TITLE Excitation Processes In The Positive Column of Electrical Discharges In Inert Gases

AUTHOR A. ZENDEHNAM

EXCITATION PROCESSES IN THE POSITIVE COLUMN OF ELECTRICAL DISCHARGES IN INERT GASES

BY A. ZENDEHNAM, BSc (Hons)

A Thesis submittted for the degree of Doctor of Philosophy of the Council for National Academic Awards.

The work was carried out at the Polytechnic of North London. Collaborating establishment: Cathodeon Ltd., Cambridge.

DECEMBER 1987

ABSTRACT

The variation with the current i, of the intensity, I, of neon spectral lines emitted from low pressure positive column discharges has been studied as part of an investigation of excitation processes in these discharges. The results indicate that two-step excitation is important for many neon lines. Measurements of emission line profiles have been made using a pressure scanned Fabry-Perot interfermometer. High resolution absorption measurements have been made to give data on the population densities of the lower excited states, and their variation with pressure and current, to assist in interpreting the intensity-current (I-i) results.

These measurements were carried out using a variety of discharge tubes with diameters from 3 to 20 mm, with current up to 30 mA, and pressures between 0.1 and 15 mbar. For comparison some measurements were also made with argon and neon-argon mixtures.

A high vacuum system capable of achieving pressure of 10^{-8} mbar was constructed and used to give high purity conditions. Various cathode systems (cold plane, hollow and heated coated) were employed; the advantages and drawbacks of the cathode systems are discussed.

The I-i, emission and absorption profile measurements were carried out for two orientations of the discharge tubes (end and side on views). The effect of self reversal was observed for the NeI lines terminating on the metastable level $3s(3/2)^{\circ}_{2}$. The number densities of the lower excited states of neon were 0.2 - 8x10 m , pressure and discharge current had marked effect on these population densities.

A modified form of I-i equation

$$I = Ai\ (1 + B\sum_{j=1}^{4} N_j(i)\ )$$

has been used for fitting the I-i results; satisfactory fits were obtained for most of the spectral lines studied.

ACKNOWLEDGEMENTS

The author wishes to thank Dr. E.B.M. Steers for his supervision and advice, and Mr D.W. Ward of Cathodeon Ltd. for guidance and for the provision of a range of specially designed discharge tubes for this work. Sincere thanks are due to Dr. M. Outred and Dr. I.W. Rogers of DECEAP of The Polytechnic of North London for their help and advice in computing.

STATEMENT

The Author attended final year honours spectroscopy courses, and attended specialist short courses on analytical atomic absorption and optical emission spectroscopy, at the Polytechnic of North London. The author was present at "Gas Discharges and their applications", Oxford, September 1985.

A poster including part of the work was presented by Dr. E.B.M. Steers at the 21st C. S. I., Garmisch-Partenkirchen, West Germany September 1985. Some part of this work was presented as a poster at SAC 86/3rd BNASS, Bristol, July 1986 and a further part was presented by the author at XVIII International conference on Phenomena in ionized Gases, Swansea, July 1987. Copies of the abstracts are given in appendix E.

CONTENTS PAGE

LIST OF FIGURES

LIST OF TABLES

CHAPTER (1) INTRODUCTION

1.1 : GENERAL

A brief introduction to the positive column discharge in general is given, together with a review of some of more relevant previous published works on the electrical and optical characteristics of such discharges.

A previous worker in this laboratory, Howard (1) investigated the spectral and electrical properties of hollow cathode discharge in pure neon, in particular the relationships between the discharge current (i) and the intensity (I) of the selected NeI, NeII and few FeI (cathode material) spectral lines. In the light of the initial hollow cathode results (Howard), the aim and program of the present work were to investigate the intensity-current relationships in the positive column discharge in pure neon for different discharge parameters (gas pressure, current, tube cross-section, length, etc), and to examine of the extent to which the intensity-current results are comparable with those obtained for hollow cathode discharge, and also to use argon as carrier gas to compare with neon, and their mixture (neon-argon) to study the variation of the spectral and electrical characteristics of the positive column discharge.

The glow discharge has distinctive arrangements of luminous and dark regions between the cathode and anode. The

positive column is a long luminous column with constant low field strength, and its colour is characteristic of the gas but is not necessarily the same as that of the negative glow, nor is it as bright. It is often uniform, but occasionally it is striated. An increase of pressure causes all the negative zones to be compressed toward the cathode, and the positive column extends to fill the remainder of the discharge tube; further increase of the pressure causes the positive column to contract radially, no longer filling the whole width of the discharge tube. A decrease of the pressure naturally causes the reverse effect.

If the anode is moved further apart from the cathode a greater potential is required to maintain the discharge, and the positive column extends to occupy the additional length. Conversely as the anode is moved toward the cathode, the positive column length becomes shorter and less tube voltage is needed.

The positive column is a neutral plasma with quite low and uniform field. The electrons tend more to a distribution corresponding to an electron temperature, with energies not often above 10-20 ev (depending on the particular discharge).

1.2 : SIMILARITY PRINCIPLE, AND VOLTAGE-CURRENT RELATIONSHIPS

The application of the principle of similarity can lead to considerable information concerning the nature of fundamental collision processes occurring in the discharge, as well as to information concerning the relationships between discharges for different conditions of gas pressure, and electrode geometry. Similar discharges (the same value of p.r where p is the pressure, r is the tube radius) between plane electrodes have the same voltage-current characteristics.

If the discharge current is raised, the length of negative glow increases slightly, and the positive column becomes shorter in length, and the required potential to sustain the discharge will increase; consequently a general increase in the brightness of the luminous parts of the discharge is caused, since more energy is being disipated in the gas, and some of this appears as additional radiation.

Abnormal discharge is obtained when the cathode surface is fully covered by the negative glow; in this work when a cold plane cathode was used, an abnormal discharge was observed. The tube voltage (v) depends on the current, the pressure, and the, dimensions of the discharge tube and the electrodes; it increases as the pressure diminishes or as the discharge current is increased, both being

characteristic of an abnormal discharge. Voltage-current curves for abnormal discharge have an increasing positive slope.

When a hollow cathode is employed in a positive column discharge tube rather than a plane cathode, a much lower tube voltage is required for a given current and pressure compared with the plane cathode situation. v-i curves for glow discharge when a hollow cathode is employed show a flat characteristic; this effect is known as the hollow cathode effect.

The electrical relationships of the hollow cathode discharge (when the arrangement of the electrodes is such that the positive column is not present) have been studied by many workers (which have been reviewed by Pillow (2)), but not many published works are available in the literature concerning the voltage-current characteristics of glow discharges when the positive column is present and a hollow cathode is used in the column tube.

A discharge tube with a hot coated filament cathode requires much less voltage compared with tubes having hollow, or cold plane cathode for like discharge conditions, due to thermionic emission, if the coated cathode is used at the right temperature.

1.3 : THE ELECTRIC FIELD STRENGTH IN THE POSITIVE COLUMN:

The longitudinal field has been measured in various ways;

the older measurements were carried out by inserting two or three floating probes into the positive column and measuring the difference between the potential they acquire. Other workers have used a movable anode and, keeping the discharge current constant, measured the extra voltage needed to sustain a short additional length of the positive column. Most measurements since about 1930 have been made with Langmuir probes spaced along the column, used to deduce the space potential, electron temperature, and electron concentration.

All measurements give the average field strength X.

$$X = \frac{\Delta V}{\Delta x} \qquad (1.1)$$

The electric field in the uniform positive column is uniform. The results of Klarfeld (3) and Groos (4) are in good agreement on measurements of field strength for different tube cross-sections, and various gas pressures. It has been mentioned by Francis (5) that at pressures about 1 mm, the dependence of the potential gradient (X) on r (the radius of the discharge tube) obeys the similarity law. i.e.

$$\frac{X}{p} = f\,(p.r) \qquad (1.2)$$

where p is the pressure.

Guntherschulze (6) has derived a semi-empirical law over a restricted range of pressure, current, and tube radius ($p \simeq$

5×10^{-2} to 0.2 mbar, $r \simeq 4 - 18$ mm, and $i \simeq 10 - 100$ mA).

$$X = \frac{C}{r+a|} \qquad (1.3)$$

where c is a constant depending on the ionisation potential and atomic weight of the gas, and a values for helium, neon, and argon respectively are given as o, 0.01, and 0.13 mm/mA (X is in v/cm, r in mm, and i in mA).

Schellenmeier (7) investigated the variation of the electric field in neon with respect to the discharge current in a tube of 10 mm bore and found that the current has very little effect on the potential gradient. Measurements by Golobovskii and his co-worker (8) show similar results.

The variation of the field strength in a neon discharge with admixture of argon was investigated by Headrick and Duffenduck (9), who observed a small amount of change in the neon electric field. This occurs when the metastable states of the main gas have energies slightly greater than the ionisation or excitation levels of the added gas; then collisions of the second kind cause the second gas to be ionised or excited. In their results admixture of neon to an argon discharge showed practically no effect on the argon discharge gradient.

1.4 : CATAPHORESIS IN GAS MIXTURES

The study of the separation of the mixtures of binary gases

under the influence of the discharge current is very important for practical applications in gas lasers, so several investigations have been carried out within the past twenty years; Hackman (10) investigated the variation of the intensity of the neon and argon spectral lines using a grating monochromator to monitor the light emission from the glow discharge in neon - argon mixtures, and found an enrichment of the minority constituent gas near the cathode, and majority gas in the vicinity of the anode. But these results have not been supported by other workers (11,12).

Sanctorum (12) studied the cataphoresis effect in six neon-argon mixtures by means of using a mass-spectrometer to monitor the neutral gas constituents present in the positive column discharge at several positions, and found in agreement with Loeb (11), Gaur and Chanin (13) an enrichment of the admixture with lower ionisation potential near the cathode region.

In this work the near anode area of the discharge tube was employed for most of the investigation (to avoid the sputtered area of the tube and problems due to striation). When a gas mixture (neon-argon) was used, this part of the tube was also used for measurements to avoid the cataphoresis effect.

1.5 : THE INTENSITY-CURRENT (I-i) CHARACTERISTICS:

A possible method of studying excitation processes under actual discharge conditions is the investigation of the relationships between the intensity of spectral lines and the discharge current.

In general, very few published works could be found concerning the relationships of the intensity and the discharge current in the positive column discharge.

Kagan et al (14) investigated the variation of the intensity of some neon spectral lines with respect to the gas pressure (1 - 30 mbar), and discharge current (10 - 400 mA) by measuring the absolute intensities in the positive column discharge; but no relationship between the intensity and current was derived from their results. Golobovskii and his co-workers (15) studied the absolute intensities of neon lines in the positive column at medium pressures to measure the population densities of the excited states of neon. Some of the intensity-current curves from their results are linear, and some show an upward curvature.

At constant electron temperature and pressure, the relationship between the intensity and electron number density is given by Frisch and Kagan (16) as follows:

$$I = An_e + Bn_e^2 \qquad (1.4)$$

where A and B are constant. This apparently assumes that population density of any intermediate state for the two-step excitation is proportional to electron number density.

Golobovskii and his co-workers (8) studied the electron concentration in neon (at pressure of 10 - 30 mbar) and in argon (at pressure of 5 - 10 mbar) discharges, in a tube with 24 mm diameter, and current of 50 - 400 mA. Measurements of the electron number density on the axis under their conditions was found difficult, due to strong pinching and pinch bends around the probe which they used. They observed a continuous spectrum in addition to the line spectrum in that pressure range. A study of the intensity of that portion of the continuous spectrum along the radius showed that the intensity changes as the square of the electron concentration, and they used this to find the electron number density on the axis from the measured concentration outside the pinch.

Some work has been carried out in order to find a relationship between the intensity of spectral lines and the discharge current in the hollow cathode discharge. Musha (17) used a log-log plot of his results and obtained very approximately straight lines of differing gradient, but there is no physical reason suggested for the various fractional powers obtained.

Howard (1) investigated the intensity-current relationships of NeI spectral lines in hollow cathode discharges, using

cathodes with bores ranging between 3 and 15 mm, pressure in the range of 1-20 mbar, and discharge current up to 20 mA.

The intensity-current (I-i) results obtained have been interpreted in terms of a model proposed by Howard et al (18), involving the balance between one-step and two-step excitation processes and de-excitation by radiation and electron collisions. Many of Howard's I-i results were fitted to this equation:

$$I = \frac{Ai(1+Ci)}{(1+Bi)} \qquad (1.5)$$

where I was the intensity of the spectral line, and i the discharge current.

A: depends on one-step excitation.

B: depends on the relative importance of collisional de-excitation compared with radiative de-excitation.

C: depends on the relative importance of two-step excitation compared with one-step excitation.

In this model, it is assumed that, for two-stage excitation via an intermediate state, the population density of the intermediate level (metastable state) is proportional to the discharge current. Subsequent work by Light and others (19,35) in a hollow cathode discharge in neon, in the same pressure range, and discharge current up to 50 mA, showed that a substantial number of the metastable neon atoms exist within the hollow cathode discharge, but their population

is not proportional to the discharge current under the experimental conditions used.

1.6 : RADIAL DISTRIBUTION OF THE INTENSITY:

As it is well known, when pressure is increased in inert gases the phenomenon of contraction of the positive column discharge is observed, - i.e., the glowing region does not fill the entire volume of the discharge tube, but contracts into a pinch near the axis. A narrow channel of discharge is also obtained when the discharge current is very low.

The constriction mechanism of the constricted positive column discharge in neon has been investigated by Mouwen (20). He argues that this strong constriction of the light intensity distribution can only be understood by assuming a strong electron temperature dependence of the excitation mechanism.

Golubovskii et al (21) studied the radial intensity distribution in the positive column discharge in neon and argon. Their results were averaged over various spectral lines, and the radial distribution contracts toward the axis with decreasing discharge current, and this contraction is more pronounced when pressure is increased. Their results show that the intensity declines much more steeply than does the electron concentration.

Milenin (22) investigated the radial dependences of

relative intensities of a number of neon spectral lines, and electron concentrations were calculated from the measured electron distribution function. His results are in good agreement with those obtained by Golubovskii and his co-workers (8). Although few workers have studied the radial distribution of the intensity in the low current positive column discharge, much work has been carried out on investigation of radial intensity in hollow cathode discharges (23,1).

1.7 : POPULATION DENSITY MEASUREMENTS OF EXCITED ATOMS:

Interest in the study of the behaviour of the metastable atoms and their concentration is due to the fact that their population densities in a discharge are usually two or three orders of magnitude higher than the concentration of other excited states. Consequently the metastable atoms play an important role in most processes of excitation at various levels, and for this reason many investigations have been carried out on population densities of excited levels in inert gases by several workers.

The metastable atoms are created during the discharge by decay from higher excited levels, which are the results of electron collisions with neutral atoms. At the same time the metastable atoms are destroyed through a variety of collisions; the most important destruction processes in a low pressure discharge are diffusion to the walls of the

container, and two-body collisions with neutral atoms (or molecules) and electrons. Three-body collisions, where metastable and two neutral atoms are involved, will be the dominating destruction process in high pressure discharges (24).

If molecules are present (intentionally or due to a leak) then collisions between metastable atoms and molecules are very effective in quenching the metastable state. If the metastable energy level is higher than the ionisation energy of the molecules involved, one gets a chemi-ionisation reaction whereby the molecules (or the associative products) are ionised, as is usually the case in a helium plasma. In an argon discharge one finds normally chemi-excitation collisions, because the metastable energy level of argon is lower than the ionisation energy of most commonly used quencher gases. In the present work we used pure gases.

There are four main experimental methods commonly used to carry out the measurements of the population density of the excited states; the hook method, the absorption method, the emission method, and the fluorescence technique.

Soldatov et al (25) investigated the population density of lower excited states of neon ($1s_3$,$1s_5$ see Fig.1) in pure neon and He-Ne mixtures; they also studied the variation of the concentrations of these levels with respect to discharge current and the pressure. Their measured number

density of the metastable level of neon 3s $(3/2)_2^o$ is 11.3 x 10^{16} $(m)^{-3}$ at pressure of 7.3 mbar and 30 mA current.

Smith and Prins (26) have measured densities of neon atoms in the 3s $(3/2)_2^o$ and 3s $(3/2)_1^o$ states in the positive column of a 130 mbar neon pressure discharge, using the fluorescence technique. Their current range was between 20 mA to 120 mA. They have plotted the number densities of the metastable state 3s $(3/2)_2^o$ and the radiative level 3s $(3/2)_1^o$ against discharge current, and found the density of the metastable atoms tends to an asymptotic value for higher current, and suggested this may be due to destruction by electrons of the metastable atoms caused by stepwise excitation and ionisation , which increases in comparison with the almost current-independent destruction by three-body collisions with neutral atoms. Their results show that for the resonant atoms this asymptotic behaviour starts at larger currents. They also carried out some measurements on the radial distribution of the metastable and resonant atoms.

Similar measurements on the atom densities of first excited states in low pressure neon discharge were carried out by Van Schaik et al (27), by means of optical fluorescence in a cylindrical discharge tube (d = 31 mm), with discharge current up to 30 mA. Their results show a very similar trend to Smith and Prins results for population densities of the same metastable level (lowest excited level) and the

same radiative state versus current.

Akhmedzhanov and his co-workers (28) determined the densities of neon atoms in the metastable state and in the radiative level in the positive column of neon discharge by the laser resonance fluorescence technique. Their measurements were carried out over a range of electron densities of 10^{14} to 10^{16} m^{-3}.

Golubovskii et al (29) studied concentrations of excited argon atoms in the positive column discharge at medium pressures and current range of 4 to 120 mA, in a discharge tube of 12 mm diameter.

Delcroix et al (30) have studied the dependence of number densities of the excited state in argon on the discharge current, and calculated the overall production and destruction coefficient for these excited states. A strong saturation behaviour can be seen on concentration of metastable level against current graph. The population densities from their results are the same order of magnitude as the results from Golubovskii et al. (29).

The diffusion of the metastable atoms of inert gases has been investigated by Lisitsyn et al (31), and the radial distributions of the concentrations of the metastable atoms were measured. It has been shown in their results that the metastable levels of neon are not destroyed completely by collision with the discharge tube walls, and destruction

parameters have been determined.

Many other workers have studied the variation of the population densities of the excited states of neon or argon in the positive column and hollow cathode discharge, but due to the difference between their current or current densities and pressure range, compared with this work, they have not been discussed in detail. (e.g. Van Veldhuizen (32) and Smits et al (33)).

The excitation of atoms from a lower excited state by electron collision (stepwise excitation) is often of primary importance among other excitation processes. Thus, information on the dependence of the effective cross-sections of these processes on the energy of the colliding particles, that is, the excitation function, is of considerable interest.

Mityureva and Penkin (34) have studied the stepwise and direct excitation function for some atomic neon and helium spectral lines. They estimated from their measurements the maximum values of the cross-sections for the stepwise processes; the values found were $Q = 10^{-15} - 10^{-14}$ cm^2 for the atoms and $Q = 10^{-16}$ cm for the ions excited from atomic metastable level. This estimate shows that the cross-section for the processes of stepwise excitation by electron collision are greater than the cross-section for direct excitation.

The investigation about stepwise excitation cross-sections in rare gases has been made by Behnke et al (35), in the positive column of a low pressure glow discharge. Also they studied the population densities of excited states of helium, neon, and argon.

CHAPTER (2) OUTLINE OF RESEARCH:

2.1 : GENERAL:

The aim of this work was to investigate the electrical and spectral characteristics of the positive column discharge in neon, argon, and their mixtures in a more systematic manner, and to compare and contrast these obtained results with those of hollow cathode discharges.

Discharge tubes with alternative anodes and different diameters and length were employed, with various cathode systems (cold plane, hollow, and hot coated filament) to find the most convenient one to work with (in respect of lower tube voltage, less sputtering from the cathode, and problems due to constricted discharge). Neon was chosen as the initial carrier gas, then similar measurements up to an extent were carried out for argon and argon-neon mixtures.

Gas purity was monitored photographically using a medium quartz spectograph. The molecular bands detected were identified being predominantly due to CO and CO^+, typical outgassing products, and to a lesser extent to OH and H. No O_2 OR N_2 bands was observed, indicating that the contamination was due to outgassing, and not a real leak. Subsequently all the results were carried out under maximum gas purity after extensive degassing.

2.2 : VOLTAGE - CURRENT (V-I) RELATIONSHIPS:

Voltage-current measurements were made for different discharge parameters (pressure, tube cross-section, positive column length, etc). Using the discharge tubes with alternative anodes, and either hollow or hot coated filament cathode allowed an estimation to be carried out on the electric field strength under various discharge conditions.

2.3 : SPECTRAL LINES:

In neon the wavelength corresponding to the strongest transitions from the p level to the s level are in the visible region. All the spectral lines which have been studied in detail in this work when neon was used were NeI lines, listed in table 1.

The majority of spectral lines were those arising from transitions between 3s, 3s' group levels and the 3p, 3p' groups. The 3s, 3s' group of four energy levels include the two metastable states $3s\ (3/2)^{\circ}_{2}$, and $3s'(1/2)^{\circ}_{0}$ and the two radiative levels $3s(3/2)^{\circ}_{1}$, and $3s'(1/2)^{\circ}_{1}$, the $3s\ (3/2)^{\circ}_{2}$ being the lowest energy level of NeI excited states.

A few NeI spectral lines were selected with the same upper energy level and different lower level (metastable and non-metastable) for studies of the variation of the intensity ratio of such spectral lines with respect to current under

similar discharge conditions.

An energy level diagram for the chosen NeI lines is shown in Fig. 1.

NeI SPECTRAL LINES STUDIED

λ/nm	Upper energy Level	Lower Energy Level
363.4	$4p\ (1/2)_0$	$3s'(1/2)_1$
540.0	$3p'(1/2)_0$	$3s\ (3/2)_1$
585.2	$3p'(1/2)_0$	$3s'(1/2)_1$
588.2	$3p'(1/2)_1$	$3s\ (3/2)_2$
614.3	$3p'(3/2)_2$	$3s\ (3/2)_2$
616.3	$3p'(1/2)_1$	$3s'(1/2)_0$
626.6	$3p'(3/2)_1$	$3s'(1/2)_0$
630.5	$3p\ (3/2)_2$	$3s\ (3/2)_1$
633.4	$3p\ (5/2)_2$	$3s\ (3/2)_2$
638.3	$3p\ (3/2)_1$	$3s\ (3/2)_1$
640.2	$3p\ (5/2)_3$	$3s\ (3/2)_2$
671.7	$3p'(3/2)_1$	$3s'(1/2)_1$
692.9	$3p\ (3/2)_2$	$3s'(1/2)_1$
703.2	$3p\ (1/2)_1$	$3s\ (3/2)_2$
724.5	$3p\ (1/2)_1$	$3s\ (3/2)_1$

Table 1.

The spectral lines which were studied in case of argon as the filling gas were ArI lines, and are listed in table 2.

ARGON LINES STUDIED

λ/nm	upper energy level	lower energy level
603.2	$5d\ (7/2)_4$	$4p\ (5/2)_3$
675.4	$5d\ (3/2)_2$	$4p'(3/2)_2$
696.5	$4p'(1/2)_1$	$4s\ (3/2)_2$
706.7	$4p'(3/2)_2$	$4s\ (3/2)_2$
727.3	$4p'(1/2)_1$	$4s\ (3/2)_1$
738.4	$4p'(3/2)_2$	$4s\ (3/2)_1$

Table 2.

2.4 : INTENSITY - CURRENT CHARACTERISTICS (I-i):

The Intensity-current relationships of most of the selected NeI spectral lines have been investigated by previous workers in this laboratory, using a hollow cathode discharge. The I-i characteristics were investigated in this work for the chosen NeI and ArI spectral lines for various gas pressures, tube cross-sections, and different orientation of the positive column discharge, (side on and end on viewing), to reveal any differences between the possible excitation processes. This would have been reflected in different intensity-current relations for certain types of spectral lines.

Additionally the spatial variation in light intensity for

neon and argon spectral lines was carried out for various pressures and currents, using end viewing of the positive column discharge.

2.5 : FABRY-PEROT SCANS (EMISSION):

The profiles of neon and argon spectral lines were recorded, using a pressure scanned Fabry-Perot interferometer (F.P.I).

Some of NeI lines having the metastable state $3s(3/2)^{o}_{2}$ as the lower energy level of the corresponding transition exhibited self-reversal when sealed hollow cathode lamps were used. This effect (self-reversal) was observed when end view of the positive column was used for emission scans experiments, but not when side-on observation was employed for investigations. Emission scans of the neon spectral lines terminating on other 3s, 3s' level groups were made, but no sign of self-reversal was observed.

No self-reversal was obtained for the chosen argon spectral lines, even though some terminate to the metastable levels.

2.6 : DIRECT ABSORPTION MEASUREMENTS:

Following observation on self-reversal of neon lines with the metastable state $3s(3/2)^{o}_{2}$ as their lower energy level, quantitive determination of the neon metastable atom

population density were made by a direct absorption method. The variation of number density of the neon metastable atoms was investigated for different currents and pressures.

Additionally population density of neon 3s, 3s' levels (radiative levels) and argon 4s $(3/2)_2$ state were measured in pure neon and argon, and in their mixtures (neon,argon) for various partial pressures.

The measurements of the radial distribution of the number density of the neon metastable atoms were carried out employing end on viewing of the positive column discharge in a tube with a mesh anode.

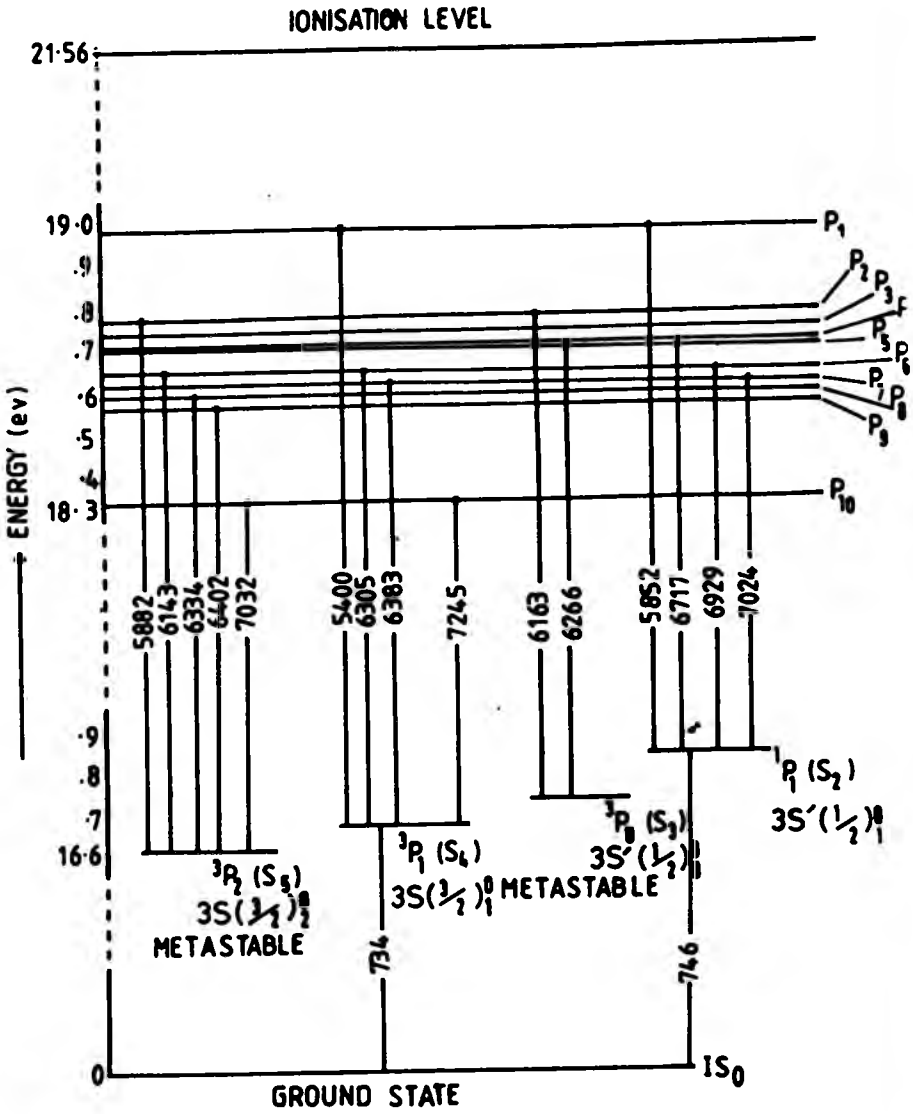

Fig. 1 Neon energy level diagram

CHAPTER (3) VACUUM - SYSTEM

3.1 : GENERAL:

In order to investigate the spectral and electrical characteristics of the positive column discharge over a wide range of carrier gas pressure, sealed column tubes would have been inconvenient. Additionally, one could not have easily ascertained how they had aged or changed over a long period. Thus, demountable tubes were required. To provide for a high gas purity a vacuum system was necessary, to evacuate the demountable column tubes prior to gas introduction.

A vacuum system was designed and built so that it could take the pressure below 10^{-7} mbar, to ensure that residuals did not contribute much to the introduced gases (pressure 15-0.1 mbar). The system was made using mainly stainless steel components for the high vacuum section. These components (tee-pieces, taps, flexible, etc) were joined together using aluminium sealing rings. Aluminium rings were used because there were more economical than copper o-rings and it was claimed by manufacturers that aluminium sealing rings could be reused.

In roughing lines aluminium components were used, and joined together using rubber o-rings. The vacuum system was also to be suitable for filling electrodeless discharge tubes containing metallic halides. The cold trap adjacent

to the tubes fixing point was made of glass, the only disadvantage of glassware was due to accidental damage, which was overcome by using expanded aluminium round those areas.

A two-stage rotary pump (Edwards 852208) with a Leybold oil vapour diffusion pump (Type 21920) were employed in the vacuum system. A schematic diagram of the system is shown in Fig. 2.

3.2 : FORELINE SECTION

A pressure of around 10^{-3} mbar, which was required before the diffusion pump could be started, was attained by the rotary pump. A foreline trap containing a 10 Å molecular sieve was employed to obtain fast pumping and to prevent contamination of the diffusion pump.

A Pirani gauge (Edwards PR-10-K) was provided to monitor the roughing line pressure over the range of atmospheric pressure to 10^{-3} mbar. 10 KF aluminium pipelines and taps with bellows-sealed drive shaft and perbunan o-ring gasket were used in this part of the vacuum system. It is claimed by the manufacturers that the leak rate of the bellows-sealed valve in aluminium taps is less than 1×10^{-9} mbar x L/S.

3.3 : HIGH VACUUM SECTION:

A watercooled Leybold oil diffusion (Type 21920) with a 35 Ls^{-1} speed of pumping at its inlet was employed, using

Fig. 2 Schematic diagram of the vacuum system

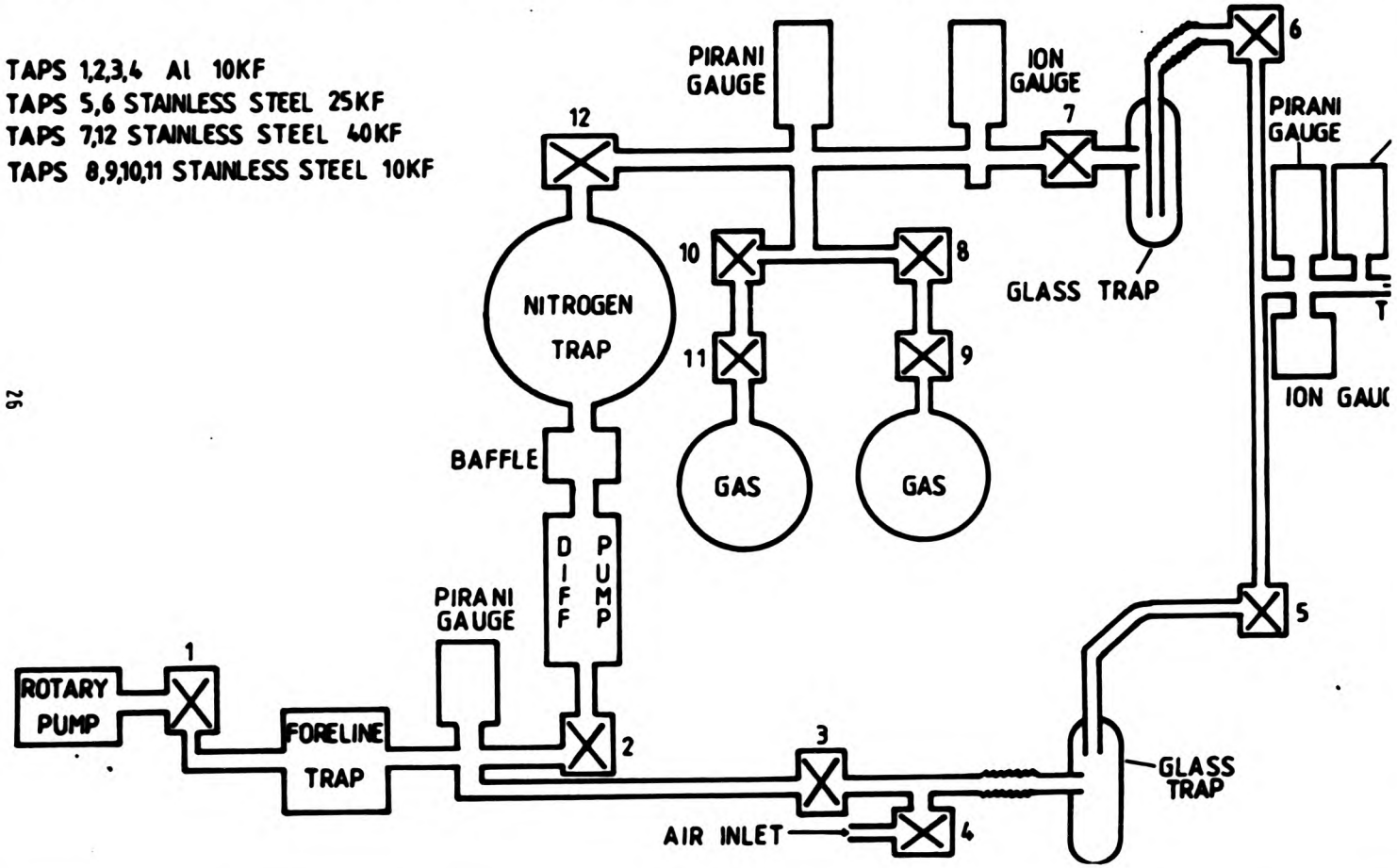

Santovac 5.

Santovac 5 has a very low vapour pressure and is not degraded by accidental exposure to atmosphere.

A baffle was used between diffusion pump and the liquid nitrogen trap to reduce the rate of distillation of pump fluid to the cold trap. This baffle was watercooled and had conductance of 60 L/S. The pumping speed value of the combination of the diffusion pump and the baffle was half the rated speed of the pump; the liquid nitrogen trap caused no further significant reduction in pumping speed.

A double iridium ionisation gauge and an ion gauge controller (V.G. Model IGC 10) unit were used for monitoring the high vacuum pressure with range of 10^{-3} to 10^{-10} mbar. A pirani gauge (Edwards PRCV 16) bakable up to 150°c was placed near the experimental discharge column tube to monitor the introduced gas pressure. Later on in this work a baratron capacitance gauge (Type 221 AHS - 10) was chosen for its pressure reading accuracy in the range 20 to 10^{-3} mbar, and because its indicated pressure is independent of gas type and was used for monitoring the gas mixture (neon-argon) pressures. The baratron was placed next to the pirani gauge and its pressure reading was calibrated against the pirani reading.

The vacuum system was constructed such that two research grade gas flasks could be used to fill the demountable

discharge tubes. All the components in this section of the vacuum system were stainless steel except the cold trap which was made of glass.

3.4 : SYSTEM DEGASSING:

An extensive degassing of the vacuum system was required, to improve the ultimate pressure. In order to do this the complete evacuated volume, including the baratron, ionisation, and pirani gauge heads could be baked.

Degassing was carried out by using heating tapes and cords which were carefully wrapped so that all components were heated uniformly. Each individual heating tape and cord was provided with a separate variable transformer power supply, several thermocouples (Chromel-Alumel) were made and placed on critical parts of the vacuum system to monitor the baking temperature. The main limiting factor on bake-out temperature of the components was the vitilan (equivalent to viton) o-ring gasket inside the stainless steel taps rated 150^{o}c.

The aluminium sealing rings which were used in the high vacuum section of the system, were found to be prone to failure if not cooled slowly, and great care was taken to ensure very gradual cooling after bake-out.

To reduce contamination dry nitrogen was used instead of air when the vacuum system was let up to atmospheric pressure.

Gas was introduced to the system and column tube by doses from research grade bottle, and pressure was monitored by the pirani gauge next to the positive column tube, this pressure reading being corrected for the gas used, as indicated by manufacturer's correction curves.

3.5 : LEAK TESTING:

This was accomplished in the high vacuum section by observing any change on ionisation gauge indicated pressure when each flange was probed with a flow of helium. Common leaks were found to be due to the aluminium sealing ring being scratched, or the clamping flanges needed further tightening. A tesla coil was used for leak detection on the glass parts of the system, as well as gas container connections and experimental demountable positive column discharge tubes.

3.6 : CONTROL SYSTEM FOR PROTECTION:

Since continuous pumping was required, a safe operation for overnight pumping was necessary, therefore a control system was built to give:

a) protection against water failure; to do this a thermal protection switch was used for the control of temperature on the cooling circuit of the pump. The heater of the pump is switched off in case of inadmissible increase in

temperature - e.g. failure of cooling water.

b) Protection against power failure; if mains power was cut off the magnetic valve of the rotary pump would close, the system was shut down completely and did not restart pumping if the power was restored. This was done to prevent the burst of gas, which occurs when a magnetic valve opens, from entering the vacuum system.

Fig. 3, shows the circuit diagram of the control system for overnight pumping.

3.7 : PERFORMANCE AND OUTGASSING PRODUCTS

After thorough baking, the ultimate pressure of 7×10^{-8} mbar was achieved.

The outgassing products were identified spectroscopically, using a medium quartz spectograph. When the vacuum system was contaminated molecular band spectra appeared, and these bands were identified as belonging to CO and CO^{+} and occasionally OH. After thorough degassing the majority of the impurities were removed, and the measurements were carried out under clean conditions.

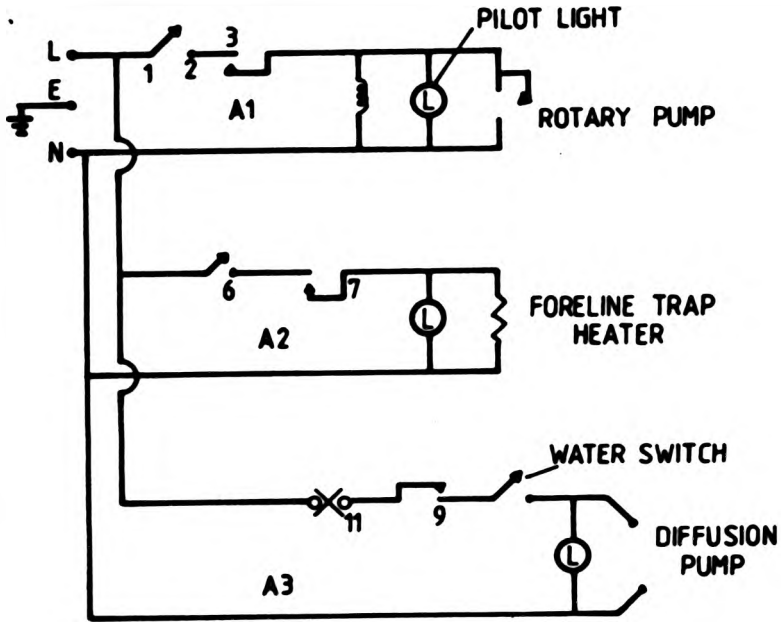

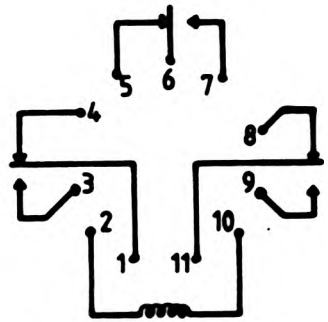

A.C. RELAY CIRCUIT

Fig. 3 Circuit diagram of control system for overnight pumping

CHAPTER (4) OPTICAL INSTRUMENTS:

4.1 : GENERAL:

To carry out the intensity measurements, a monochromator was needed to select the individual spectral lines, with high resolution to separate the close spectral lines.

Initially an Ebert mounting spectrometer was employed for the earlier part of this work, then in the later part an Eagle mounting was used which was part of an optical arrangement for Fabry-Perot interferometric measurements which was set up by a previous worker (19) in this laboratory. After some alteration this optical arrangement (see Fig. 4) was used to investigate the spectral characteristics of the positive column discharge.

Basically for intensity measurements an image of the light source to be investigated was focused by lens L1 (see Fig. 4) on the pinhole aperture, which acted as a near point source. Then parallel light was focused on the centre of the monochromator entrance slit by using lens, L2, L3. When interferometric (emission and absorption) measurements were carried out, the Fabry-Perot interferometer housing containing F.P. Etalon was placed between L2, L3 lenses. The Etalon plate was fully illuminated by parallel light, and the light from the Fabry-Perot was focused to the slit of the spectrometer by lens L3.

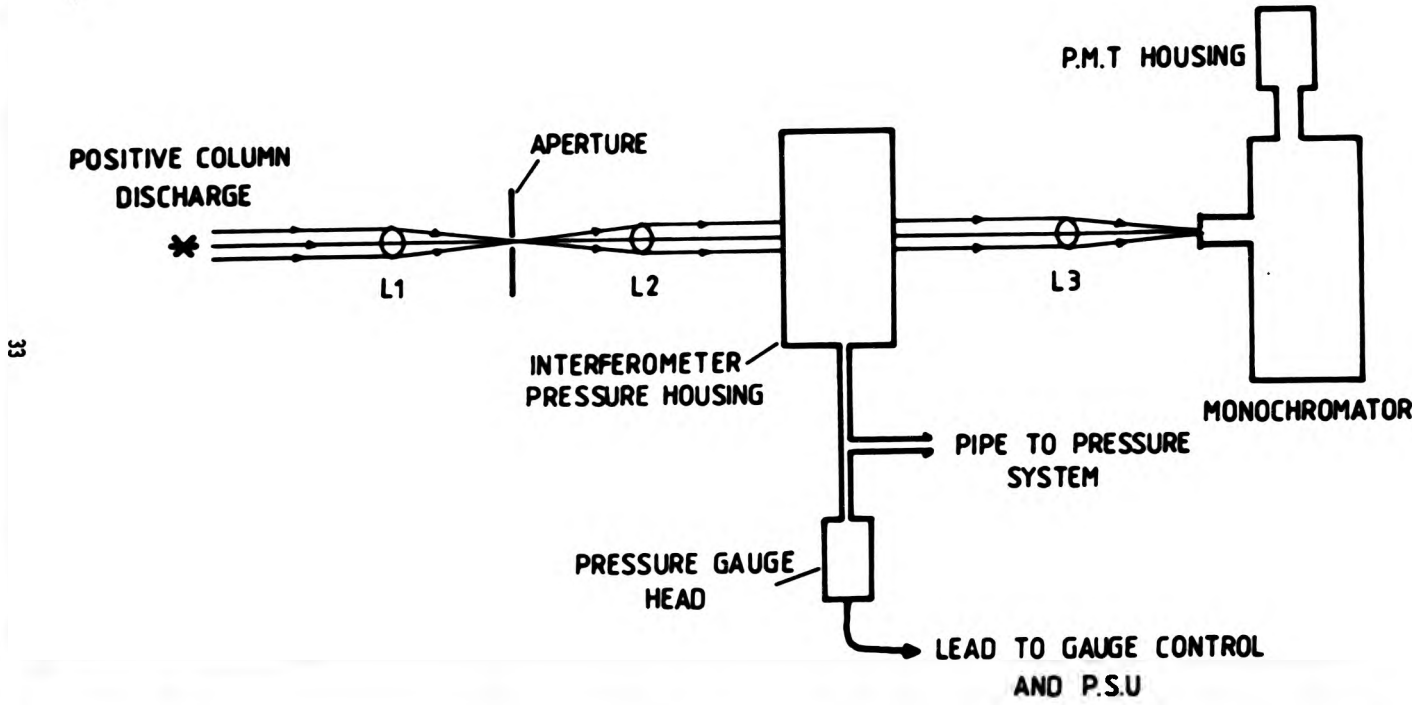

Fig. 4 Optical arrangement for the I-i and F.P.I. emission measurements

The light was detected by a photomultiplier tube (PMT) which was housed behind exit slit of the Eagle mounting. A d.c amplifier was used to amplify the signals, and for absorption measurement a phase sensitive amplifier was employed. When intensity measurements were made signals were recorded on a chart recorder, while the emission and absorption line profiles were directly recorded on a x-y recorder.

4.2 : EBERT MOUNTING

As already was mentioned initially a 1.5 metre Ebert mounting spectrometer with 11.1 Å/mm dispersion in first order was used. This spectrometer had a plane grating of 600 grooves/mm and 10 cm projected width (15 cm x 12 cm). Both entrance and exit slits were 2 cm high curved slits, in order to remove the effect of astigmatism and image curvature, and to increase the energy flux passing at any given wavelength, without decreasing the resolving power.

The grating was driven by one of the two electric motors which could rotate the grating in either direction by changing current phase; the scanning speed could be changed easily by changing the gear box levers. This grating instrument, which had been constructed in this department, was built in a cylindrical tank of 40 cm diameter and 167 cm length. The optical arrangement of this instrument is shown in Fig. 5.

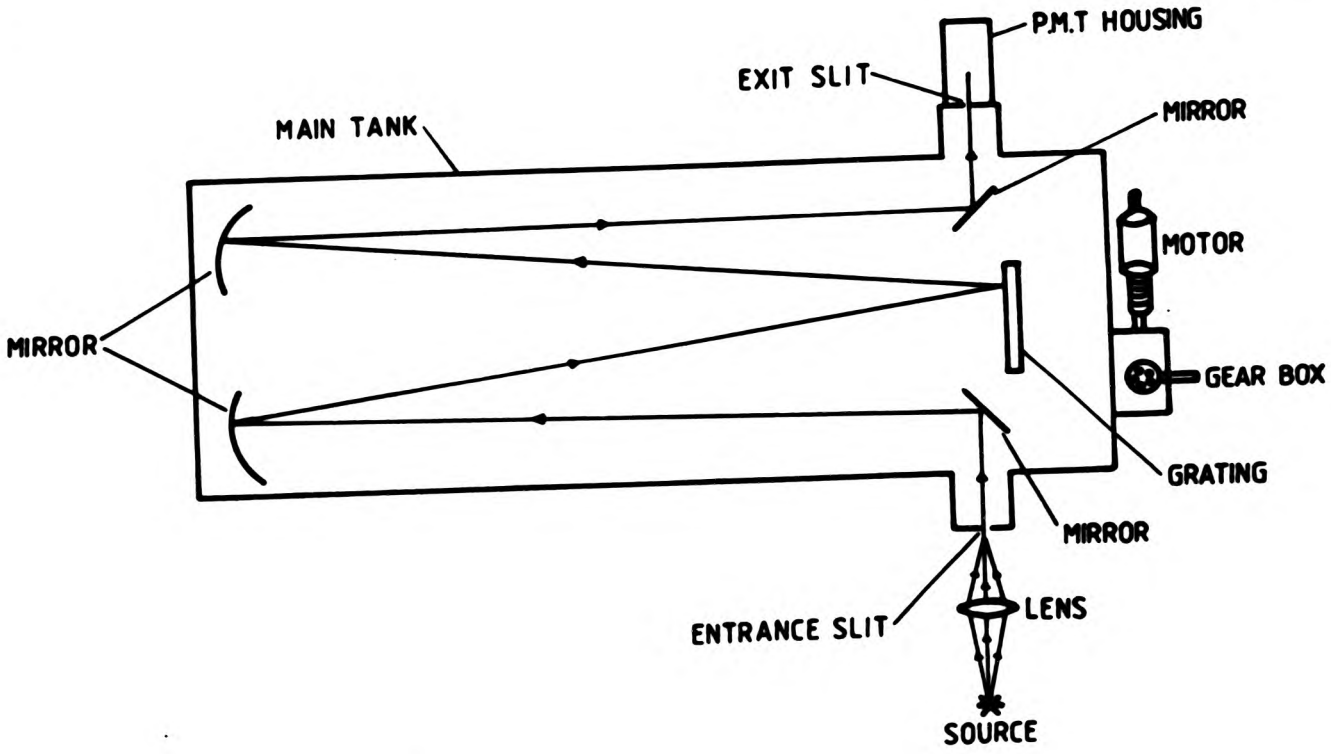

Fig. 5 Optical arrangements of Ebert mounting

4.3 : EAGLE MOUNTING

In the later part of this work, the vacuum system was moved to another laboratory where an optical arrangement was set up for interferometric measurements, and a concave grating spectrometer with Eagle mounting was used.

This spectrometer had a right angle prism, made of high quality fused silica to ensure that the monochromator could be used in the ultra-violet region. Fig.6 shows the optical arrangement of this monochromator.

The grating was ruled with 600 lines/mm, had a radius of curvature of 1 meter, and was blazed for use in first order for the optical range of wavelength. The grating was mounted in a holder on the grating table, the table was free to rotate about a vertical axis for wavelength selection, and to travel linearly toward and away from the exit slit for focusing (see Fig. 7). These motions were controlled via mechanical linkages. Rotation of the table could be driven manually or electrically. The rotation and focus setting were indicated by counters and wheel marking. A calibration was carried out for rotation and focus setting against wavelength, using a series of standard Philips lamps of various elements Hg, Zn, and Cd. The correct focus was obtained by repeated rescanning of chosen spectral lines, the best focus being that which gave maximum peak height on the chart recorder.

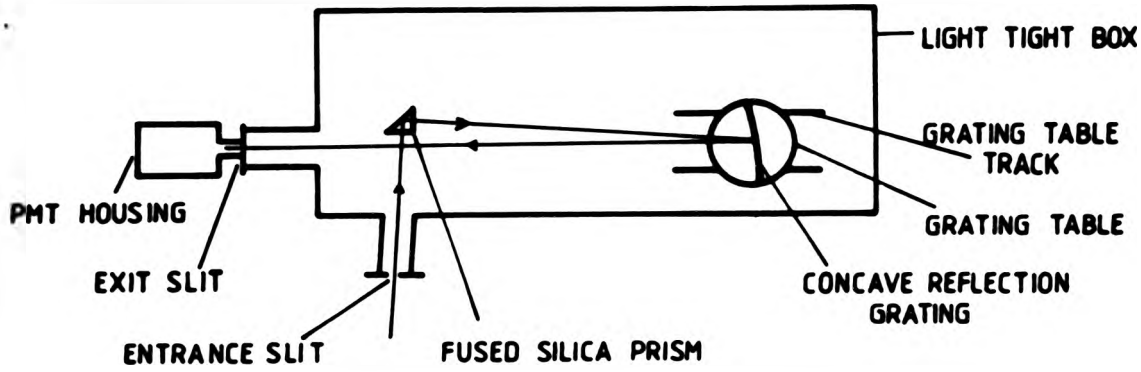

Fig. 6 Optical arrangements of Eagle mounting

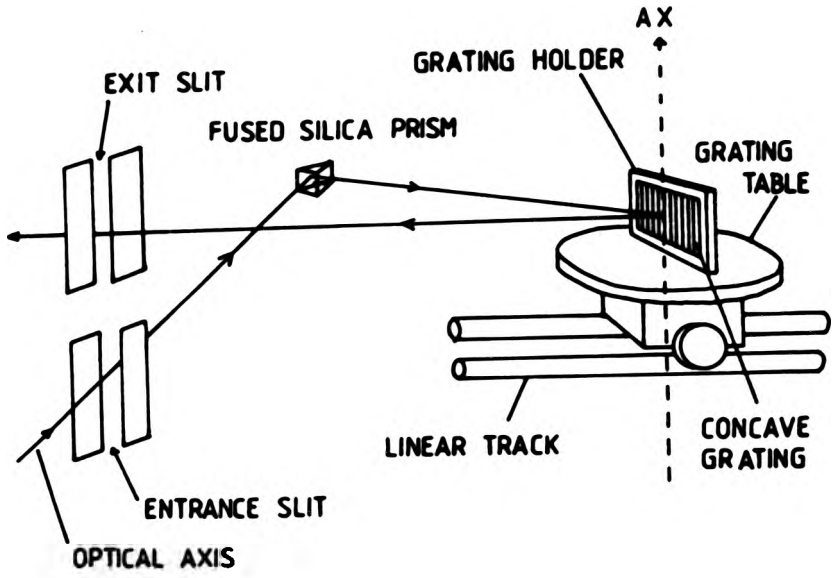

Fig. 7 Optical set up and grating in Eagle mounting

To define the optical axis and alignments of the monochromator and whole optical system a He-Ne laser was employed and after final adjustments had been carried out, the laser spot occurred at the centre of the exit slit of the monochromator, irrespective of rotation setting to different orders. After final adjustments and calibration of rotation and focus settings, this instrument functioned satisfactorily as a spectral line isolator, with a critical slit width of about 15μm, and resolution of order of 0.03 nm.

The slit width was increased in the experimental measurements, in order to provide adequate light level for all the spectral lines to be studied, whilst giving freedom from interference due to other close lines. In a few cases, in particular the line of NeI at 363.3 nm, noise was a problem, it was considered better to lose some data on this spectral line rather than to upset the instrument calibration for the rest of the data.

4.4 : DETECTING AND RECORDING SYSTEMS

4.4.1 : PHOTOMULTIPLIER TUBE:

An EMI 9558QB photomultiplier tube (PMT) with spectral response S20 was employed to detect signals. The PMT was housed behind the exit slit of the spectrometer and was powered by a stabilised EHT power supply (Thorn EMI type 28B).

The photomultiplier potential (v) was monitored with a calibrated digital voltmeter. The voltage range used for detection of the spectral lines in this work was between 500 to 1000 volts. This photomultiplier had good response from the ultra-violet to the near infra-red region.

Since the source line intensities sometimes were too large, resulting in an over range signal on the chart recorder, the supply voltage to PMT was calibrated, by plotting a graph of log (recorded intensity, I) versus log (photomultiplier voltage, V), and measuring the slope, m, and intercept, log A. This gave an equation of the form:

$$I = AV^{m}$$

where m = 10.2, and intensities at different supply voltages could thus be compared by using:

$$\frac{I_{V_1}}{I_{V_2}} = \left(\frac{V_1}{V_2}\right)^{10.2}$$

For each set of measurements the above relationship was checked, and very small changes were obtained.

4.4.2 : **AMPLIFIERS**

A d.c amplifier with a wide range of gain was used for the intensity-current, measurements and emission profile scans. By controlling photomultiplier voltage and load resistance R (1,2,5,10,20,50 MΩ), the overall amplifier output level could be chosen to have suitable values for a large range

of spectral line intensities. The amplifier was prone to slight drift, and balance controls were provided so that the baseline could be checked before and after each measurement run. A phase sensitive amplifier (Brookdeal, type 401) was employed when absorption measurements were carried out. Microwave excited electrodeless tubes filled with neon or argon (pressure 2 mbar) were used as the primary source for the absorption experiments. The probe beam was modulated at 33 ⅓ Hz by a chopper which also provided a reference signal for the phase sensitive amplifier used to amplify the photomultiplier output.

4.4.3 : CHART RECORDERS

For intensity-current measurements the signals were displayed on a X-T chart recorder (YEW - type 3021) with the range of 10 mv to 50 v.

A X-Y recorder (RIKADENKI model BN-133 A) was employed for recording the spectral line profiles (emission and absorption). This recorder provided a choice of scales from .05 mV/cm to 5 V/cm.

The x-axis of the x-y recorder was controlled by Fabry-Perot housing pressure, while the y-axis was controlled by the amplifier output of the photomultiplier.

4.4.4 : FABRY-PEROT INTERFEROMETER (F.P.I)

A pressure scanning Fabry-Perot system, which had been developed by Reed (36), and Light (19), (previous workers in this laboratory) was used to investigate the emission and absorption profiles of neon, and argon spectral lines. The optical arrangement of this system is shown in Fig. 4 for emission, and in Fig. 5 for absorption measurements.

The interferometer plates were separated by a quartz spacer 6mm thick and held together by the pressure of three leaf springs transmitted by lever arms pressing on ball bearings. The tension on the leaf springs could be altered from outside the housing, and in this way the parallelism of the plates was adjusted. The plates which were used had peak reflectivity of 93% at 700 nm and a bandwidth of 140nm; quoted flatness was $\lambda/150$ (36). The optical alignment was carried out with a He-Ne laser and a finesse of $\simeq$ 30 was obtained.

The line profiles were directly recorded on a x-y recorder. The pressure in the interferometer housing was sensed by a Schaevitz P744-002 pressure transducer.

The portion of the output corresponding to atmospheric pressure was subtracted by means of an offset amplifier. By raising the gas pressure within the housing and then allowing the gas to escape very slowly through a needle valve, the refractive index of the gas in the Fabry-Perot housing would be varied and hence the F.P.I. made to scan the spectral lines isolated by the monochromator. The

determination of instrument function, finesse, and adjustment of the F.P.I. will be discussed in chapter 6 in more detail.

Fig. 8 Optical arrangements for absorption measurements

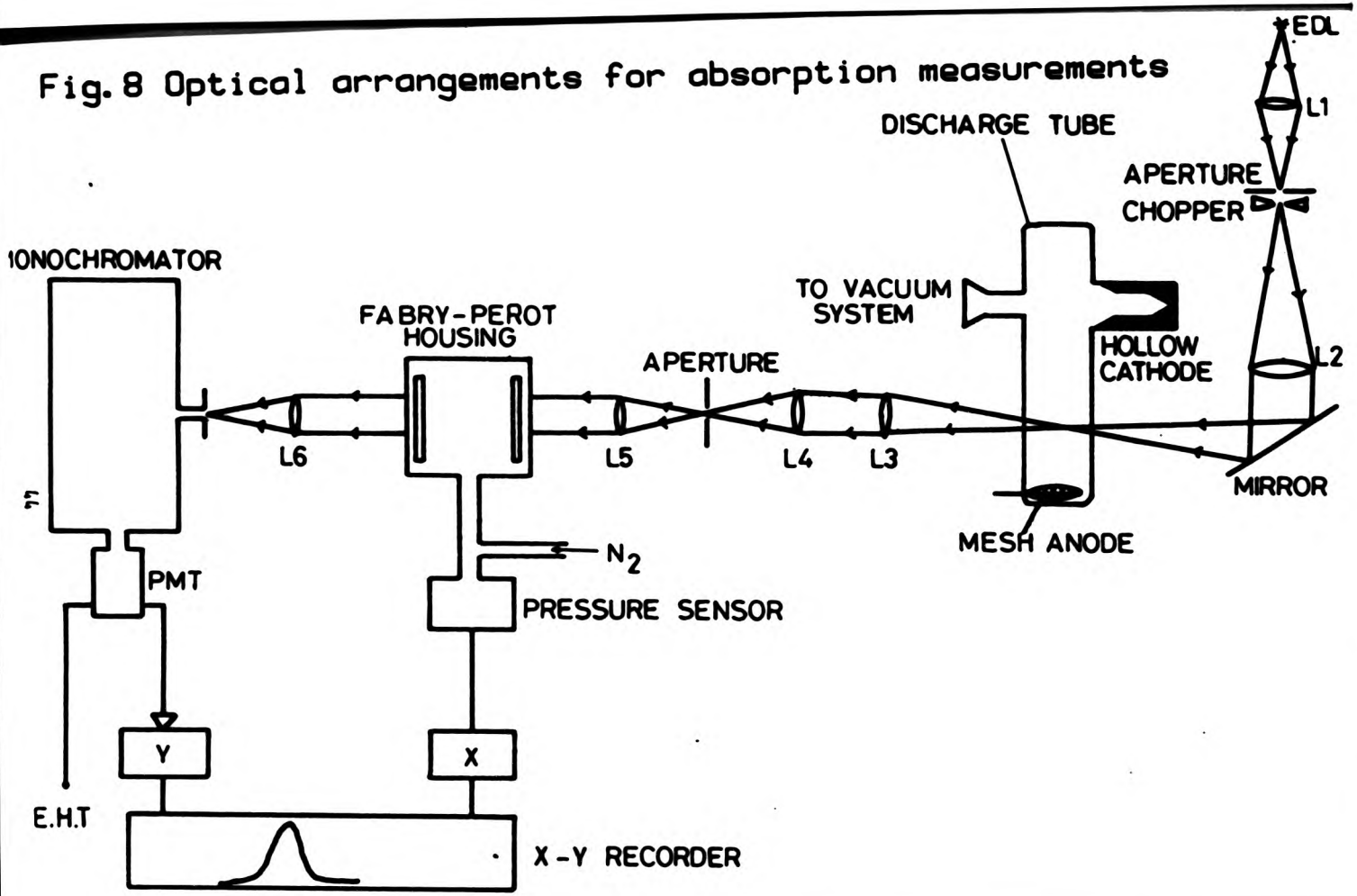

CHAPTER (5) DISCHARGE TUBES, CATHODE SYSTEMS, AND THEIR TREATMENT

5.1 : GENERAL

All the discharge tubes for this work have been specially made by Cathodeon, Ltd; some were made of 8250 glass and some of quartz with a spectrosil viewing window.

Every time a new column tube was connected to the vacuum system, a gentle flaming was given to the tube if it was made of glass; when a quartz discharge tube was used, a hot flaming was applied to it, particularly around the electodes. Then, using heating cords, the tube was baked up to 120 c for at least 48 hours.

A clean discharge using neon gave a red brick colour positive column and orange negative glow, and a few mm length Faraday dark space, when a cold plane cathode was used. In the high pressure case (10-20 mbar), most of the distance between the electrodes was occupied by the positive column, with one or two striations at the beginning or head of the column near the cathode. A constricted discharge was observed when gas pressure was higher than 10 mbar and current was lower than 5 mA, and was more noticeable in wider tubes. The constriction was more pronounced when argon was used as carrier gas.

Reducing the pressure resulted a shorter positive column, and longer length of the negative glow, and the required potential to sustain the discharge increased. By

further reduction of the pressure, a paler coloured positive column was obtained, and sputtering from the cathode became heavier.

5.2 : PLANE COLD CATHODE

The first discharge tube, Fig.2 was designed with tungsten electrodes. The reason tungsten was chosen was that the sputtering effect is apparently less from tungsten cathodes (5). This effect is due to bombardment of the cathode surface by gas ions from the discharge, and results in the deposition of cathode material on the glass envelope.

The current and pressure ranges in this work were limited due to sputtering when a plane cold cathode was used; in some cases the cathode acted as a hollow cathode due to sputtered material around it, which caused changes in discharge characteristics. Low pressure, and higher current, resulted in a heavy sputtering. This deposition of the cathode material on the glass envelope was not removed when chromic acid was applied.

Stocker (37) found an empirical relation between the sputtering rate R (proportional to number density of cathode atoms in the discharge), discharge current i and pressure p in the form:

$$R \quad (i/p)^{1.5}$$

It was decided to shield the cathode in the column tube

mentioned above for two reasons:

i) Often discharge took place behind the cathode, and changed the characteristics, (electrical and spectral).

ii) To be able to use the discharge tube for a longer period. (It was found very difficult to remove the sputtered layer).

The discharge tube was mounted to the vacuum system via a demountable glass-metal connector with viton O-ring seal, and the shielding of the cathode was done by using 3cm length silica tubing, which could easily be replaced by a clean one when the silica tube was coated with material. The width of shielding tube was just enough to go over the cathode; although the shield prevented the discharge tube from being permanently affected by sputtered metal, it was necessary to let the vacuum system up to atmospheric pressure every time the shielding tube was changed. Furthermore, the chance of the cathode acting as a hollow cathode was greater owing to the narrower bore tube.

Another problem was that, if the silica tubing did not cover the pin behind the cathode completely, then an arc would take place between the beginning of the negative glow and the area which was not covered by shielding tube. One way of overcoming the problems due to sputtering was using a hot oxide coated cathode rather than a cold one.

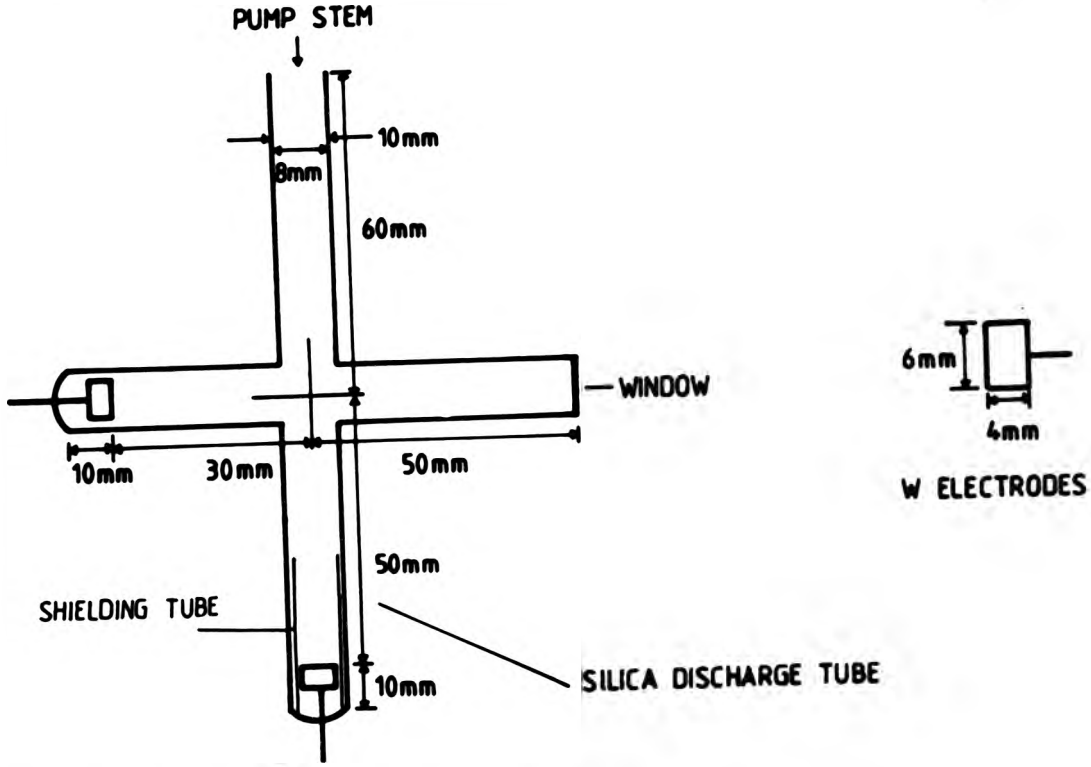

Fig. 9 Discharge tube with plane cold cathode

5.3 : THERMIONIC EMISSION

When a hot cathode is employed in a discharge tube and is used properly, then current through the discharge is less than primary emission of its cathode, and secondary emission is not necessary to sustain the discharge.

The main difference between a cold and a hot cathode discharge lies in the cathode dark space near the hot cathode. There is a space charge of electrons, whose density determines the electron current leaving the cathode. This current is almost equal to the total current through the discharge tube, whereas the electron current from a cold cathode is about a tenth of the discharge current. The cathode fall in a hot cathode discharge is very small compared with a cold cathode.

A hot cathode may be oxide-coated or thoriated, which improves its emission, but bombardment with positive ions energetic enough to cause secondary emission would destroy the emission surface of the cathode, and shorten its life; also an oxide-coated cathode gets chemically poisoned if exposed to air or other reactive gas after activation.

There is usually a visible dark space in front of the hot coated cathode, and the negative glow is either very small or absent. If the discharge current required is greater than the thermionic emission from the cathode, an accelerating field must develop at the cathode surface and

a positive ion current is required. The cathode fall must then become positive, the dark space disappears, and the negative glow can be seen round the hot oxide-coated cathode, furthermore if the voltage across the hot cathode is very low, then the negative glow will cover the hot filament cathode.

5.4 : COLUMN TUBE WITH HOT COATED CATHODE

A discharge tube with barium oxide-coated filament (tungsten) see Fig. 10 was designed, made by Cathodeon Ltd, and mounted to the vacuum system.

The cathode filament was activated using a 30v d.c power supply. This activation process was carried out by increasing the voltage across the filament cathode by .5 and 1 volt steps; a disappearing filament pyrometer was employed to estimate the filament cathode's temperature.

The coated filament in this column tube was poisoned after a short period. As was mentioned before, the discharge tube was connected to the vacuum system via a glass-metal connector with viton O-ring seal, which was found to have a small leak, and OH bands were observed. This could be the reason for the filament cathode acting as a getter and getting poisoned. The other reason for the hot coated filament becoming unsatisfactory after a while could be due to incorrect activation process (e.g. not a good background pressure).

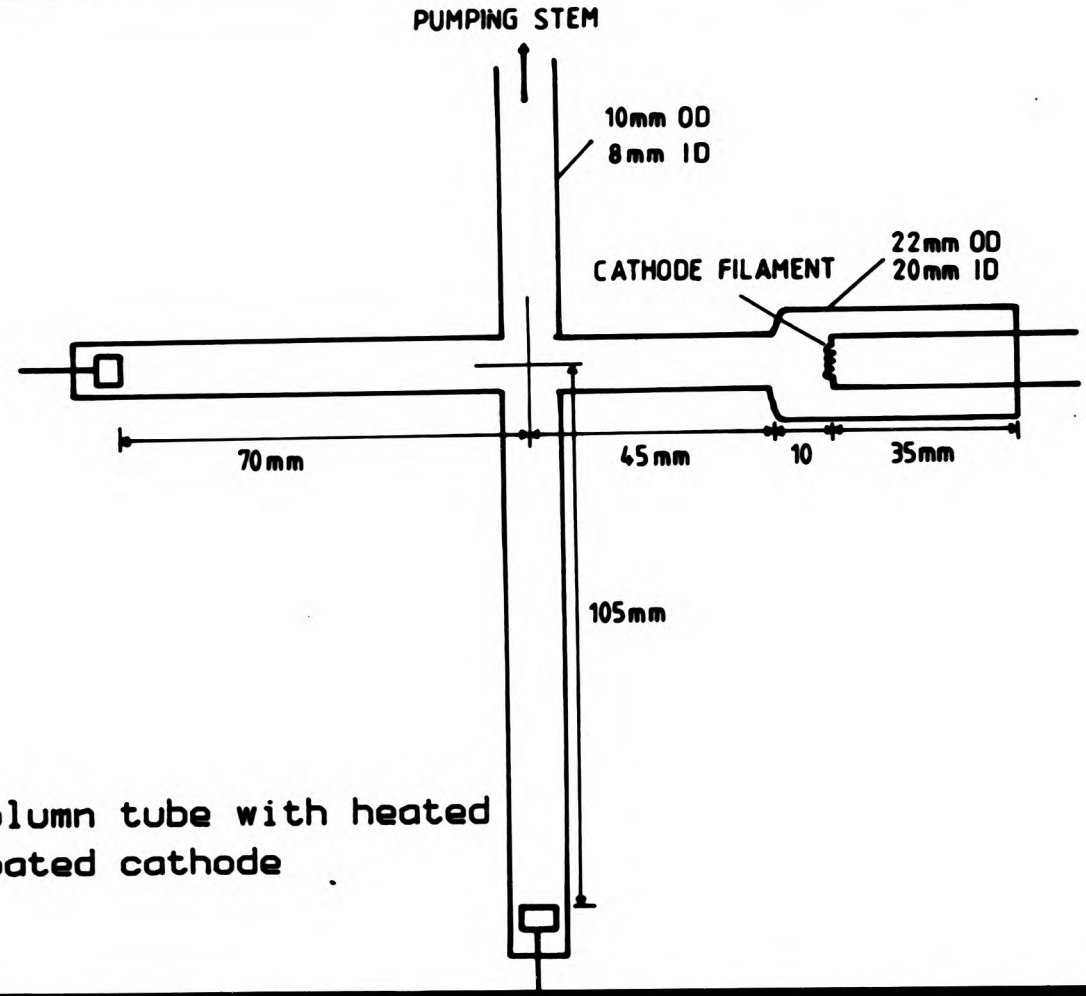

ig. 10 Column tube with heated coated cathode

The filament voltage, pressure rise, time taken to reach the background pressure and temperature estimation for the coated-filament activation for this column tube are given in table 1.

Later on an ion gauge was mounted to the vacuum system near the new discharge tube, (Fig.11) with a hot coated filament cathode, which was connected to the vacuum system via a glass-to-metal seal, and a very clean discharge was obtained.

A SAES getter (type ST 171/HI/7-6/150° c) had been placed in this tube; every time the getter was activated, the filament cathode was kept hot during the activation to stop impurities landing on the filament and damaging its coating. An anode plate was included in the discharge tube near the coated cathode to check the diode characteristics of the cathode.

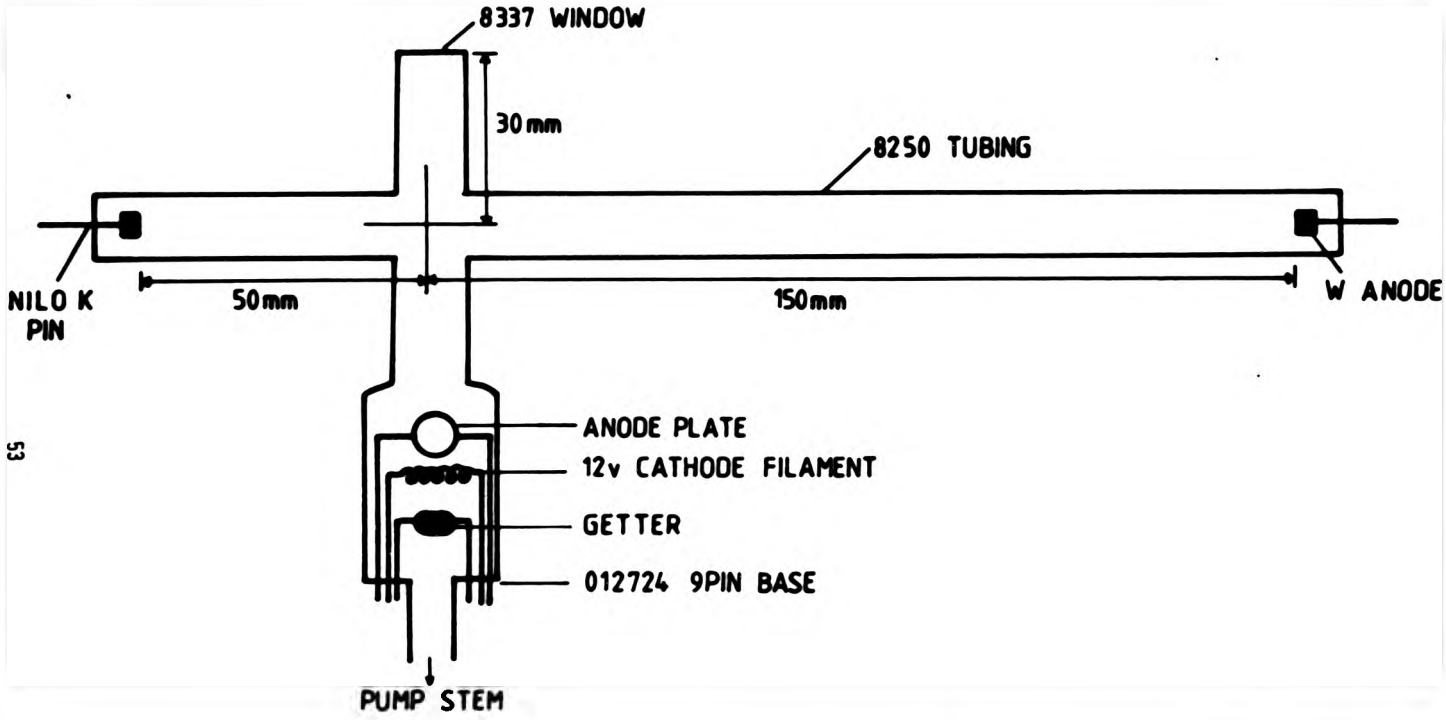

Fig. 11 new design discharge tube with hot coated cathode

Table 3 shows the activation process data of the first discharge tube with coated cathode.

FILAMENT VOLTAGE (v)	BACKGROUND PRESSURE (mbar)	PRESSURE RISE (mbar)	TIME (MIN)	TEMPERATURE (° c)
.5	$8x10^{-7}$	$2x10^{-5}$	2	
1	$6x10^{-6}$	$4x10^{-5}$	6	
1.5	$1x10^{-6}$	$2x10^{-4}$	13	
2	$4x10^{-5}$	$7x10^{-4}$	21	
2.5	$7x10^{-5}$	$8x10^{-4}$	28	
3	$6x10^{-5}$	$4x10^{-4}$	31	
3.5	$7x10^{-5}$	$5x10^{-4}$	28	
4	$8x10^{-5}$	$4x10^{-4}$	30	
4.5	$1x10^{-4}$	$8x10^{-4}$	25	
5	$1x10^{-4}$	$6x10^{-4}$	32	720
5.5	$3x10^{-4}$	$7x10^{-4}$	41	
6	$4x10^{-4}$	$8x10^{-4}$	35	760
6.5	$7x10^{-4}$	$8x10^{-4}$	20	
7	$3x10^{-4}$	$7x10^{-4}$	12	830
7.5	$3x10^{-4}$	$5x10^{-4}$	7	
8	$6x10^{-5}$	$2x10^{-4}$	2	910

Table 3.

Activation process data for the coated cathode in the new discharge tube is given in table 4.

FILAMENT VOLTAGE (V)	BACKGROUND PRESSURE (mbar)	PRESSURE RISE (mbar)	TIME (MIN)	TEMPERATURE (^{o} c)
.5	$2x10^{-7}$	$1x10^{-6}$	1	
1	$1x10^{-6}$	$1x10^{-5}$	5	
1.5	$2x10^{-6}$	$5x10^{-5}$	15	
2	$3x10^{-6}$	$9x10^{-5}$	20	
2.5	$1x10^{-5}$	$2x10^{-4}$	30	
3	$1x10^{-5}$	$3x10^{-4}$	30	
3.5	$1x10^{-5}$	$5x10^{-4}$	41	
4	$1x10^{-5}$	$7x10^{-4}$	47	
4.5	$2x10^{-5}$	$6x10^{-4}$	40	
5	$2x10^{-5}$	$6x10^{-4}$	45	710
5.5	$1x10^{-5}$	$1.5x10^{-4}$	48	
6	$1x10^{-5}$	$6x10^{-5}$	35	780
6.5	$1x10^{-5}$	$5x10^{-5}$	21	
7	$2x10^{-5}$	$6x10^{-5}$	16	850
7.5	$9x10^{-6}$	$2.6x10^{-5}$	8	
8	$9x10^{-6}$	$2x10^{-5}$	5	930
8.5	$8x10^{-6}$	$1.6x10^{-5}$	2	
9	$8x10^{-6}$	$1.2x10^{-5}$	2	980

Table 4.

By comparing table 3 and 4 it can be seen a lower background pressures and longer period of time to reach these background pressure resulted in a satisfactory activation process, and the discharge tube was used without having any problem due to poisoning of the hot coated filament cathode.

5.5 : TUBE WITH HOLLOW CATHODE:

Another way to overcome the problems due to heavy sputtering from the plane cathode was by using a discharge column tube with a hollow cathode. A positive column discharge tube with hollow cathode and two anodes was designed in such way that two positive column arms had different length (5 and 10 cm).

Since a lower voltage (compared with cold plane cathode) was required when a hollow cathode is employed in a discharge tube enabled an estimation of the electric field strength (gradient) along the positive column to be carried out by switching from one anode to another under identical discharge conditions. A diagram of the discharge tube with hollow cathode is given in Fig.12.

Sputtering from the hollow cathode was far less than from the plane cathode, and if there was any sputtering it was inside the hollow cathode itself, hardly any deposition of the cathode material was found on the discharge tube envelope. Having less sputtering from the hollow cathode allowed investigation on the electrical and optical characteristics of the positive column to be carried out at lower pressures and higher currents than in the case of a plane cathode.

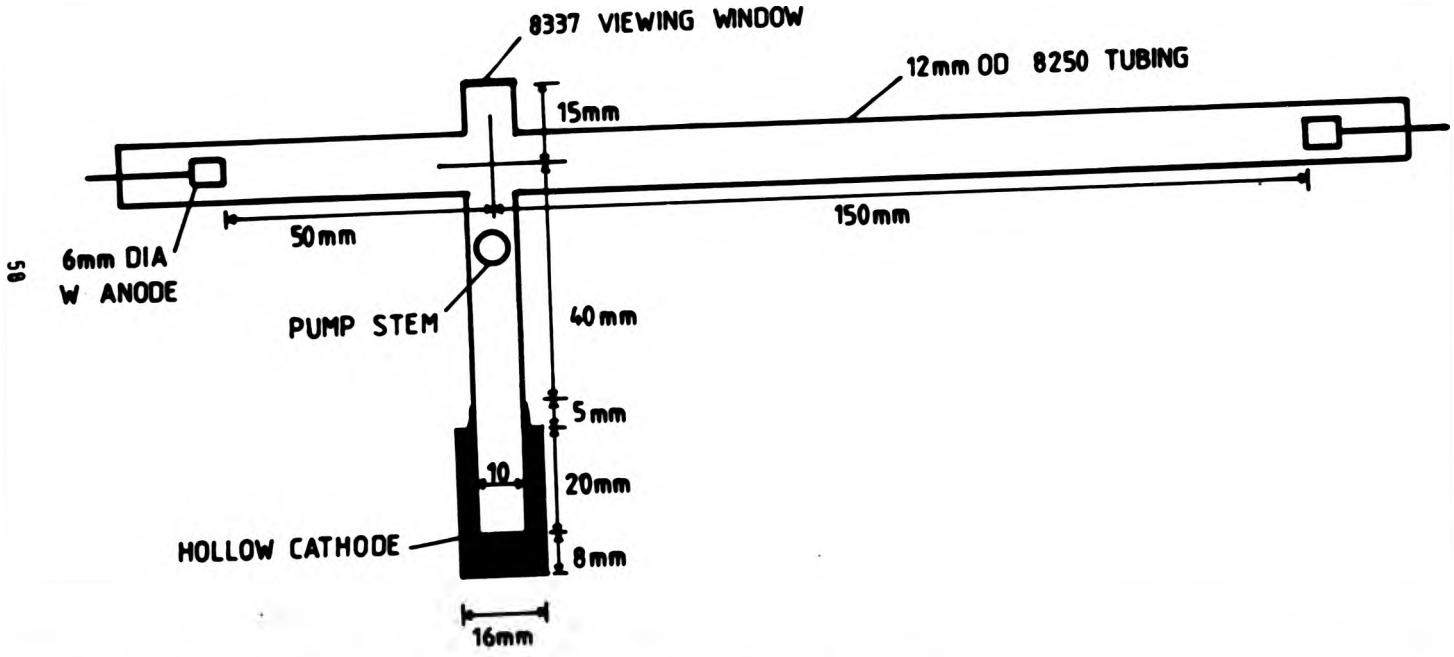

Fig. 12 Column tube with hollow cathode

5.6 : SUMMARY OF COMPARISON OF THE CATHODE SYSTEMS:

The drawbacks of the cold plane cathode were due to:

i) using a plane cathode in a discharge tube required high tube voltage (500 - 2000 volts).

ii) limitation of the current and pressure range due to heavy sputtering from the plane cathode, which changes the electrical and spectral characteristics of the discharge.

iii) because of sputtering, after one or two sets of measurements depending on the pressure and current range, the discharge tube had to be changed, which would be expensive, and letting the vacuum system up to atmospheric pressure, which would mean baking the vacuum system and could cause delay for continuous study.

The advantages of the column tube with hollow cathode were:

i) Less maintaining tube voltage was required, so this allowed on estimate of the electric field along the positive column to be made using a tube with two positive column arms, since small changes on the tube voltage could be noticeable.

ii) Much less sputtering was produced compared with plane cathode under the same conditions, therefore a wider range of pressure and current could be used.

iii) Using a hollow cathode in a discharge tube was more economical than plane cathode, since changing the tube was not required so often.

The drawback of using a hollow cathode was that, since the negative glow was present in the discharge, one could not carry out the measurements for end on viewing observation of the positive column.

By employing a hot coated filament cathode in the discharge tube the problems caused by sputtering were solved, and a very low potential was required compared with hollow and plane cathode to maintain the discharge. This made estimation of the field much easier, and more accurate.

The absence of the negative glow (with right filament temperature) allowed the measurements to be carried out for the positive column with end on viewing. The disadvantage of using a hot coated cathode was that, once the cathode filament has been activated, it gets chemically poisoned if exposed to air, so if changing the discharge tube was required for any reason, the column tube had to be sealed using a tap, which could be expensive. If it is sealed for a long period of time, due to a gradual leak from the tap the coated filament cathode would be poisoned and not reusable.

Various other tubes with different column lengths, and diameters have been tested in this work to find the most

convenient ones to work with. The common problems with some of these discharge tubes were as follows:

i) if the discharge tube was wide (20 mm), a constricted discharge was observed, and discharge was found to be unstable occasionally (specially in low current range and higher pressure).

ii) if the column tube was too narrow (3 mm), sputtering from the cathode was heavy (if a plane cathode was used).

For radial intensity measurements, end viewing of the positive column was used. A discharge tube was designed with hollow cathode, and a mesh anode (Ni), see Fig. 13. This tube also was employed for direct absorption measurements, and investigation of radial distribution of the population densities of the neon metastable atoms.

Figs. 14 and 15 show the various discharge tubes which have been tested and used for side viewing investigation of the positive column.

The majority of the results obtained in this research, were made with discharge tubes having hollow or hot coated cathode, with 10 mm bore diameter, because of the above mentioned reasons.

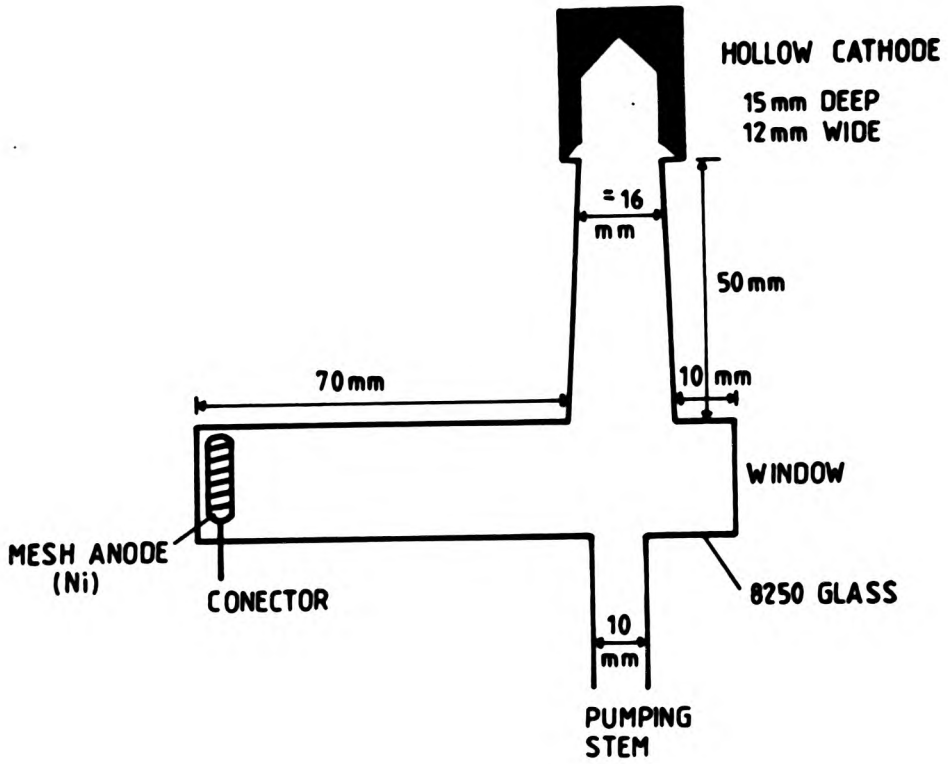

Fig. 13 Positive column tube with mesh anode

Fig. 14 Two of the tested discharge tube diagrams

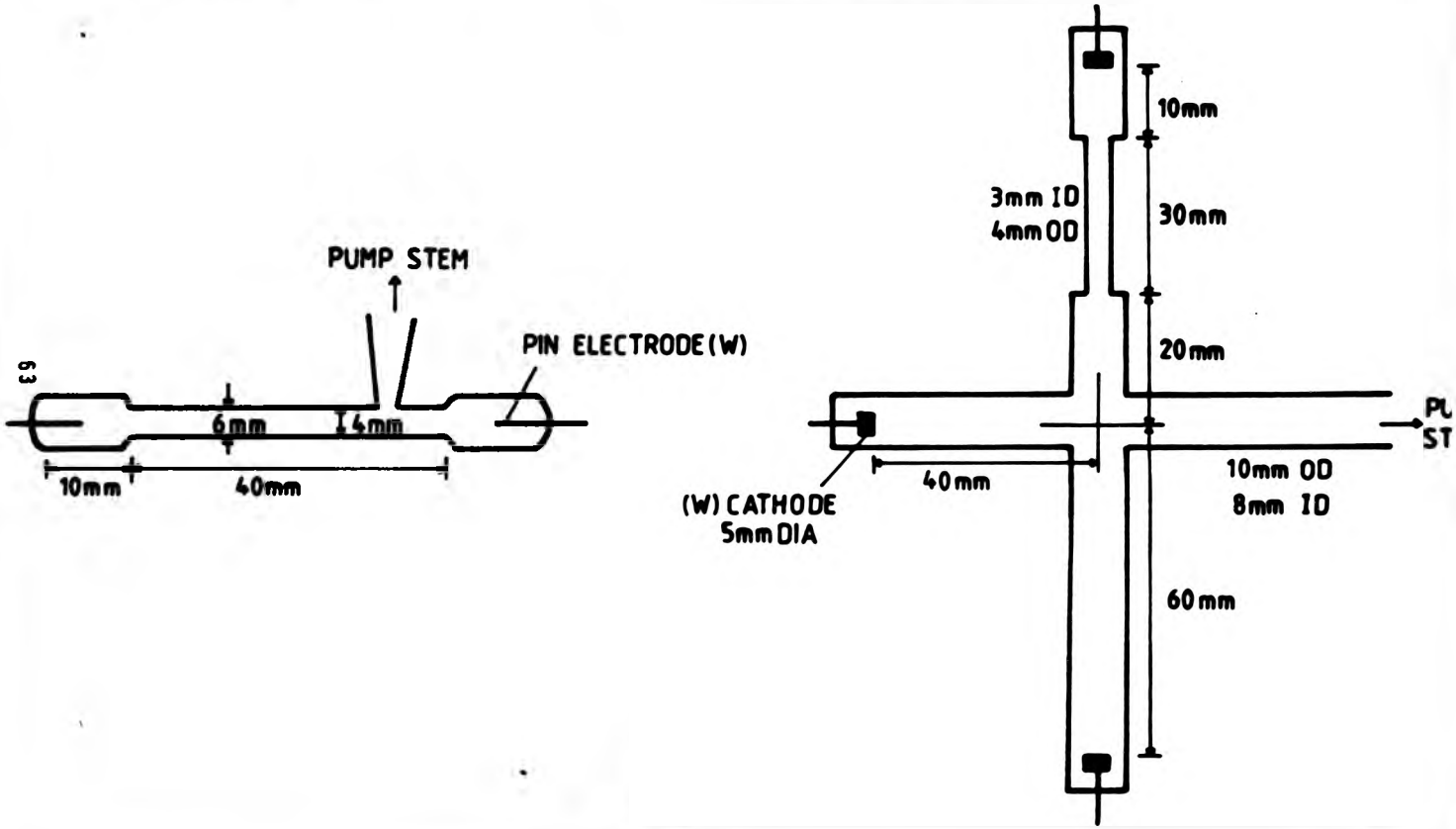

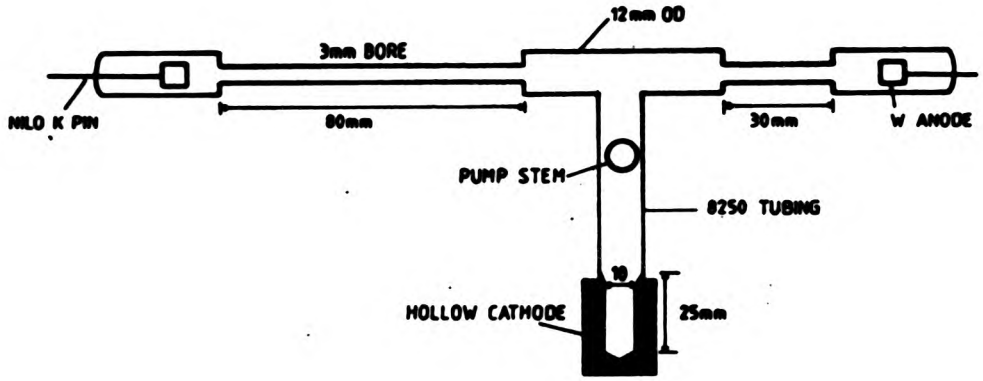

Fig. 15 Diagram of two tested discharge tubes

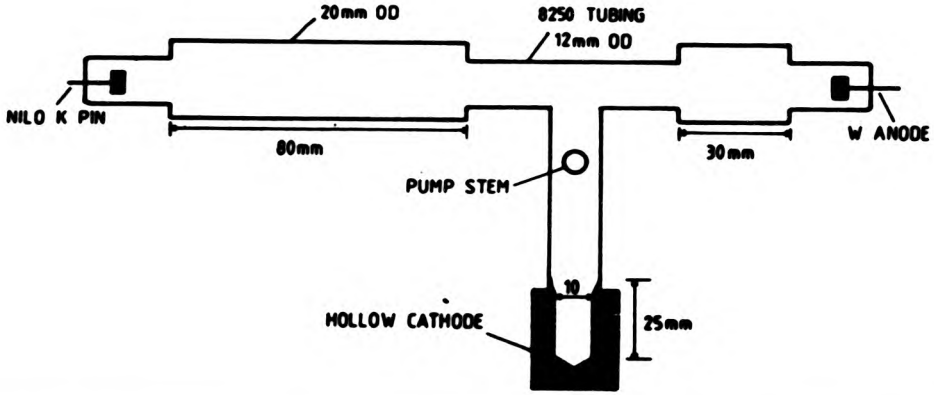

CHAPTER (6) EXPERIMENTAL METHODS

6.1 : GENERAL:

The removal of contamination from the vacuum system by baking and gettering (inside the discharge tube) were described in sections 3.4 and 5.4 respectively. After isolation of the experimental tube from the pumping system, the necessary amount of filling gas (neon or argon) to the required pressure was introduced to the system. To run the discharge a KSM (type HI 2200) current-controlled stabilised power supply unit (p.s.u) was employed.
The p.s.u could provide a maximum current of 200 mA and maximum voltage of 2.0 KV. The minimum controlled current that the power supply could stably supply was about 0.3 mA depending on load conditions. A load resistance, 10 or 20 K depending on maximum current was included in the circuit to improve stability at low currents which were used. The cathode was earthed and, to monitor the tube's voltage and the discharge current safely on the digital multimeter (DMM) and the recorders, a circuit was built, see Figs.16 and 17.

When a discharge was struck, a series of photographic plates were taken on the medium quartz spectrograph under various discharge conditions (pressure and current) from side and end viewing of the positive column discharge to identify spectral components of the discharge.

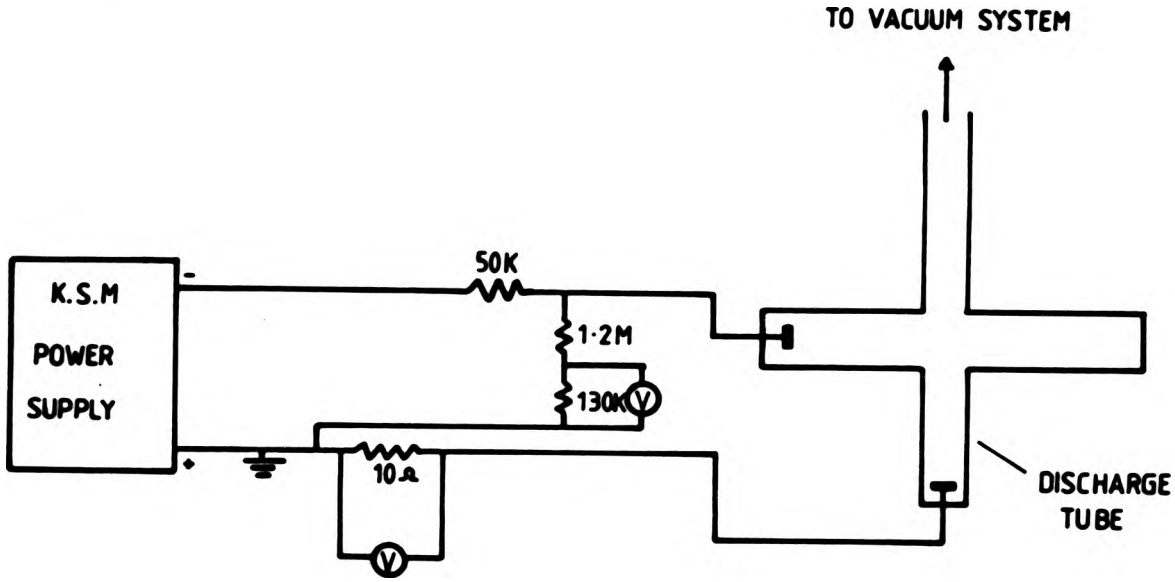

Fig. 16 Circuit diagram for running discharge with cold plane cathode

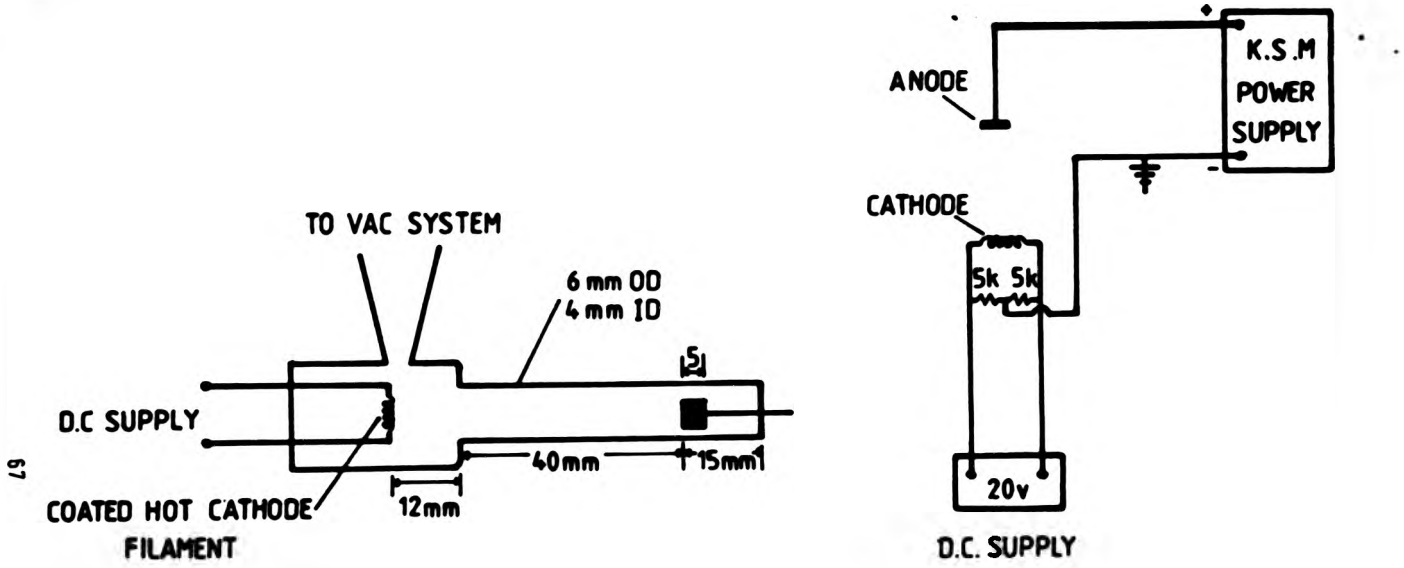

Fig. 17 Circuit diagram for running discharge with heated coated cathode

Occasionally CO and CO^+ bands were observed, and their intensity increased with discharge operation time, indicating some outgassing. The discharge colour then became more pinkish rather than red (in neon), and maintenance potential increased at given current and pressure with time. Fresh gas was introduced to the discharge tube, after the dirty gas had been pumped out, and the molecular bands had disappeared, and the tube voltage decreased under similar conditions (pressure, current) compared with the impure gas situation.

Since a large volume of gas inside the system was used, the gas temperature would be unchanged over the measurement period. Results were not reproducible until the discharge had warmed up and stablised.

6.2 : VOLTAGE-CURRENT (v-i) MONITORING:

It was necessary to determine whether the discharge electrical characteristics were stable and reproducible over the current range studied. Any large change in the electrical characteristics during the optical measurements would have affected the electron and ion distribution within the discharge and the spectral line intensities.

It was also found that whilst commissioning the vacuum system, the voltage-current curves changed, when the system became contaminated. Therefore monitoring the discharge

electrical behaviour was required during the spectral measurements. The voltage did not change for the same discharge conditions over the measurement period after the vacuum system was thoroughly degassed, indicating a reproducible characteristic within the experimental accuracy of about + 3 volts.

The measurements were carried out from a minimum current of 1.0 up to 30 mA and occasionally to 40 mA. A smaller minimum current (less than 1.0 mA) than the controlled current power supply could stably supply would have been attainable by putting a ballast resistance in the circuit, but due to more constriction of the positive column discharge at very low current, specially at high pressure, it was justified to carry out the measurements from 1.0 mA current.

Voltage-current measurements were made with increasing current by steps of 2 or 3mA, and voltage was recorded from a digital voltmeter for each current step. The results were checked by decreasing current through the same current steps. Occasionally a hysteresis effect was noticed, see Fig.18.

Voltage versus current curves were checked with time to ascertain their reproducibility, and to show any changes in gas purity.

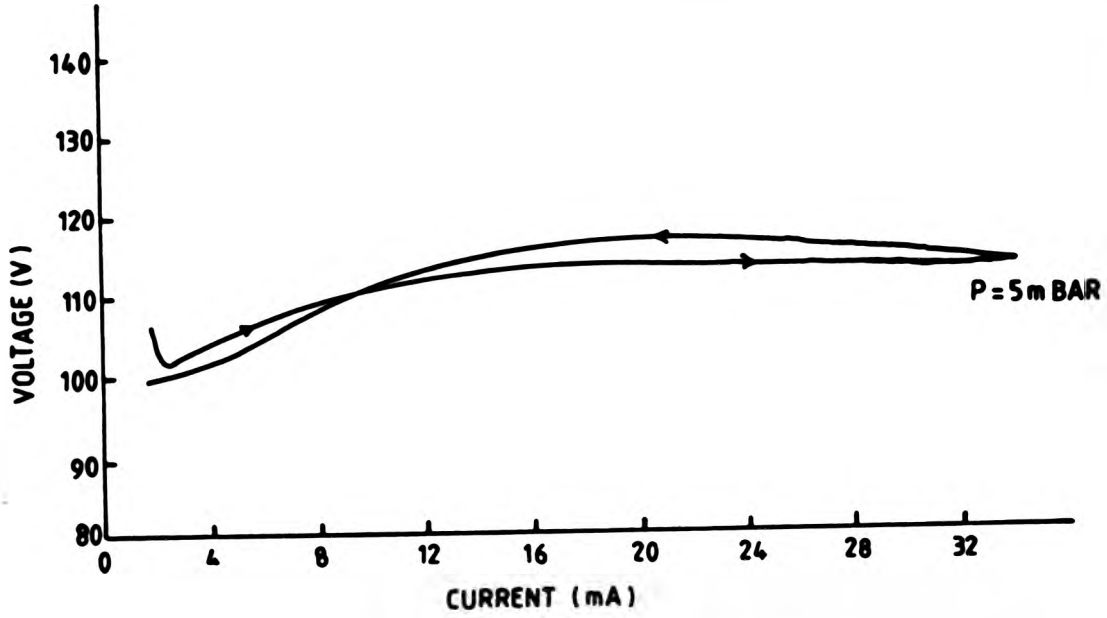

Fig. 18 Showing hysteresis effect on v-i characteristics

6.3 : INTENSITY-CURRENT (I-i) MEASUREMENTS:

There are three main methods of describing intensity against current relationships:

i) Axial intensity versus current.

ii) Intensity of a diametrical slice against current.

iii) Total integrated intensity versus current.

If one is interested in the explanation of excitation processes at the centre of the discharge, by interpretation of the intensity-current relations, then one is justified to choose method (i) as only processes occurring at the discharge axis will determine the light intensity there. On the other hand,if one is concerned with investigation of the balance of processes within the plasma cross-section as a whole then method (iii) is appropriate.

In this work investigation of the intensity-current characteristics were carried out by using method (i). The centre of the discharge was focused on a aperture of 1.5 mm width and the image was focused to the entrance slit (centre) of the monochromator. The optical arrangement for I-i experiments is shown in Fig.4. (The Fabry-Perot housing was removed).

Constricted discharges were noted, specially in the wider column tube, and for this reason, using the centre of the plasma was a more convenient way for I-i measurements to be

carried out. Constriction of the positive column was more noticable when argon or argon-neon mixtures were used.

Occasionally striations were present at the beginning of the positive column near the cathode, and varying the pressure or the current caused displacement of these striations. The uniform section of the positive column (near anode area) was chosen for the investigation of the I-i experiments when side on viewing of the positive column was used.

When I-i relationships were studied in the case where argon-neon mixtures were used, once again the area near the anode of the tube was employed, since it was found that the intensity of a given spectral line under the same conditions varied along the positive column length, due to the separation of the gases or so called "cataphoresis". This matter will be discussed in more detail in the results and discussion chapter.

The current was stepped up by 2 or 3 mA, and the signals were recorded on the chart recorder, and the voltage for every step was noted.

For radial distribution of the light intensity measurements two adjustable plane mirrors were employed, and end viewing of the positive column was used. Fig.19.

6.4 : FABRY-PEROT INTERFEROMETRY (F.P.I.)

Scans were carried out to optimise adjustment of the Etalon

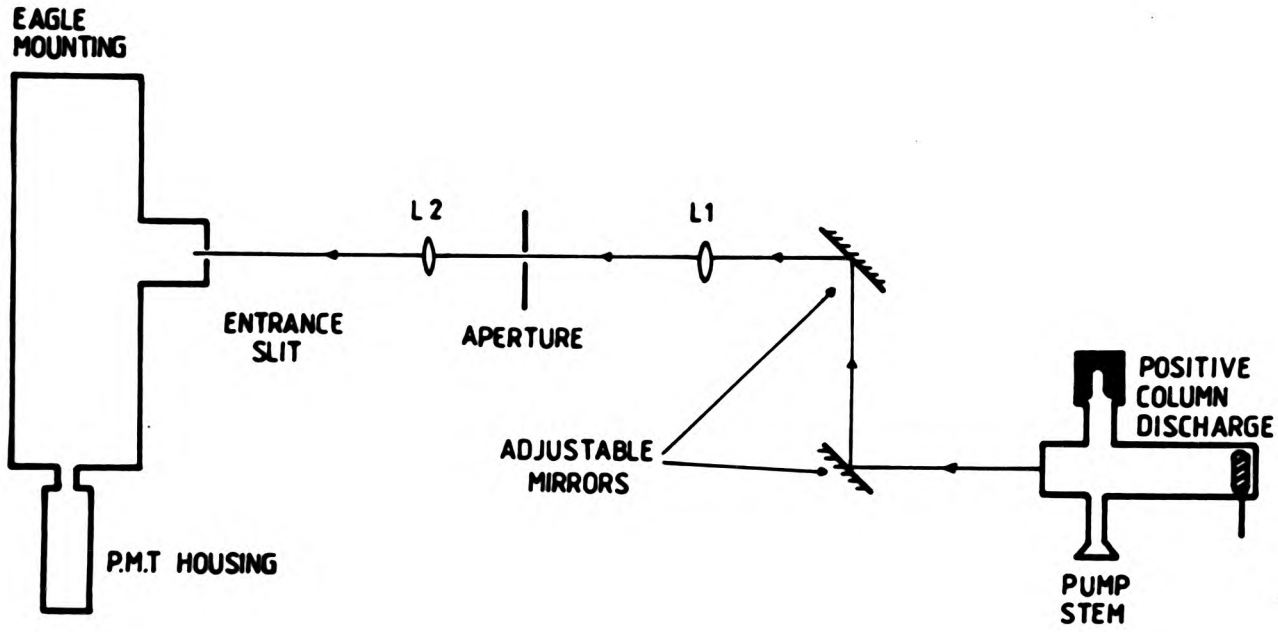

Fig. 19 Optical arrangement for radial intensity measurements

and to determine the instrument function and finesse. Fine adjustment of the interferometer could be done either by scanning a spectral line which is structured and adjusting for maximum resolution, or by scanning a laser line and adjusting for maximum peak height.

To record the instrument function of the Fabry-Perot interferometer experimentally, a light source producing a very narrow spectral line was required; in practice a spectral line of width much less than the instrument width is sufficient (a diffused laser beam).

6.4.1 : <u>He-Ne LASER SCANS:</u>

All the interferometry investigations in this research were carried out in the red region of the spectrum, and for this reason a He-Ne laser was used for the determination of the instrument function.

The F.P.I. instrument function and its width (usually expressed in terms of finesse $F = \frac{\Delta\delta}{\delta\delta}$) are particularly sensitive to error in the orientation and parallelism of the Etalon plates.

The laser beam was diffused with a ground glass screen, and the light was focused on an aperture, ensuring that the Etalon area was fully illuminated. The laser emission profile (λ = 633 nm) was repeatedly recorded, and Etalon orientation and parallelism were adjusted for minimum width and maximum peak height of the profile, Fig.20. A finesse

of $\simeq$ 30 was obtained after final adjustments.

The Fabry-Perot interferometer which was used in this work has been used by previous workers in this laboratory (A.Reed, C. Light). The F.P.I. had been adjusted by C. Light (19) using a mode-stablised laser just before this present research was started using Fabry-Perot interferometer.

The reason for using a mode-stablised laser was that ordinary lasers usually are unstable, commonly known as 'mode hopping'. This arises from temperature drift of the laser cavity, and causes changes in the amplifying mode, see Fig. 21.

The adjustment of the F.P.I was checked every time measurements were made. Occasionally readjustment was required, due to variation of room temperature, and this was done by using three screws outside the F.P.I. housing.

6.4.2 : EMISSION MEASUREMENTS

The emission profile studies were carried out for selected NeI and ArI lines (with the metastable, and non-metastable lower level), by means of the pressure scanned Fabry-Perot interferometer. The variation of these profiles with respect to pressure, current, different cross-section and orientation of the discharge tube (side, end on viewing) were investigated.

The Etalon was fully illuminated, after light from the

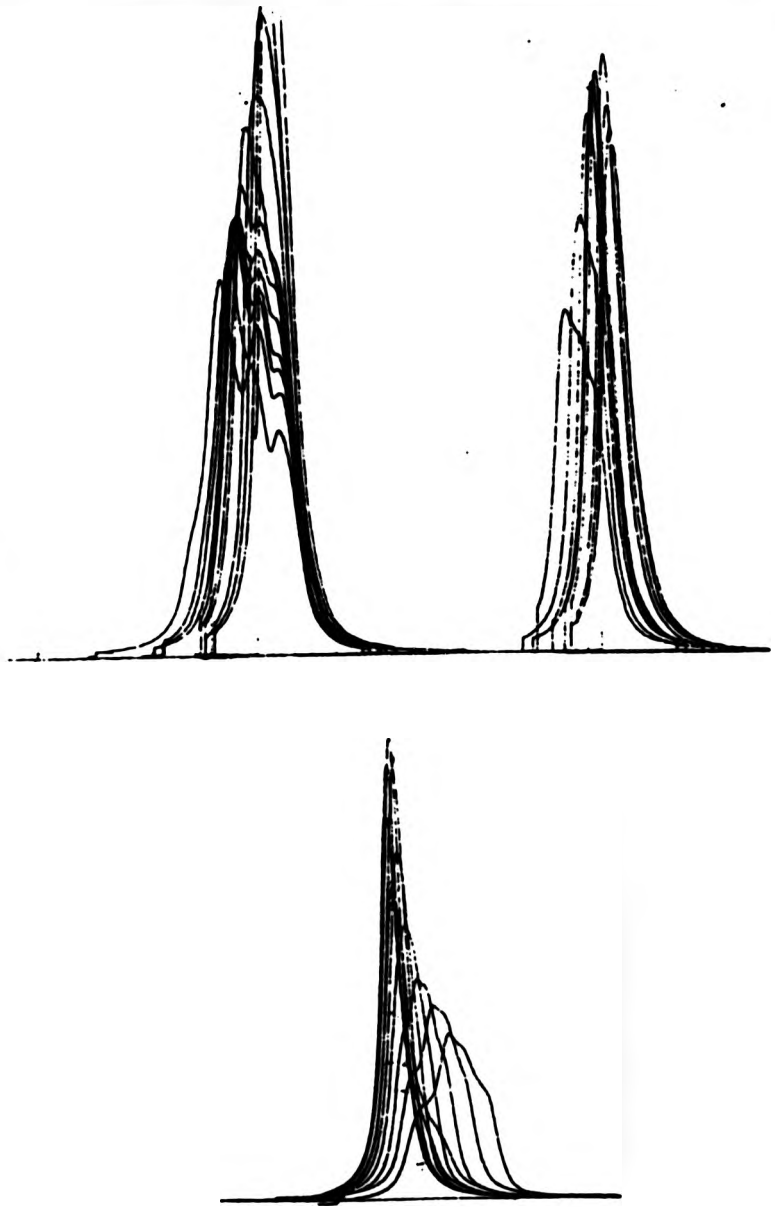

Fig. 20 Adjustments of the F.P.I. using He-Ne laser

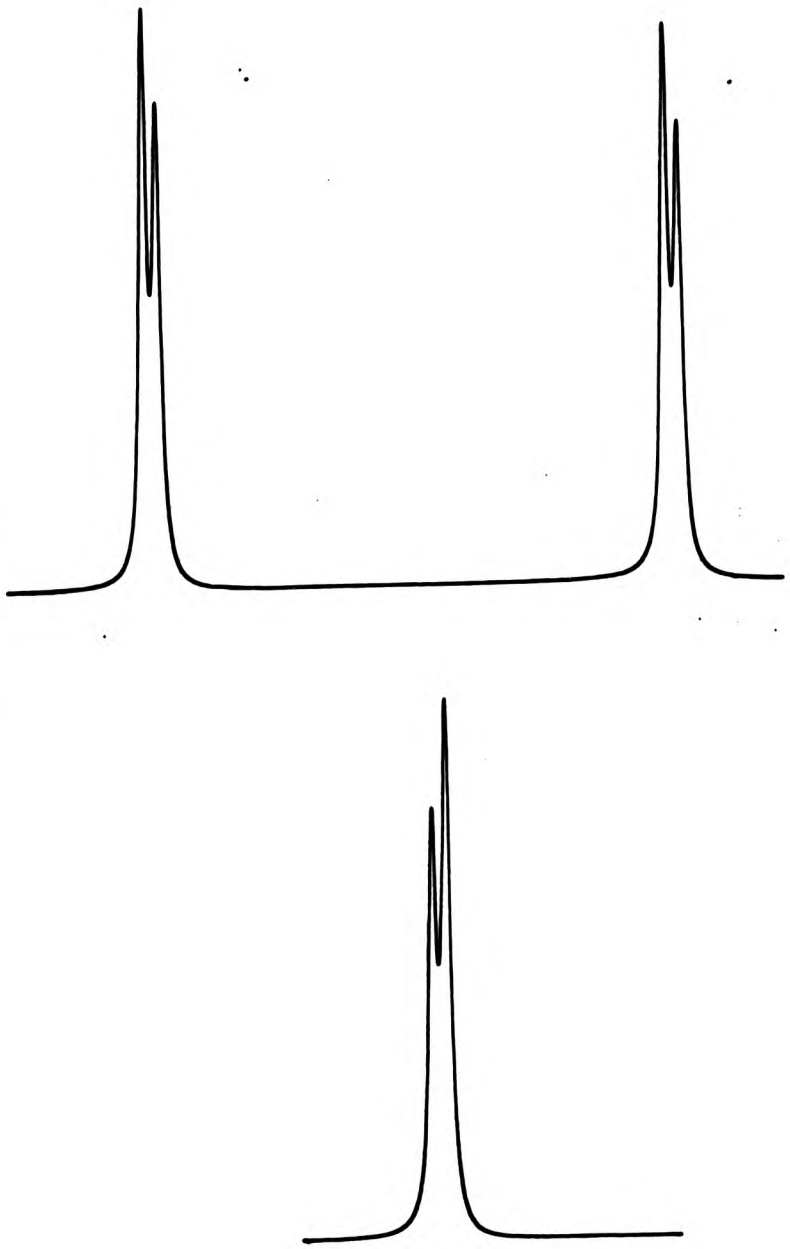

Fig. 21 Showing the effects of 'mode hopping' of He-Ne laser.

positive column was passed through a small aperture. The profiles were directly recorded on the x-y recorder, and amplification was adjusted for each wavelength.

Initially a few commercial hollow cathode lamps filled with neon or argon with different pressure (made by Cathodeon Ltd) were used. Side view and end on view of the positive column were employed later on, and great differences were obtained in those results, which will be discussed fully in chapter 8.

6.4.3 : ABSORPTION MEASUREMENTS

In order to measure the number density of the neon metastable atoms within the positive column discharge, under various conditions, direct absorption measurements were carried out.

A neon, microwave excited, electrodeless discharge tube (EDL) was used as the primary source for absorption measurements. The EDL had a fused silica envelope containing neon or argon at 1 mbar, and was inserted in a tunable microwave cavity which was water cooled and driven by a microwave generator (EMS Microtron 200), via a reflected power meter (EMS Mark I), and coaxial cable inter connection.

The EDL was run for at least 30 minutes before measurements were taken, to allow conditions to stablize. Microwave

generator power was set at 50 W and cavity tuning screws were adjusted for minimum reflected power 15W. The probe beam was modulated at 33 Hz by a chopper which also provided a reference signal for the phase sensitive amplifier used to amplify the photomultiplier tube output. This frequency was chosen to eliminate harmonic interference from the mains.

Fig. 8 shows the optical arrangements used for the direct absorption measurements with Fabry-Perot interferometer and a simplified circuitry

Light emitted from the EDL was focused as a near point source at the centre of the positive column tube. NeI spectral lines were isolated by the monochromator, and the profiles were recorded by means of the pressure scanning Fabry-Perot interferometer, with the positive column discharge tube off (current i = o), then with the discharge running at current values of 1, 3, 5, 10, 20, 30 mA, then decreasing through the same current steps, and finally with the discharge tube off again. In this way reproducibility of the results could be checked. The microwave power was kept at a constant value (50 watts input power) throughout the measurements.

To investigate the radial distribution of the neon metastable atoms two plates with ten very close holes (1.5 mm diameter) along their axis were designed, and one of the plates was placed on the back of the discharge tube and

one in front of viewing window of the positive column tube, see Fig.22. This was done to ensure that a parallel light beam travelled through the discharge tube when the entire vacuum system was raised or lowered by adjusting three jacks on which the vacuum system was mounted. By having those two plates one could see if the system was tilted during adjustment of the jacks.

The light beam was sent through the first hole of the first plate behind the anode window (very close to the tube), and passed through the mesh anode and came out of the first hole of the second plate, in front of the viewing window. The image was focused on the pinhole aperture by L3. The Fabry-Perot plate was illuminated by parallel light and by use of lens L5, the image was focused on the centre of the entrance slit of the monochromator. The optical arrangement for the investigation of the radial distribution of the metastable atoms is shown in Fig.22.

Investigation of the radial distribution of the neon metastable atoms could not be carried out for the horizontal axis of the discharge, since there was a bent positive column, and for this reason these measurements were made on the vertical axis of the discharge tube. The entire vacuum system was mounted on three jacks, which could be easily and uniformally adjusted for height.

6.5 : ERRORS:

All the Fabry-Perot scans are accurate to the same error

limit. The results were recorded directly on the graph paper with the x-y recorder.

Adjustments were repeatedly carried out and reproducible results with similar order of accuracy as that to which the graphs could be read i.e. 2-3% were obtained.

The error for the voltage-current results was about 2%, voltage and current being monitored by digital voltmeters. The intensity results were less reproducible, having errors of 4-5% and in the case of weak spectral lines (e.g. 363.3 nm), the accuracy of the intensity measurements was 7-8%.

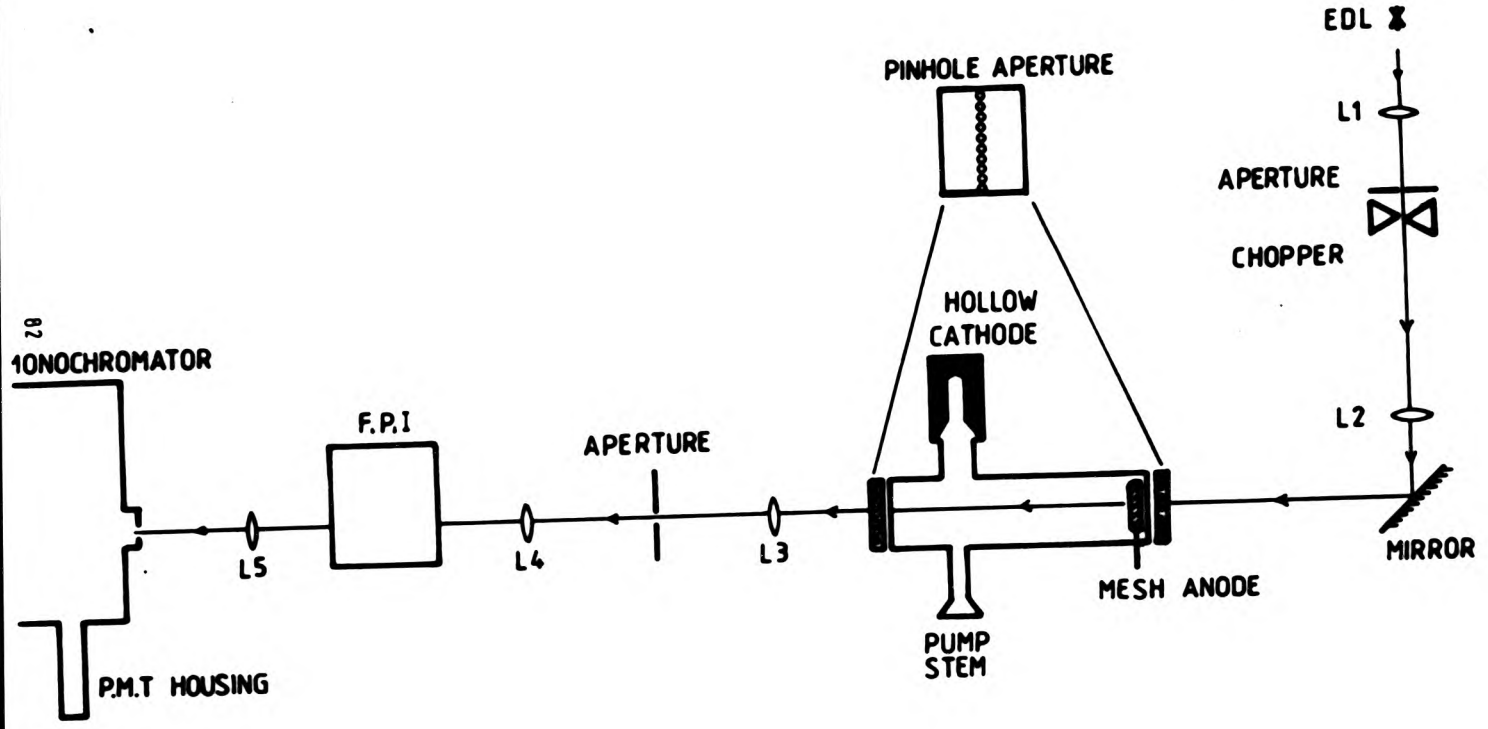

Fig. 22 Optical arrangements for investigation of radial distribution of the metastable atoms

CHAPTER (7) VOLTAGE-CURRENT RESULTS

7.1 : GENERAL:

The electrical characteristics of the positive column discharge were studied by monitoring the tube voltage and the discharge current over a wide range of gas pressure (0.1 to 15 mbar) for each experimental discharge tube.

The voltage-current (v-i) results have been divided in three sections, dealing with cold plane cathode, hollow cathode, and hot coated filament cathode tubes. In all cases the presence of impurities caused the potential to be greater than in the pure gas situation, under identical discharge conditions; all the measurements were carried out under maximum gas purity.

Occasionally a hysteresis effect was observed for v-i curves, when the discharge current was stepped down through the same steps that the current had been increased to carry out the voltage-current measurements, see Fig.18.

The discharge voltages are similar in magnitude to those reported in the literature for like electrode systems, tube cross-section, and pressure.

7.2 : VOLTAGE-CURRENT CHARACTERISTICS:

7.2.1 : DISCHARGE TUBE WITH PLANE CATHODE:

Voltage-current curves for different pressures using neon

and argon as carrier gases are given in Figs. 23 and 24, respectively, for the discharge tube which is shown in Fig. 2.

An abnormal discharge was obtained in this work, since the cathode surface was fully covered by the negative glow when a positive column discharge tube with cold plane cathode was employed. As can be seen from the v-i curves, the tube voltage increases with increasing discharge current for a given pressure; this is one of the characteristics of an abnormal discharge where X/p (X is the potential gradient, and p is the pressure) is no longer optimum, and the discharge current is attended by an increase in running voltage (or an increase in current produces an increase in cathode fall) as otherwise the glow could not be maintained. The voltage against current curves for the abnormal discharge has an increasing positive slope.

The required voltage for a given current increased when the pressure diminished; this is another characteristic of an abnormal discharge. For a given gas pressure and discharge current a higher tube voltage was needed for a narrower discharge tube than for wider diameter tubes. Longer positive column length required a greater potential than short column length for sustaining the discharge for the same conditions (pressure, current, and tube cross-section).

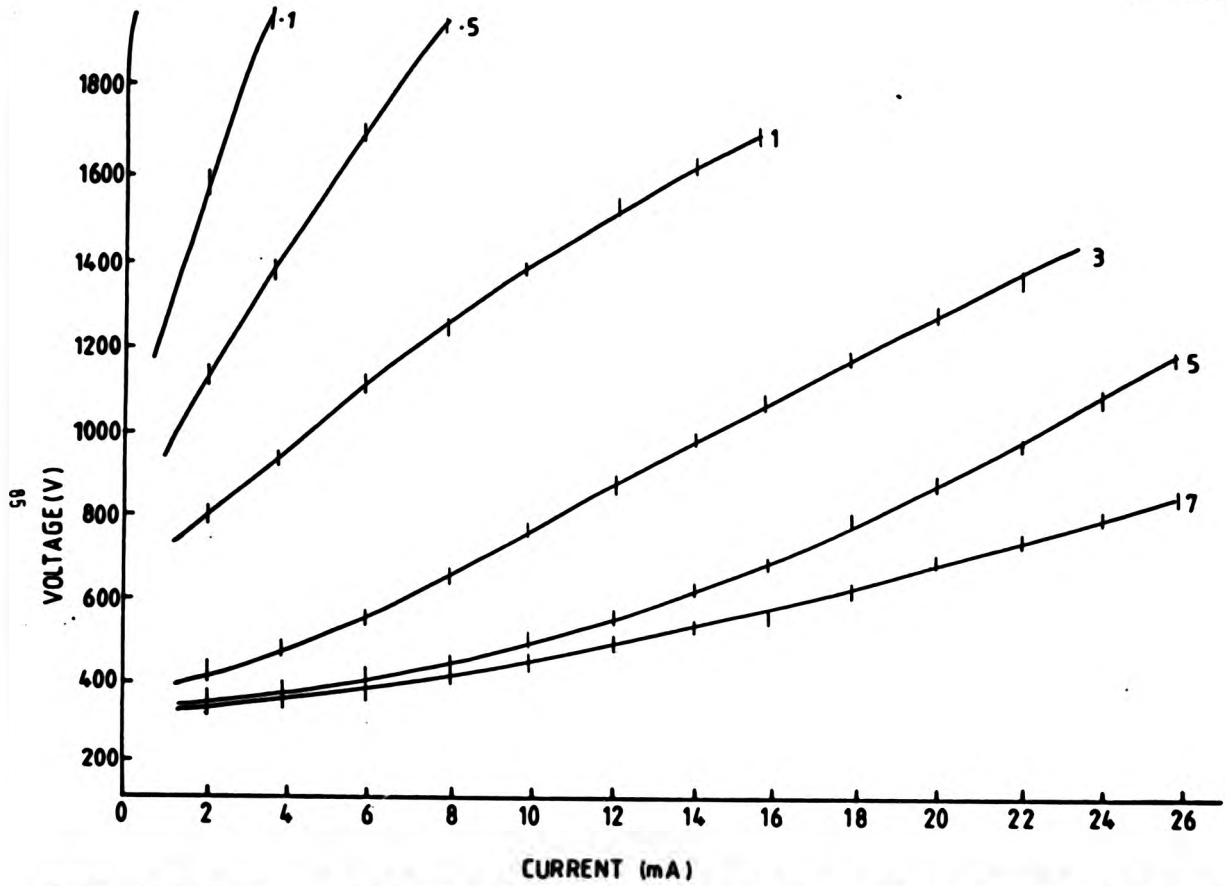

Fig. 23 V-i chracteristics for various neon pressures (mbar) of column tube with plane cathode

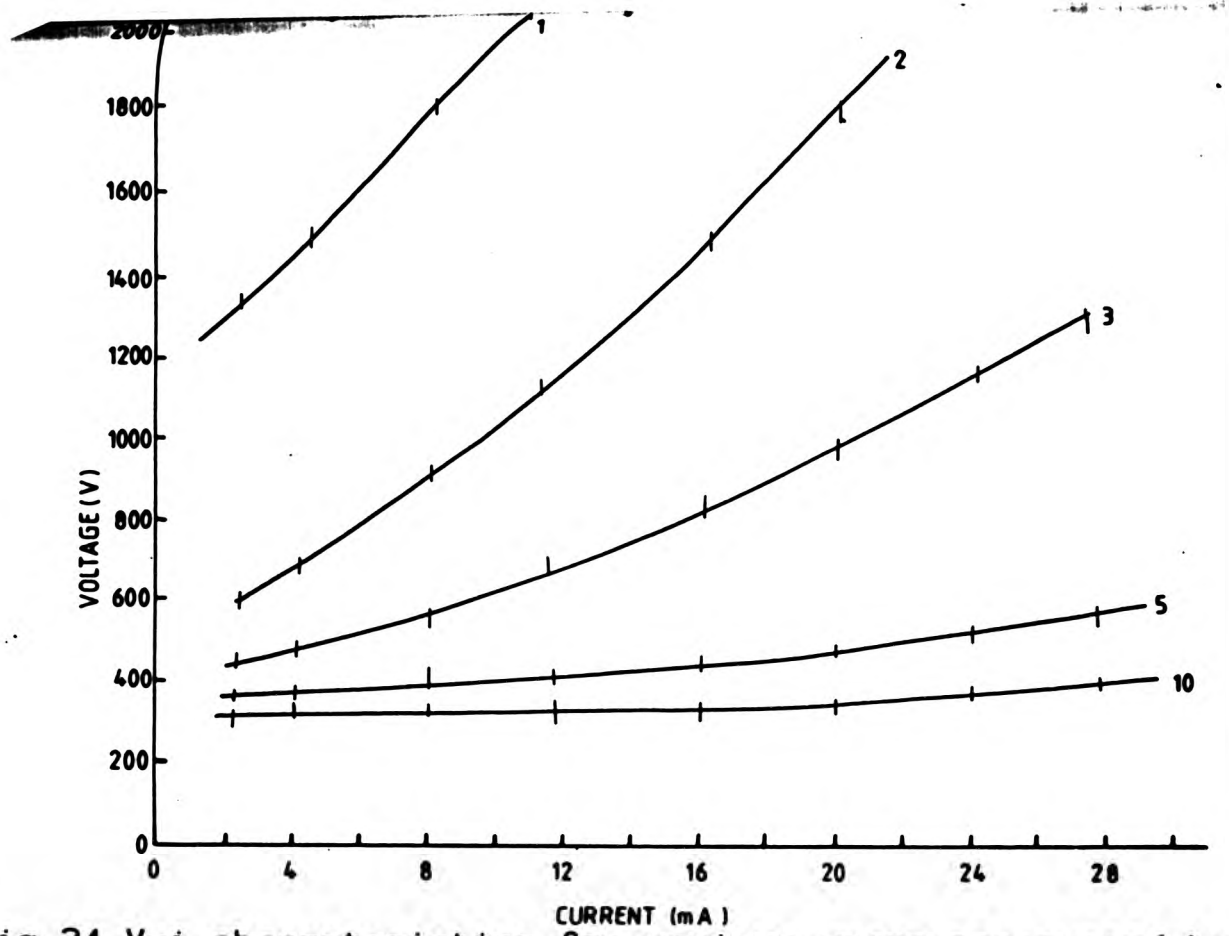

Fig. 24 V-i characteristics for various argon pressures (mbar) for column tube with cold cathode

Voltage-current curves for argon showed the same pattern as in neon discharge, except that the tube potential was higher than that for a neon discharge under identical conditions. Sputtering caused changes in the electrical characteristics of the discharge in the tubes with a plane cathode.

7.2.2 : TUBE WITH HOLLOW CATHODE

The difference in electrical potential between anode and cathode required to maintain a given discharge current is considerably lower in the case of a hollow cathode in a positive column tube than that of a plane cathode of similar dimensions.

The discharge current in low pressure inert gas discharges is largely determined by the efficiency of the processes related to releasing electrons from the cathode. The dominant processes contributing to electron release are considered to be collisions by inert gas ions accelerated by the cathode fall, and photoelectric emission caused by the ultra-violet resonance radiation from the inert gas.

In a cold plane cathode discharge, a reduction of the pressure or an increase of the discharge current resulted a shorter positive column length, and a longer negative glow, whilst in the hollow cathode case (or when the plane cathode and sputtering area round it acted together as a hollow cathode) the length of the negative glow remained

constant, and stayed within the hollow cathode. This means that the probability of either ions or photon produced by the discharge striking the cathode is much higher than if the cathode is plane. For this reason the efficiency of electron release from a hollow cathode is much higher than that from a plane cathode; more efficient electron release gives a greater current density and therefore higher current for a given potential.

Voltage-current curves for various pressures using neon and argon in the discharge tube with hollow cathode (Fig. 12) showed a flat characteristic; see Fig.25.

A "bump" at the beginning of the v-i curves at low current could be linked to widening of the discharge to fill the tube's cross-section, and a change of discharge colour.

7.2.3 : TUBE WITH HOT COATED CATHODE

v-i graphs are shown in Fig.26 for neon discharge for different gas pressures in a discharge tube with a hot coated filament cathode which was shown in Fig.11.

A much lower running voltage was required for similar conditions (pressure, current, and discharge tube diameter) compared with the tube having either plane or hollow cathode. The main factor in the hot coated cathode case was the correct filament voltage (right temperature).
With a low filament voltage, it was observed that the

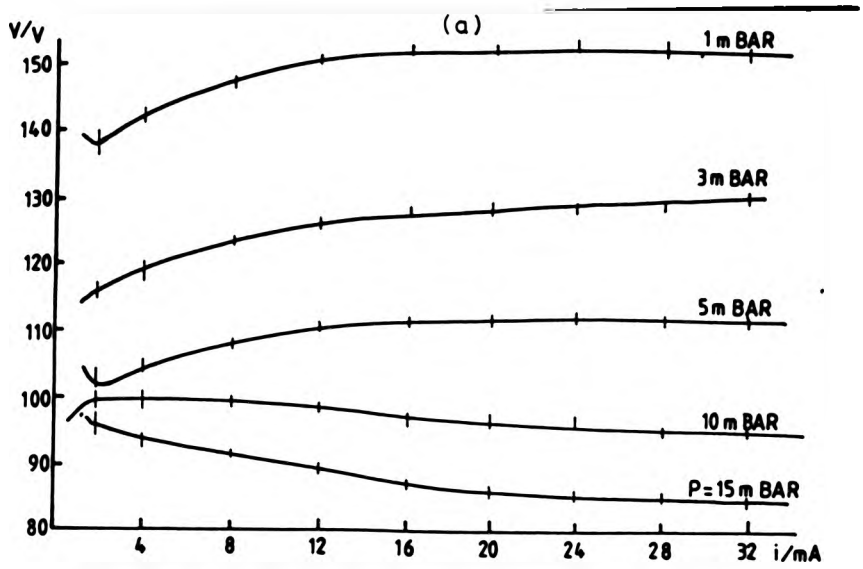

Fig. 25 V-i characteristics for tube with hollow cathode (a) in neon (b) in argon

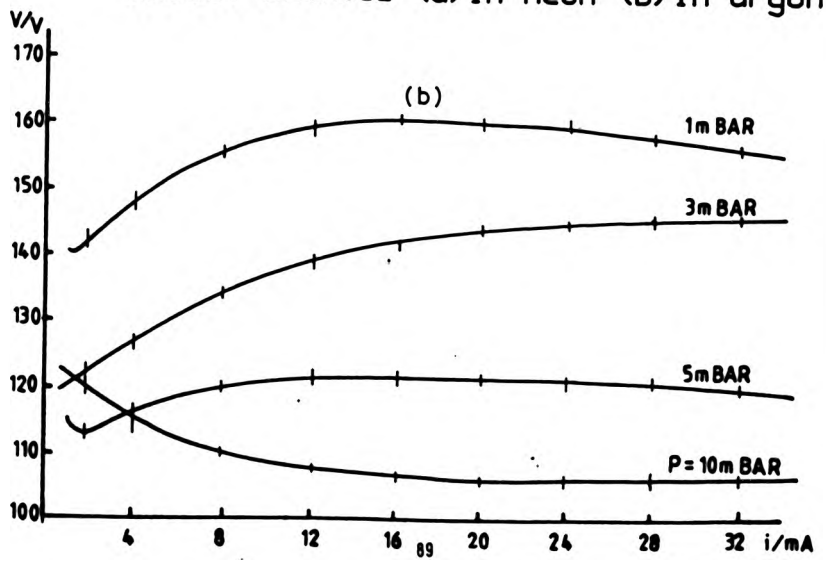

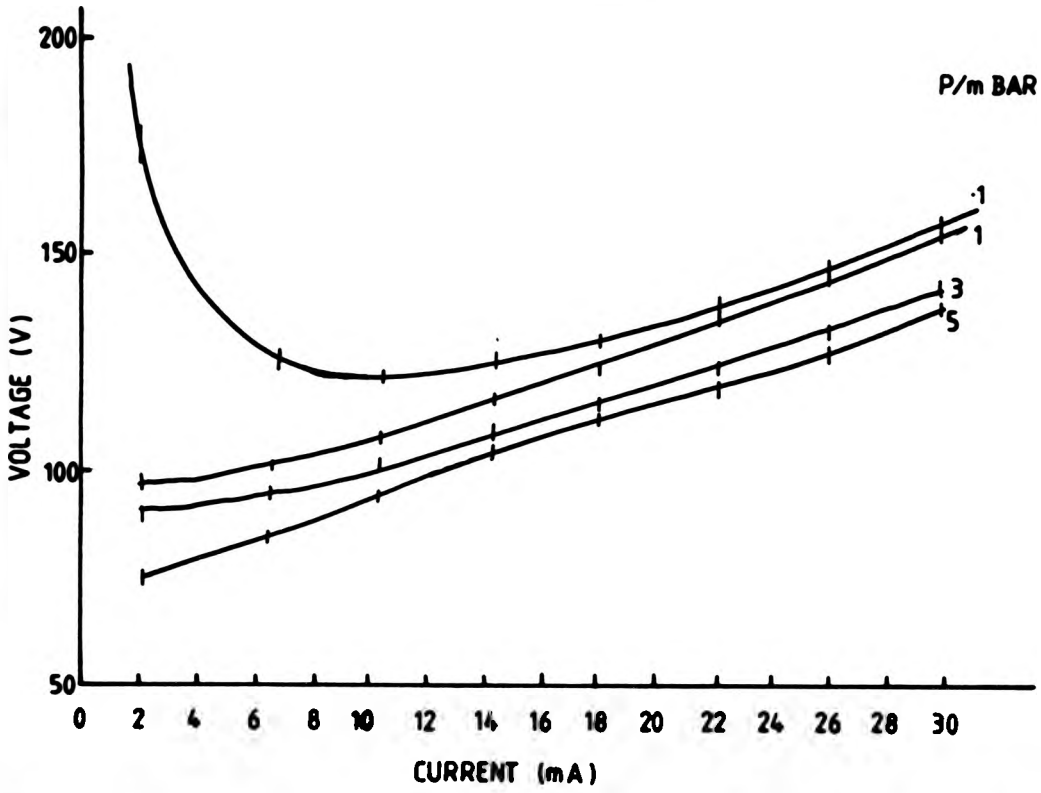

Fig. 26 V-i graphs for tube with heated coated cathode in neon for various pressures

negative glow appeared, and covered the coated filament, which resulted in an increase of the tube voltage. Lower filament cathode temperature was required to maintain the discharge in the lower pressure case. In Fig.27 voltage-current curves are shown for the same pressure and various filament voltages.

7.3 : ESTIMATION OF THE ELECTRIC FIELD STRENGTH (X)

Most measurements of the potential gradient since 1930 have been made with Langmuir probes spaced along the positive column, and used to deduce the space potential, electron temperature, and concentration.

Since the electron temperature and electron concentration were not studied in this work, the field strength in the positive column discharge in neon, argon, and Ne-Ar mixtures was estimated by using a discharge tube with alternative anodes (1 and 2), and a common cathode, hollow or hot coated (see Figs.11 and 12,) rather than using probes.

Use of discharge tube with two anodes, gave two different lengths of the positive column by switching from one anode to other. The extra voltage needed by the longer length of column was measured, and the average field $X = \frac{\Delta V}{\Delta x}$ (where x was usually 5 or 10 cm) was estimated.

The diameter of the discharge tube had a marked influence

Fig. 27 V-i graphs for column tube with heated coated cathode in neon for various filament voltages

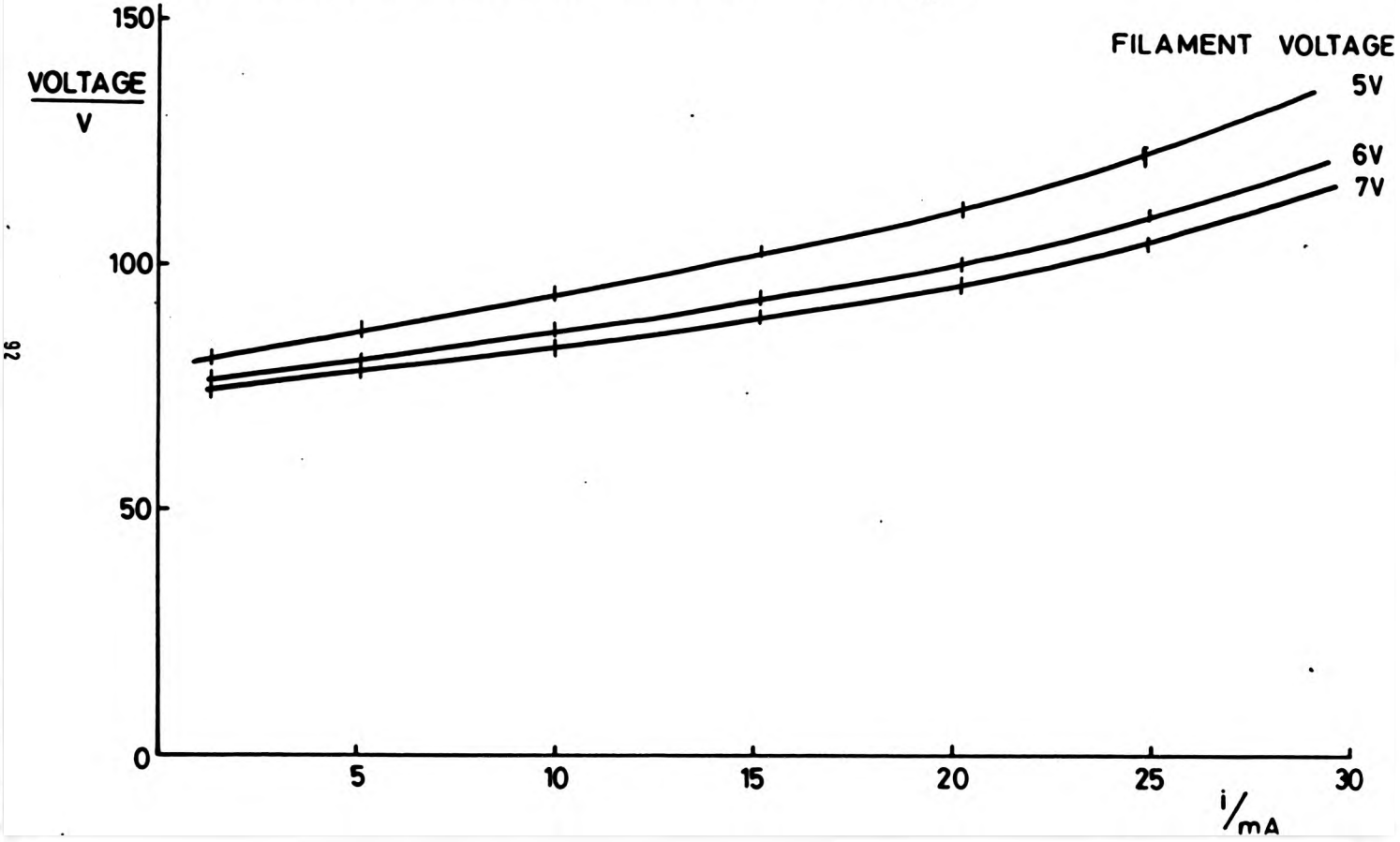

on the gradient, which decreases as the column tube becomes wider. It was found that the decrease of the field strength is less rapid at higher pressures. Fig.28 shows the variation of the electric field in the positive column in neon with respect to the discharge tube radius for different pressures. The gradient increases as pressure is increased whilst discharge current had little effect on the positive column field.

Fig. 29 shows the gradient of the positive column as a function of pressure in an argon discharge for various currents. The electric field was slightly lower for an argon than for a neon discharge under identical discharge conditions, which is due to lower ionisation potential.

When a small amount (1-2%) argon was added to a neon discharge, the field strength diminished by a small amount; whilst adding 1-2% neon to an argon discharge had practically no effect on the gradient of the positive column in argon.

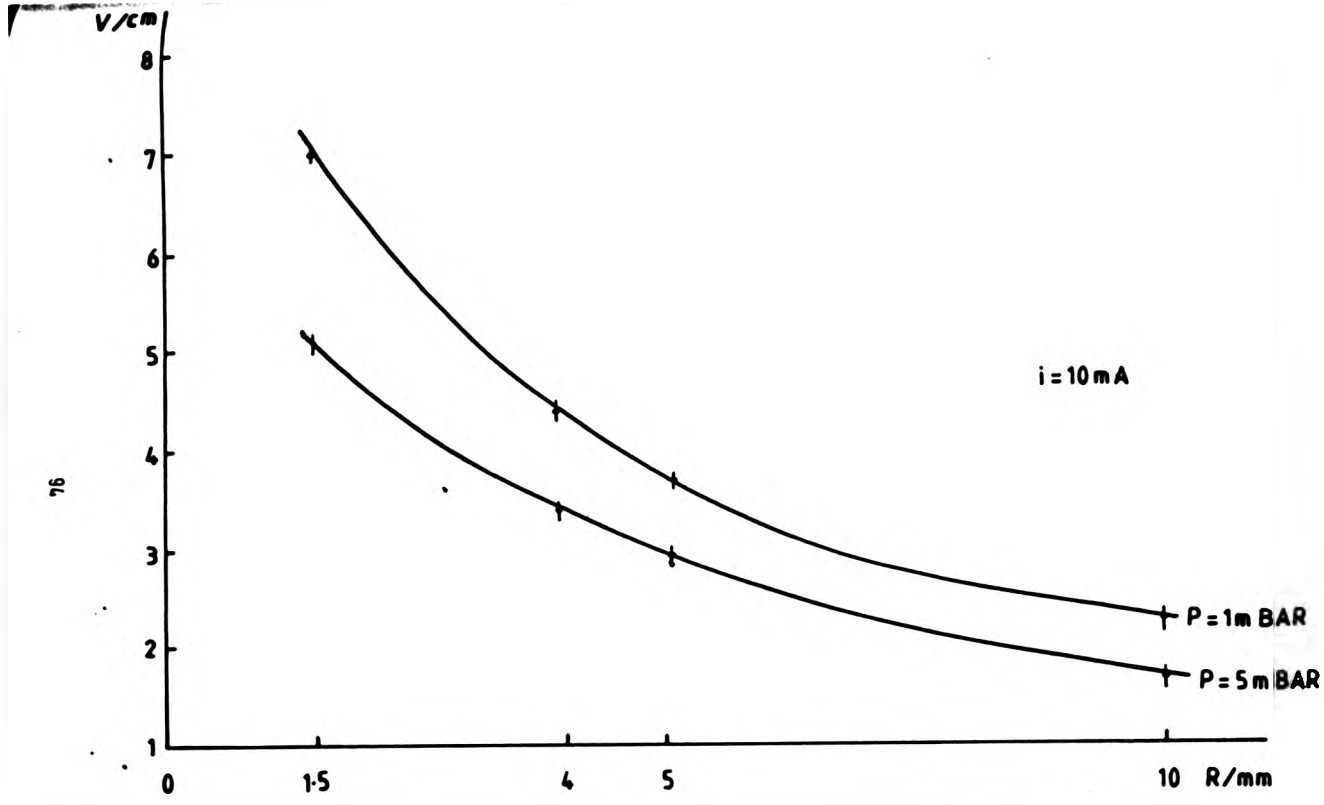

Fig. 28 Variation of the gradient with tube radius in neon discharge

Fig. 29 Variation of the gradient with pressure in argon discharge

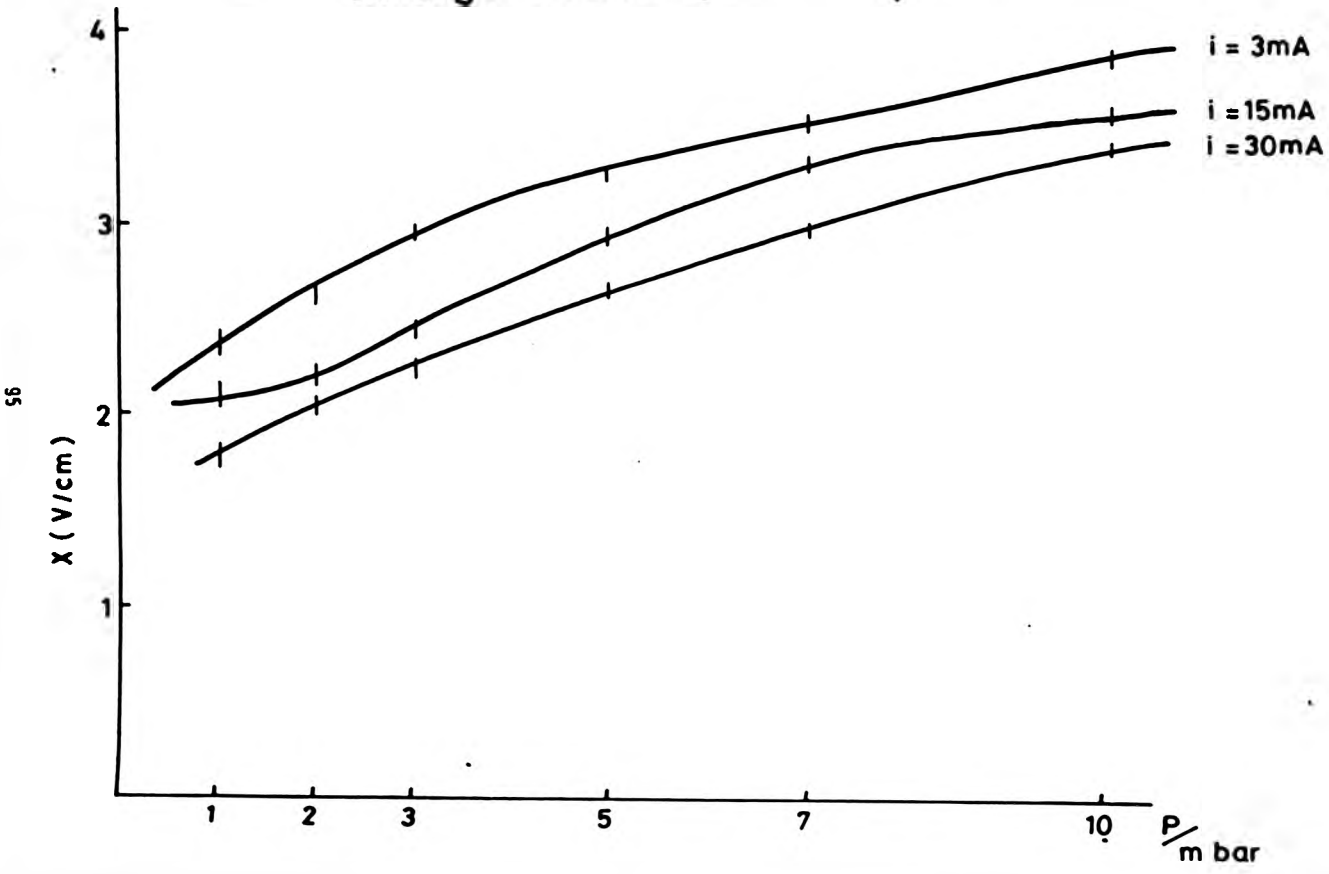

CHAPTER (8) FABRY-PEROT INTERFEROMETRIC RESULTS

8.1 : FABRY-PEROT EMISSION SCANS (F.P.I.)

8.1.1 : F.P.I. EMISSION IN NEON

Fabry-Perot interferometry (F.P.I.) results from a hollow cathode discharge in neon (19) have shown a self-reversal effect for the NeI spectral lines with the metastable state 3s (3/2) as the lower energy level of the transition.

Initially in the present work, two sealed hollow cathode lamps (HCL) (Cathodeon 3QNY/Fe) of the type manufactured for use in commercial atomic absorption spectrometers were used. Both these similar lamps C12 and 22639 were filled with neon, C12 at 10-1 torr, and 22639 at 15-1 torr and both had a cylindrical mild steel hollow cathode of 3mm bore and 10mm deep.

The self-reversal effect was observed for those spectral lines with the metastable state 3s $(3/2)^{\circ}_{1}$ as their lower energy level (640.2, 614.3, 703.2 nm) when the sealed hollow cathode lamps (C12 , 22639) were employed for emission measurements. F.P.I results for the positive column did not show any sign of self-reversal for the spectral lines terminating on the 3s $(3/2)^{\circ}_{2}$ level when side viewing of the positive column discharge was used, but when end viewing of the column tube (with hot coated cathode shown in Fig. 13) was used, then the effect of self-reversal for those spectral lines was observed.

Self-reversal of a spectral line only occurs if a significant number of atoms in the lower energy level of the corresponding transition are between the observer and the main emitting atoms.

Self-reversal was observed for the NeI lines when end viewing of the neon discharge was used. Not only was there a longer length of the positive column discharge compared with side viewing but also there was 3cm of tubing in front of the discharge, in which there was no discharge taking place (see Fig.13), into which the metastable atoms could diffuse. Therefore to observe the self-reversal effect for NeI spectral lines with the metastable lower state 3s $(3/2)_2^o$, not only must significant population of neon atoms in the metastable state be generated, but also these metastable atoms must survive long enough to diffuse to the cooler region of the discharge in order to absorb.

F.P.I. results in hollow cathode work by Light (19) and in this work show self-reversal for all selected neon spectral lines with the lower energy level 3s $(3/2)_2^o$ except the line 588.2nm. The reason for not observing self-reversal for this line could be due to lower values of transition probability (A) and statistical weight (g) for this spectral line (588.2 nm) compared with others. The effect of self-reversal for this line was not observed when sealed hollow cathode lamps were used.

Some NeI spectral lines, with their corresponding A,g,f (oscillator strength) values, are given in table 5, (38).

VALUES OF TRANSITION PROBABILITIES, STATISTICAL WEIGHT, AND OSCILLATOR STRENGTH FOR SOME NeI LINES.

λ/nm	A_{ki} (10^8 sec^{-1})	g_k	f_{ik}
640.2	0.433	7	0.373
614.3	0.216	5	0.122
703.2	0.192	3	0.0852
633.4	0.136	5	0.818
588.2	0.128	3	0.0398

TABLE 5.

Fig. 30 shows the emission scans of NeI line (640.2nm) for end viewing of the positive column discharge for neon pressure of 5 mbar for various discharge currents. F.P.I scans of some NeI spectral lines are given in Fig.31, for current at 20 mA, and 2 mbar neon pressure. Heights for this figure have been adjusted for comparison. Emission scans of 588.2nm for 1 mbar pressure for various current steps is given in Fig.32.

As the discharge current was increased the degree of self-reversal and overall line profile width was increased. Self-reversal of NeI spectral lines was found to be very sensitive to the presence of impurities produced by outgassing; therefore a thorough degassing of the vacuum

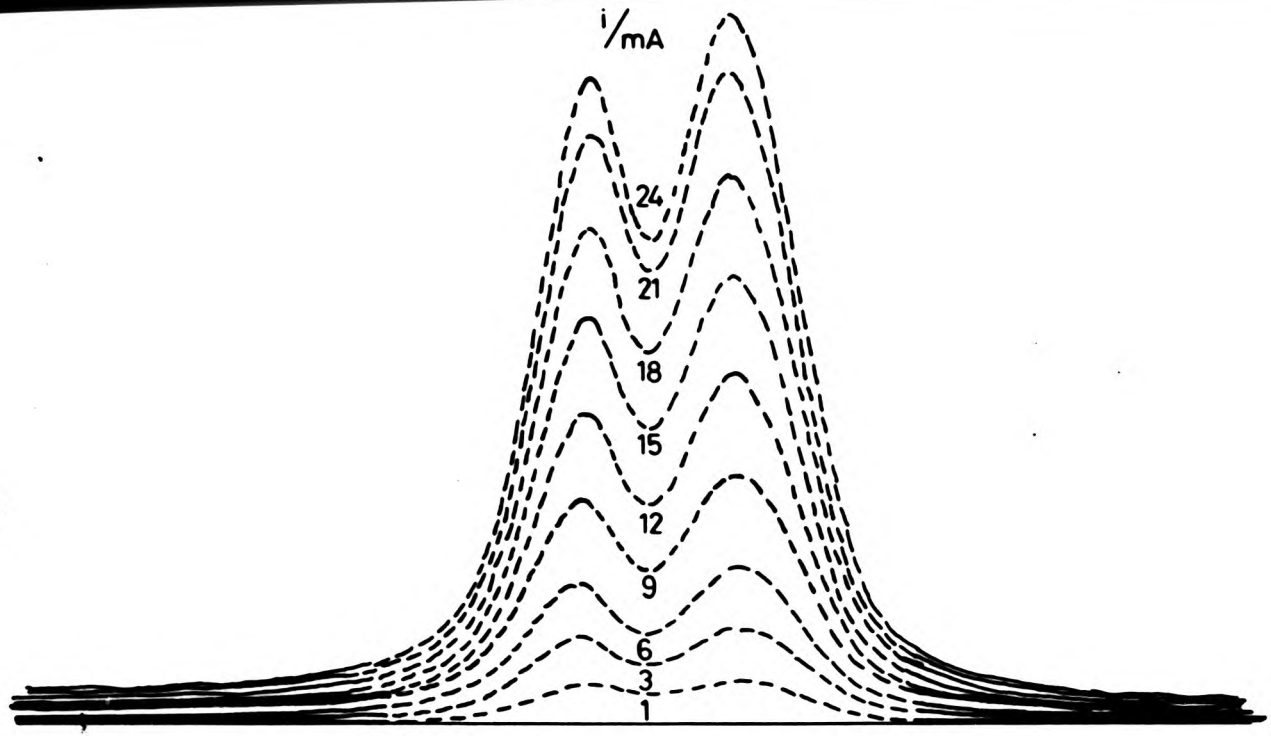

Fig. 30 F. P. I. scans of 640. 2nm (end on viewing) at P=5 mbar .

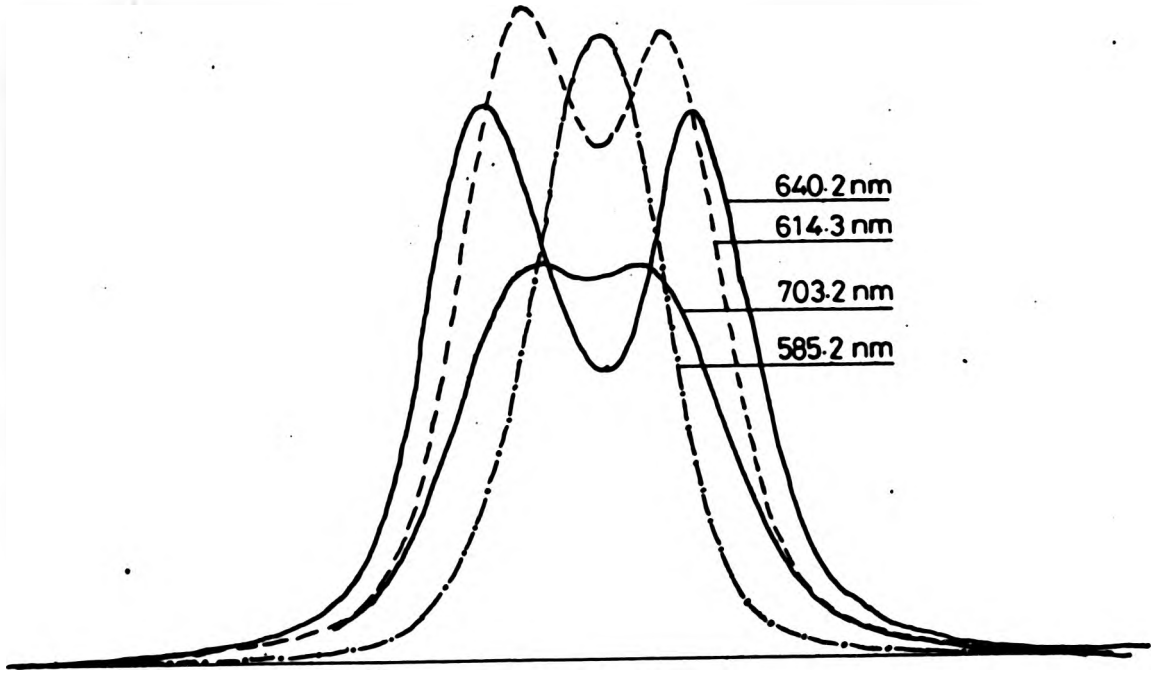

Fig. 31 F.P.I. scans of some of NeI lines at P=2 mbar

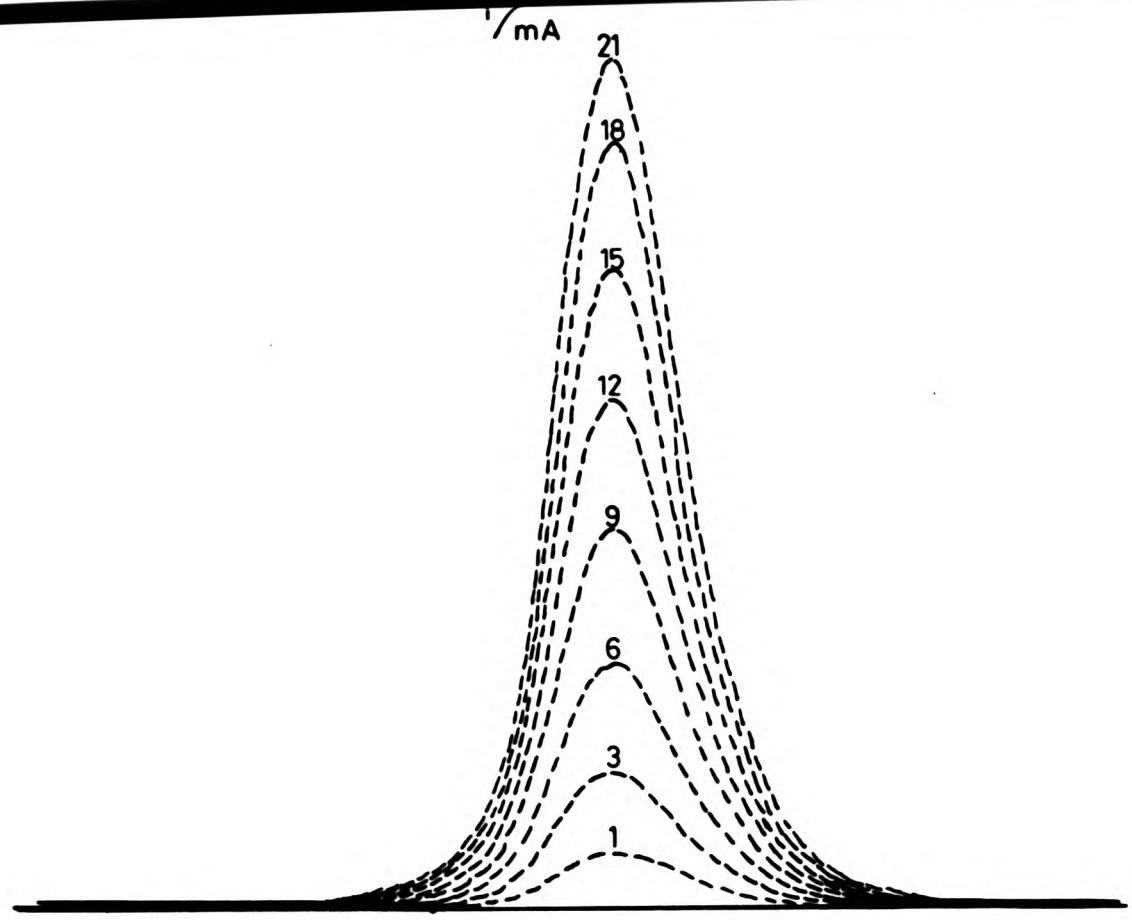

Fig. 32 Emission scans of 588.2nm at P=3 mbar

system was necessary before reproducible results could be obtained.

Fabry-Perot results on NeI lines with the metastable level $3s'(1/2)^{o}_{o}$ as their lower energy level did not show any sign of self-reversal effect, see Fig.33, which shows the emission scans of NeI lines terminating on the $3s'(1/2)^{o}_{o}$ and non-metastable states.

8.1.2 : **F.P.I EMISSION IN ARGON:**

A hollow cathode lamp filled with argon pressure at 10 + 1 torr made by Cathodeon Ltd (3QAY/Fe serial no. 73608) with 3mm bore and 10mm deep mild steel cathode was employed to carry out Fabry-Perot emission measurements with argon; no sign of self-reversal was observed for ArI lines with the metastable state $4s\ (3/2)_2$ as their lower energy level.

F.P.I. results for chosen argon spectral lines did not show any self-reversal when side and end viewing of the positive column discharge was used, although a few of these selected ArI lines had the metastable state $4s\ (3/2)_2$ as their lower level. Once again the reason for not observing self-reversal for these argon spectral lines from the F.P.I measurements could be due to the values of A,g corresponding to these lines. Table 6 shows the values of A,g,f for some of the chosen argon spectral lines (38).

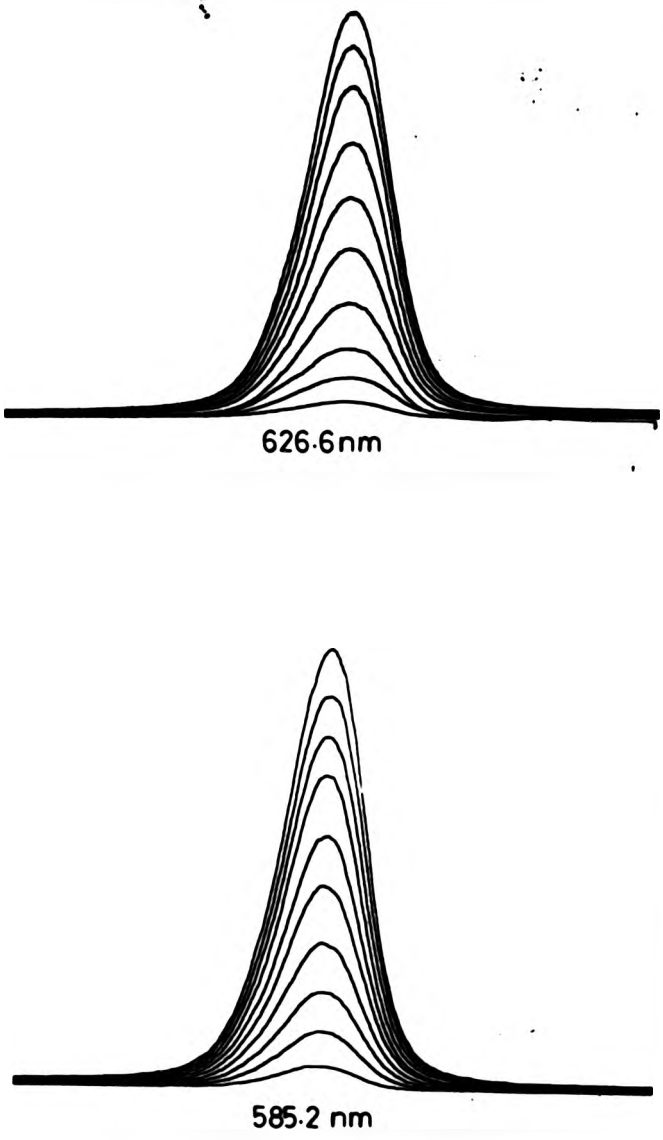

Fig. 33 F. P. I. scans of 585. 2 and 626. 6nm at P=7mbar for i=3 to 30mA by steps of 3

A.g.f VALUES FOR SOME ArI LINES.

λ/nm	A_{kI} (10^8 sec^{-1})	g_K	f_{iK}
696.5	0.067	3	0.0292
706.7	0.0395	5	0.0296
727.2	0.020	3	0.0156
738.3	0.087	5	0.119

TABLE 6.

The ArI line 696.5 nm is analogous to the line 588.2nm of neon, which did not show the self-reversal effect. The measurements on ArI lines 811.5 and 763.5nm which are respectively analogous to the NeI lines 640.2 and 614.3nm, which both exhibited self-reversal could not be carried out, without changing the Fabry-perot interferometer plates and the photomultiplier tube. Due to lack of time at the end of this project, these measurements were not made.

Fig.34 shows the F.P scans of ArI line 696.5nm for pressure of 3 mbar and different currents. Self-reversal of NeI spectral lines disappeared when a small amount of argon was introduced to a neon discharge. Adding a few percent of neon to an argon discharge did not make any marked changes on the argon spectral line profiles.

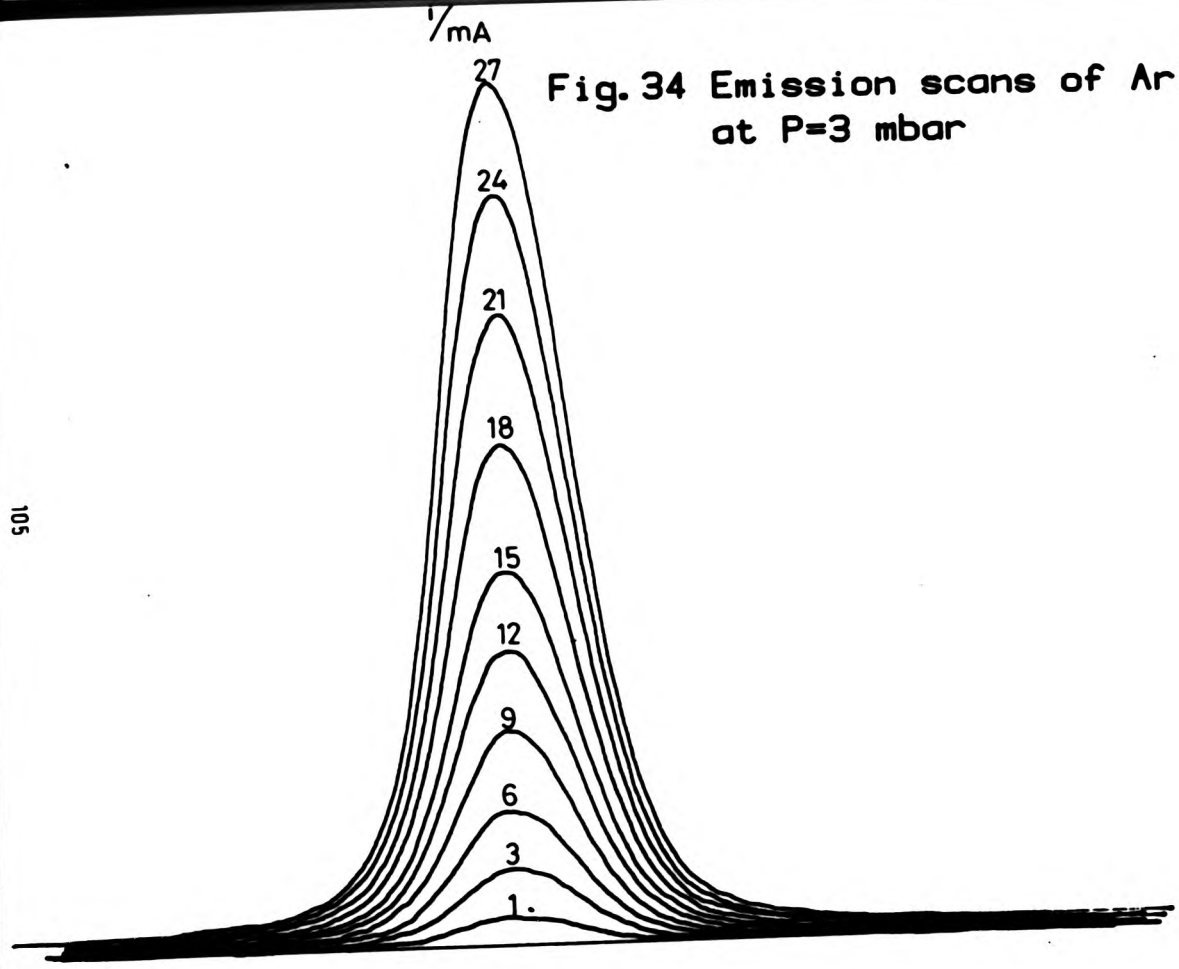

Fig. 34 Emission scans of ArI line 696.5nm at P=3 mbar

8.2 : DETERMINATION OF NUMBER DENSITIES OF THE METASTABLE AND RADIATIVE STATES

8.2.1 : GENERAL

The observation of self-reversal and broadening of the profiles of NeI spectral lines corresponding to transitions terminating in the metastable state $3s(3/2)^{\circ}_{2}$ was evidence of a significantly high number density of neon atoms in this level. By the absorption method the concentrations of neon atoms in this state and other 3s and 3s' states were determined.

Investigation of variation of the population densities of these four lower excited states (3s, 3s') of neon were carried out with respect to discharge current and pressures in pure neon and admixture of argon to neon discharge.

8.2.2 : THEORY:

Several methods for calculation of number densities of the excited atoms are described by Mitchell and Zemansky (39). The method used in this work for determination of the population density of the metastable atoms is similar to the method used by Jarrett and Franken (40).

The observed primary source and transmitted line profiles ($I(\nu)$ and $I'(\nu)$ respectively) are given by:

$$I(\nu) = \int f(\nu)\, g(\nu-\nu')\, d\nu' \qquad (8.1)$$

$$I'(\nu) = \int f(\nu) \exp[-\kappa(\nu')\ell]\, g(\nu-\nu')\, d\nu' \qquad (8.2)$$

and the apparent absorption coefficient K' ( ) is given by:

$$K'(\delta) = \ell^{-1} \ln \left[I(\delta) / I'(\delta) \right] \qquad (8.3)$$

where:

$f(\delta)$ is the primary source line profile

$g(\delta)$ the Fabry-Perot interferometer instrument function

$K(\delta)$ the true absorption coefficient

$K'(\delta)$ the apparent absorption coefficient

ℓ the absorption path length

and δ the wavenumber.

The absorption coefficient is defined by the exponential decay of a light beam travelling through the plasma;

the population density (N) of absorbing atoms is:

$$N = \frac{8\pi \times g_1 \times C}{\lambda_0^2 \times g_2 \times A_{12}} \times \int K(\delta)\, \partial\delta \qquad (8.4)$$

Where: λ_0 is the central wavelength of the spectral lines.

g_1 the statistical weight of the lower energy level.

g_2 the statistical weight of the upper energy level.

A_{12} the transition probabilities

and C the speed of light

In order to calculate the population densities of the excited states, the true absorption coefficients could be determined from the observed profiles, and be corrected for the Fabry-Perot interferometer instrument function if it is large. The problem associated with this is that of using high enough resolution to obtain a true line profile. Ideally the instrument width, or resolution limit, should be much less than the line width. If this condition is not fulfilled then the results would give a low value for the area under the profile. But in the present case the instrument function is much narrower than the observed profiles, and hence apparent absorption coefficients are approximately the same as the true coefficients.

If the light transmitted after passing through a gas is measured as a function of frequency or wavenumber, the absorption coefficient may be calculated and plotted against the frequency or wavenumber. By graphical integration, then the integral $\int k(\nu)\partial\nu$ or $\int k(\delta)\partial\delta$ may be obtained, and from knowledge of the statistical weights (of upper and lower energy level) and transition probabilities, N (the population density of the excited states) may be calculated.

8.2.3 : LINE SHAPE

The Voigt (combination of Lorentzian and Gaussian) profiles are frequently used in spectroscopy, since doppler broadening is usually important and the Lorentz distribution is a characteristic feature of pressure broadening for a wide range of conditions. The instrument function can very often be described approximately by a Lorentzian distribution. Although the Voigt profile can not be solved analytically it has been computed and tabulated by several authors (41, 42, 43).

The observed line profile results were checked by means of using tabulated values of the Voigt profiles, and good agreements were found for some NeI spectral lines (e.g. 585.2 and 692.9 nm). But for other lines agreement was less satisfactory which could be due to the effect of the wings of the observed profiles or a self-absorption effect. This proved that the observed line profiles were not well presented by the Voigt integral.

8.2.4 : ANALYSIS OF THE ABSORPTION RESULTS

The number density of the metastable level 3s $(3/2)^{\circ}_{2}$ of neon was estimated, using the apparent absorption coefficient in the equation 8.3. These estimations were carried out by graphical analysis of some of the obtained absorption results. Figs.35,36 show the Fabry-Perot profiles of NeI spectral lines 640.2 and 630.5 nm transmitted through the

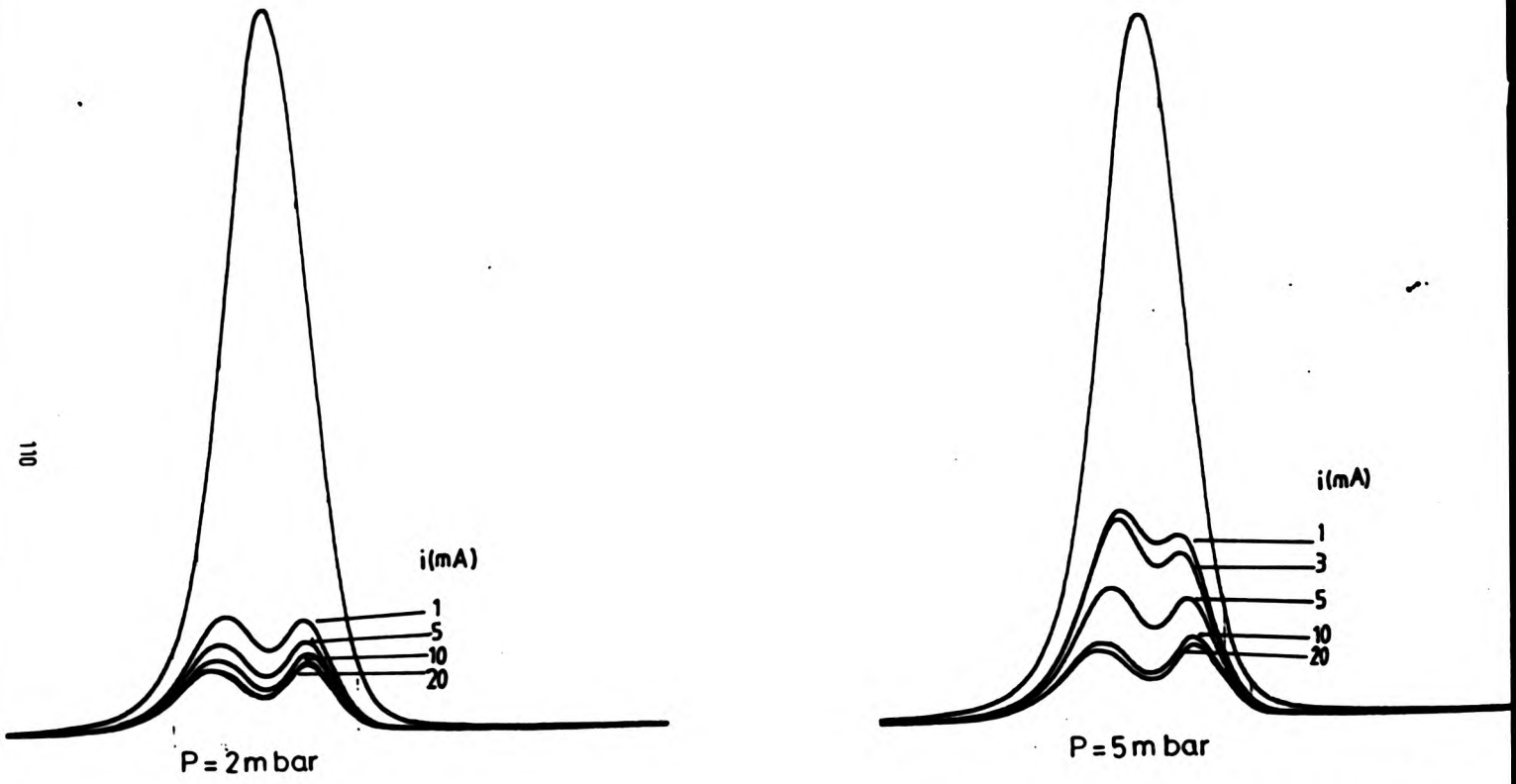

Fig. 35 Transmitted profiles of 640.2nm for various pressures

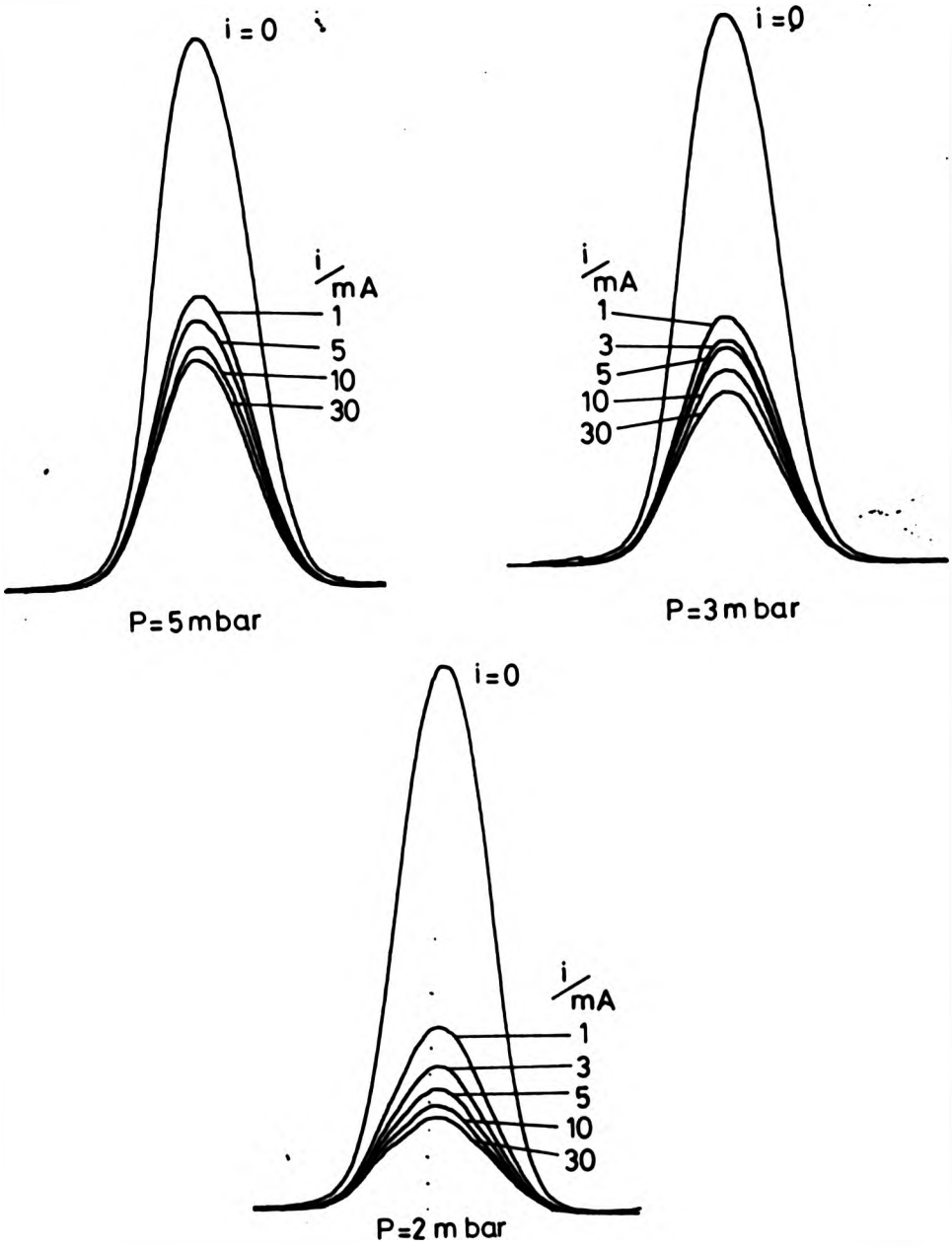

Fig. 36 Transmitted profiles of 630.5nm for various pressures

positive column discharge for various gas pressures.

The apparent absorption coefficient was determined by using the observed profile divided in to twenty evenly spaced bands across the spectral profile, (see Fig.37), and plotting a graph of these points against wavenumber (see Fig.38). Then the area under this profile (apparent absorption coefficient) was substituted in the equation:

$$N' = \frac{8\pi \times g_1 \times C}{\lambda_0^2 \times g_2 \times A_{12}} \times \int k'(\delta)\, d\delta \qquad (8.5)$$

N' is the estimated number density of the excited atoms using apparent absorption coefficients.

N' was calculated for different currents and various pressures, for a given wavelength. Fig. 39 shows the variation of estimated population density of the metastable level 3s $(3/2)_2^o$ of neon with respect to discharge current for various pressures, using the absorption results on the NeI spectral line 640.2 nm.

The graphical method was also used for calculation of concentration of neon excited atoms in the other metastable state 3s' $(1/2)_0^o$ and the two radiative levels 3s $(3/2)_1^o$ and 3s'$(1/2)_1^o$.

The absorption measurements were carried out for several NeI spectral lines, to be able to check the results. At least two wavelengths were chosen which both terminated on

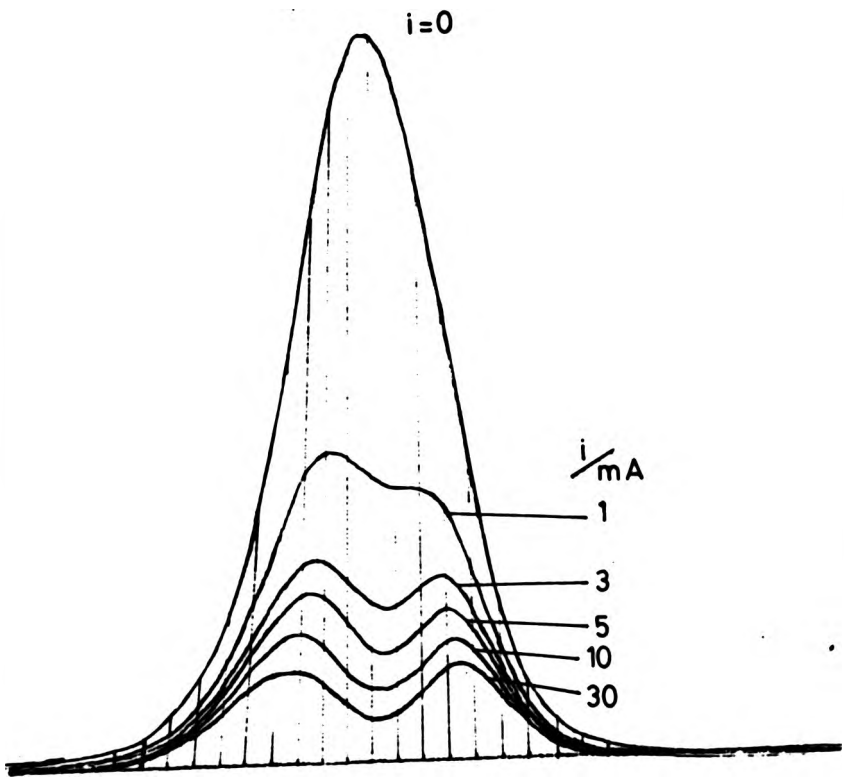

Fig. 37 Twenty evenly spaced profile of NeI line 640.2nm at P=1 mbar

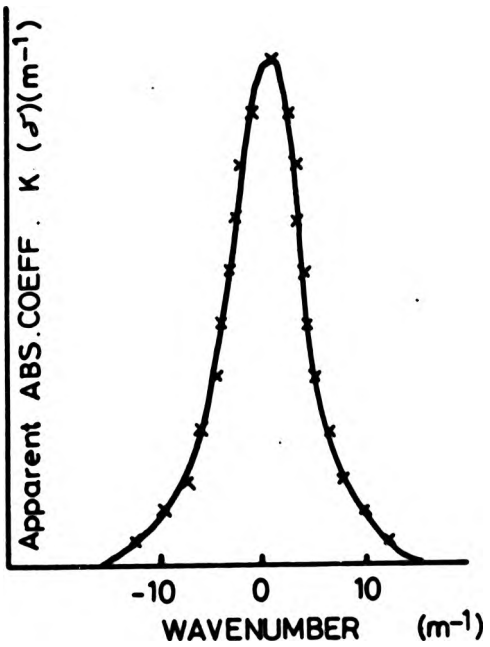

g. 38 Apparent absorption coefficient profile

Fig. 39 Variation of number density of the $3s(3/2)^0_2$ state versus current for various pressures

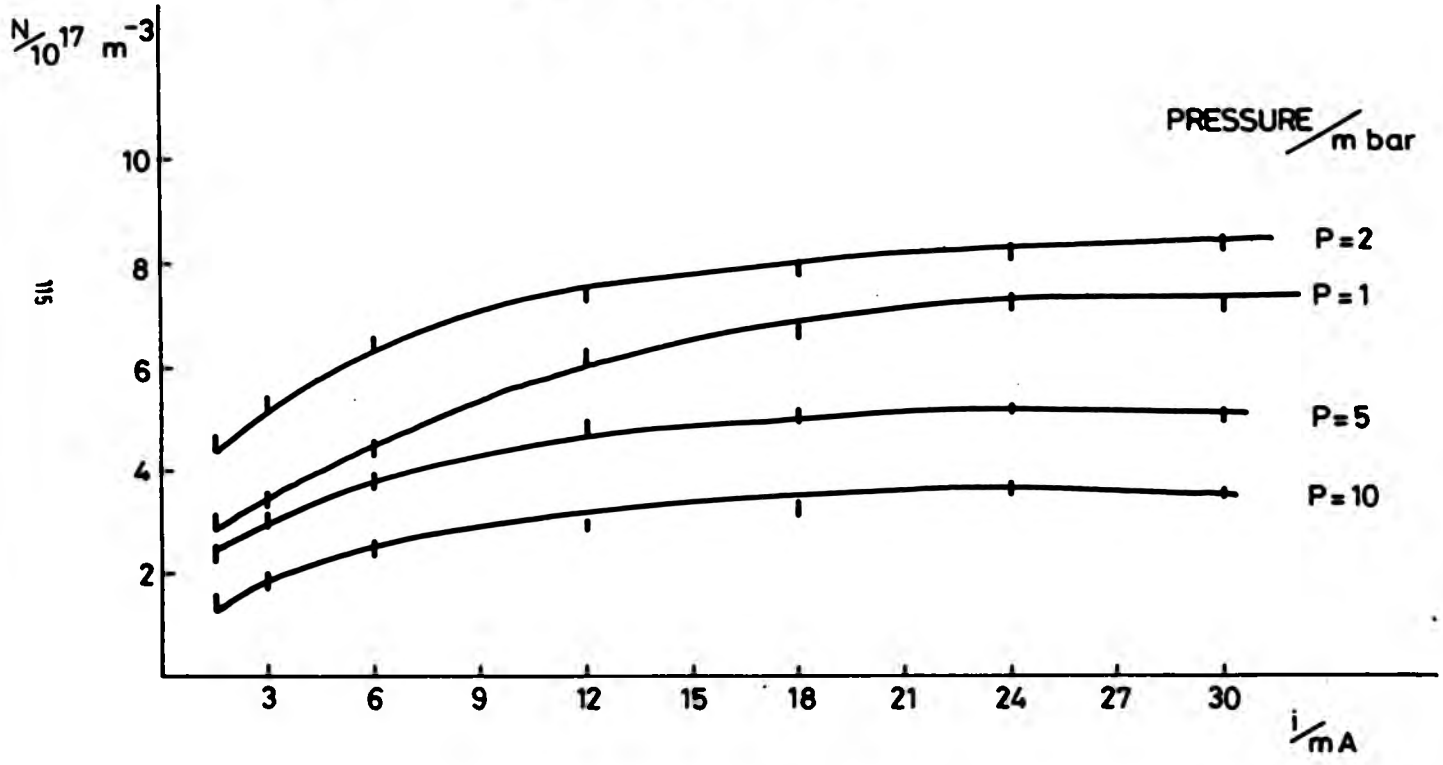

a common lower energy level. Calculations of the population density of a given excited level using different spectral lines terminating on that state were in good agreement (see Fig.40) except in a few cases, which could be due to either the effect of self-absorption or the degree of accuracy of the atomic transition probabilities (38). (The values of transition probabilities used and their uncertainty limits were tabulated by N.B.S. (38). Some of these values had 10-25% uncertainty, giving an error of 15% in the values of calculated number densities. This means that the population density of a given excited state should agree within 20% if various spectral lines terminating to that level are used. Also a drift of 5% should be allowed for the recorded profiles).

C. Light (19) has developed a curve fitting program for a DEC 10 computer to carry out the calculation of the number densities of the excited states of neon in a hollow cathode discharge, and found little difference between the calculation of concentration of excited neon atoms using the computer, and calculation of them by graphical method, but the form of the number density of the metastable atoms (N) versus the discharge current (i) graphs were slightly changed at higher currents.

Carrying out the calculation of the population densities of the excited atoms could take a long time by the graphical analysis method, and is prone to introduce some errors, so it

was decided to carry out these calculations by use of computer.

A computer program was written in basic for a Hewlett Packard computer (H.P. 87) with a double disc drive (82901M flexible) and a plotter (7470 A). A digitizing sight could be used, by placing it in one of the two pen holders of the plotter. The computation by this program (Appendix A), was carried out as follows:

First an observed profile (which was obtained on an A4 paper directly by the x-y recorder) was placed on the plotter base, and by calling program TRY 1 the emitted (positive column discharge off) and transmitted (discharge on) profiles could be digitized for a maximum of fifty equally spaced points across the base line of the spectral profile. After choosing the first and last point on the profile, the profile was digitized by controlling the digitizing sight moving along the intensity axis.

After all points had been digitized, program TRY 2 could be chained (called) to check the data points, in case of an error during the digitizing process, then using program TRY 3 enabled any mistake be corrected; using TRY 5 would plot the original profile after being digitized to compare with the raw profile before being digitized. Fig.41 shows an example of the comparison of observed profile with the one which was digitized for 35 points across the base line.

By chaining the program TRY 4 the calculation of the log ratios were carried out, and a plot of them against the wavenumber could be seen on the V.D.U. or obtained on the paper using the plotter. To determine the area under the absorption coefficient profile, the limits of integration had to be chosen. These limits were chosen as the position where the wings of the absorption coefficient profile either touched the base line or each side of maxima were getting close to the base line. Some fluctuations were present on the wings of the profile due to calculations of the ratio of two small values. Data were saved on a datafile on a floppy disc, and could be checked at any time.

The results obtained by using the graphical integration and those obtained by employing the computer were found to be in good agreement (differences of 2-5%). For calculation of population densities of the excited state of neon the absorption results of those NeI spectral lines in which self-absorption was negligible were used.

Results of computation of number densities of the excited neon atoms in 3s and 3s' levels are tabulated in table 7 for various discharge currents and in table 8 for different gas pressures. Dependence of the population density of the metastable and radiative states of neon on the discharge current are shown in Fig.42.

Table 7 and 8 give the population densities of the neon

excited states (3s, 3s' group levels) and their variation with discharge current (at neon pressure of 2.0 mbar) and with pressure (at current of 20 mA) respectively.

Excited States	CURRENT/mA				
	1	5	10	20	30
	N (10^{17} m^{-3})				
3s $(3/2)^o_2$	3.9	6.3	7.2	7.9	8.4
3s $(3/2)^o_1$	2.1	3.5	4.2	5.3	6.0
3s'$(1/2)^o_0$	.9	1.8	2.3	2.7	3.1
3s'$(1/2)^o_1$	.1	.21	.36	.51	.79

TABLE 7.

Excited States	PRESSURE/mbar					
	.5	1	2	5	10	15
	N (10^{17} m^{-3})					
3s $(3/2)^o_2$	5.8	6.8	7.9	4.6	2.6	2.3
3s $(3/2)^o_1$	3.4	3.5	5.3	3.6	2.2	1.7
3s'$(1/2)^o_0$	2.4	2.6	2.7	2	1.3	1.2
3s'$(1/2)^o_1$	.45	.47	.51	.44	.3	.21

TABLE 8.

The number density (N') of the metastable level 3s $(3/2)^o_2$ of neon showed a linear increase with current at low currents (less than 10 mA); then as the discharge current increased, the population density of this state tended to

Fig. 40 Comparison of plots of number density of $3S(3/2)^0_2$ level versus current using different wavelength

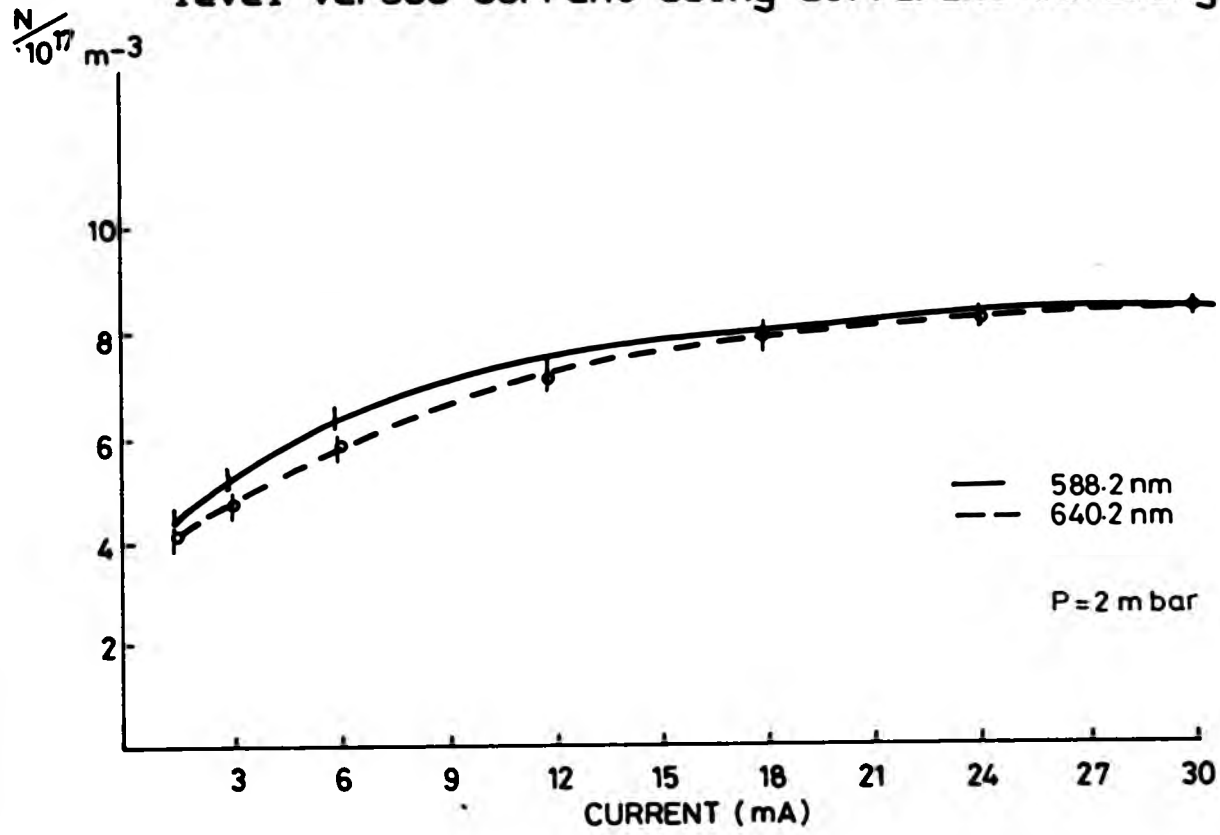

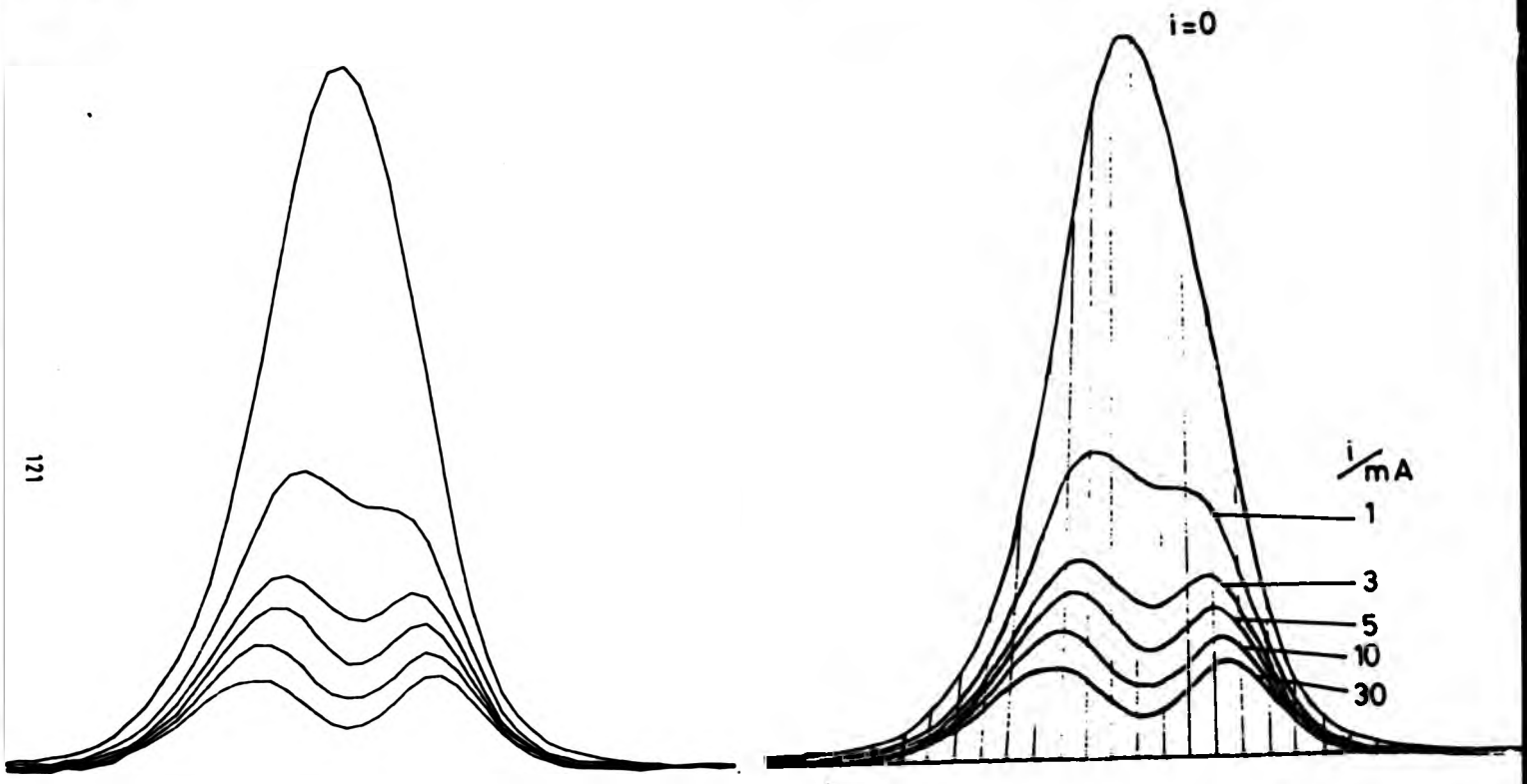

Fig. 41 comparison of the observed and digitized profile of 640.2nm at P=1 mbar

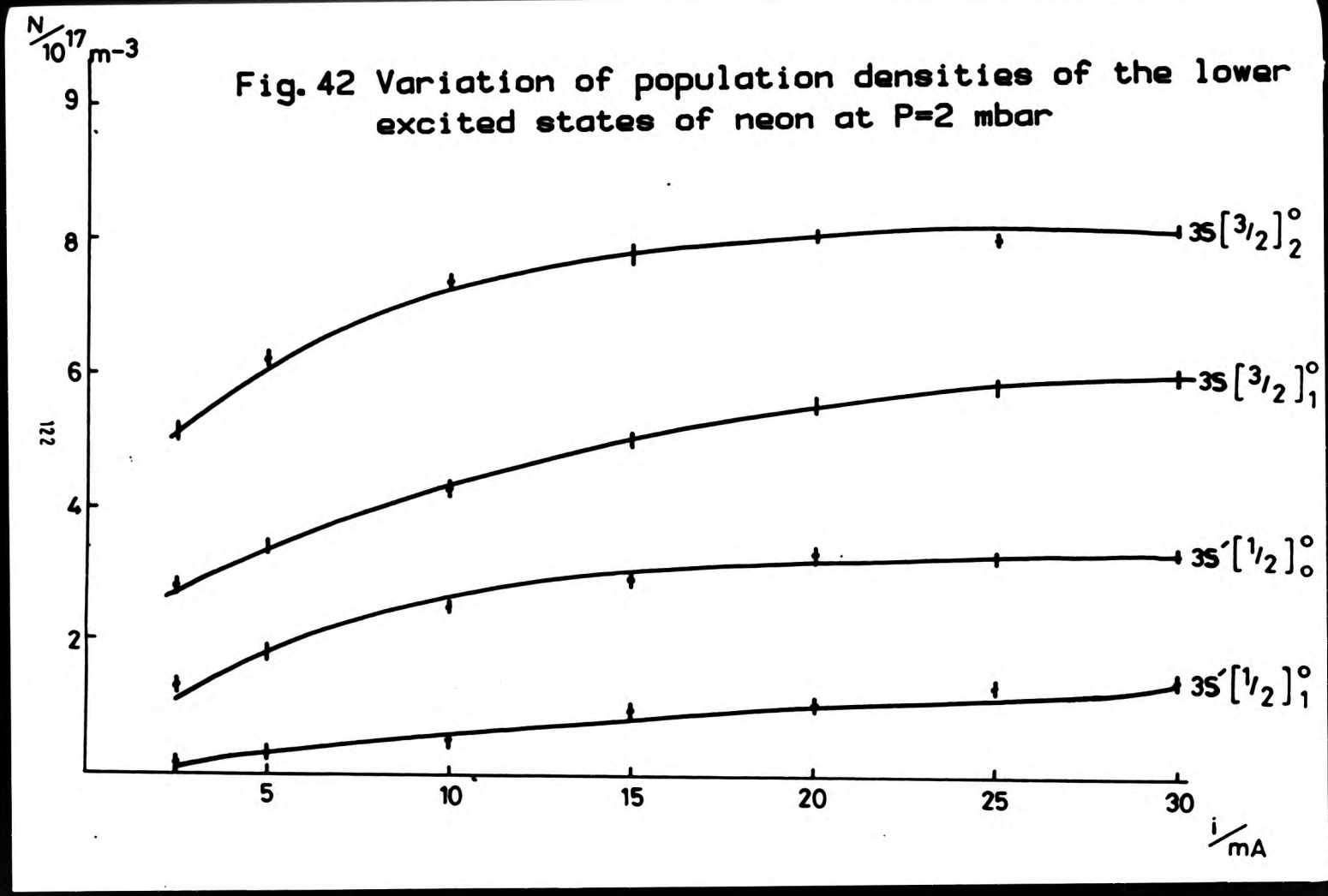

Fig. 42 Variation of population densities of the lower excited states of neon at P=2 mbar

saturate. This saturation behaviour was also observed for the other metastable level 3s'(1/2) of neon, in agreement with results of Valignat and Leveau (44) and Behnke et al (33).

Fig. 43 shows the variation of concentration of the metastable atoms in 3s $(3/2)^o_1$ state of neon against gas pressure for currents of 5 and 30 mA. As can be seen, at pressures of around 2 mbar the population density of the metastable atoms in 3s $(3/2)^o_1$ level has maximum value. This is due to the fact that the metastable atoms are lost by diffusion to the discharge tube walls, and by two-body collisions with neutral atoms and electrons at low pressures, and by three-body collisions, where a metastable and two neutral atoms are involved, at higher pressure.

Delcroix et al (30) derived an expression for the number densities of excited atoms at low current densities:

$$N = \frac{n_e \times n_o \times C}{\nu} \qquad (8.6)$$

Where:
- N is the number density of excited atoms
- n_e is electron number density
- n_o is number density of ground state atoms
- C is overall production rate coefficient
- ν is loss frequency

According to this expression, N is a linear function of n_e at constant pressure in low discharge current region. As discharge current increases, $\nu \longrightarrow n_e D$ (where D is overall

destruction rate coefficient), and the population density tends to saturate. In this saturation region the concentration of the metastable atoms is given by:

$$N = \frac{n_e \times n_e \times C}{n_e \times D} = n_e \frac{C}{D} \qquad (8.7)$$

This saturation behaviour for number density of the metastable atoms versus current occurs because of:

a) A significant number of electrons have the energy required to ionize atoms (to nearby states) in the metastable level ($\simeq$ 5 ev for neon).

b) The collisional cross-section for ionising the metastable atoms is greater than the cross-section for excitation of ground state atoms.

Therefore increasing electron density not only increases the rate of creating the metastable atoms, but also increases the rate of their loss ($N \times n_e \times D$).

In neon the lowest radiative state $3s(3/2)^o_1$ is located very close (see Fig.44) above the lower metastable state $3s(3/2)^o_2$, so the that process of excitation to the nearby higher radiative level is energetically possible. The upper metastable state $3s'(1/2)^o_0$, can be destroyed by de-excitation to the lower radiative level $3s\ (3/2)^o_1$ as well as by excitation to the upper radiative state $3s'\ (1/2)^o_1$, this is one of the reasons that the population density of this metastable level $3s'(1/2)^o_0$ is low compared with the

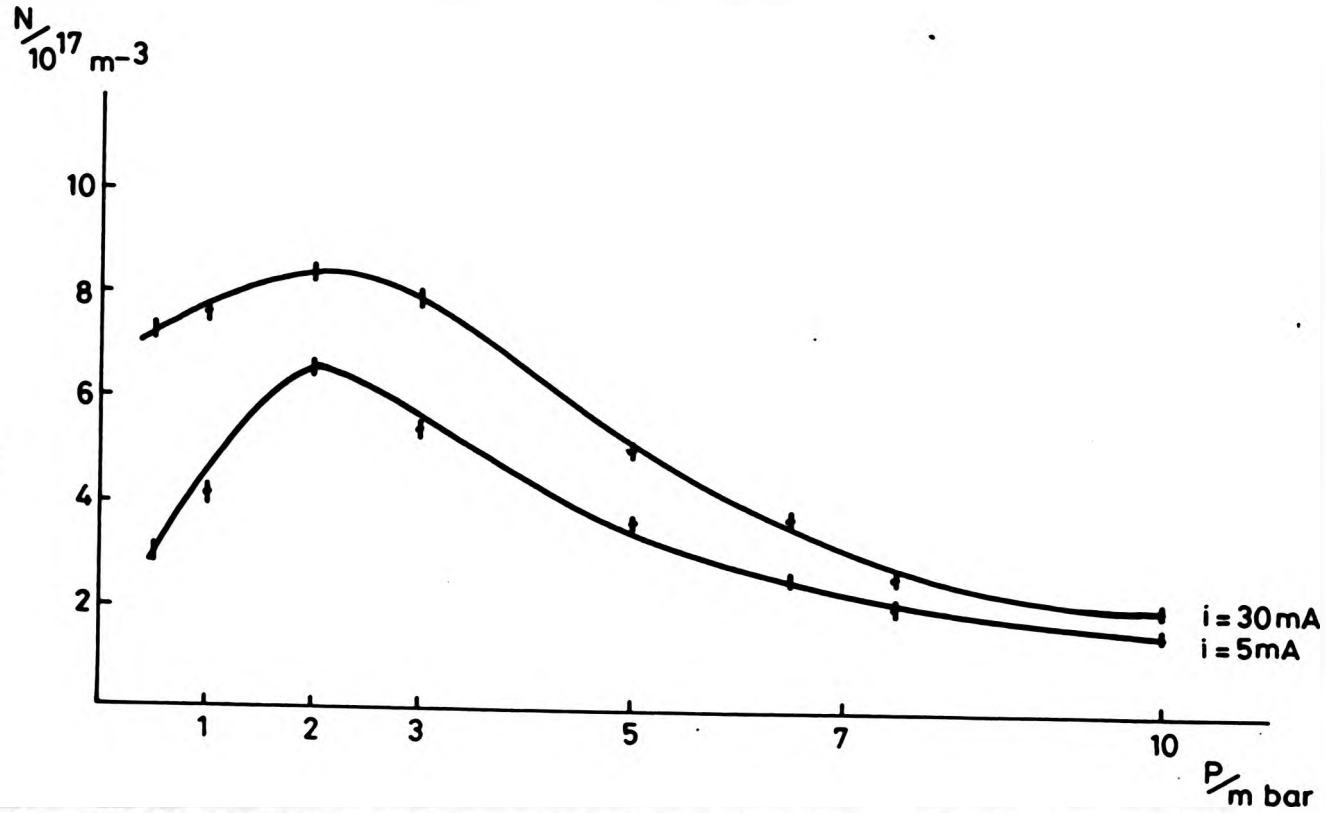

Fig. 43 Variation of population density of the $3s(3/2)^0_2$ level with pressure for various currents

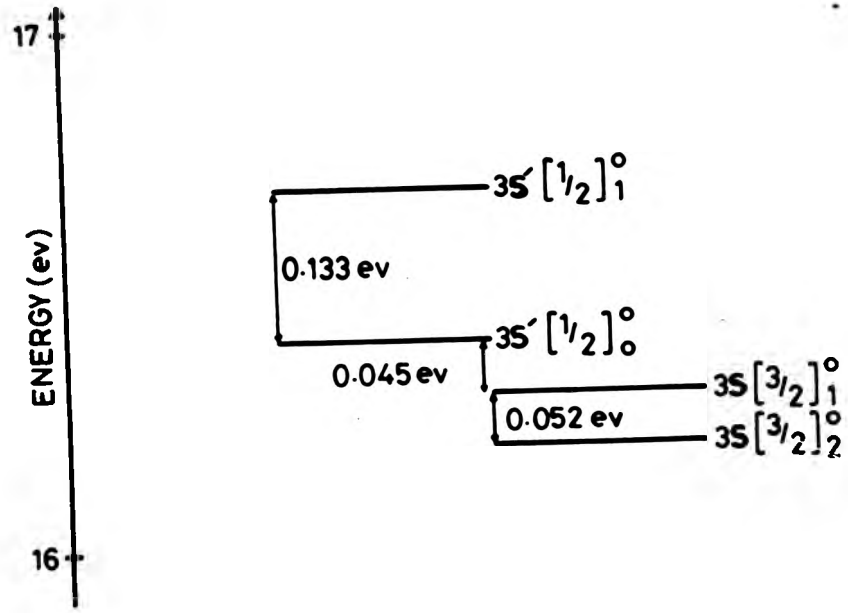

Fig. 44 Simple diagram of first excited states of neon

other metastable state, and the number density of the radiative level 3s $(3/2)_1^0$ is high.

The saturation behaviour which was observed for population density of the metastable atoms versus the discharge current was not found for the number density of the radiative state against current. Because of radiative de-excitation to the ground state, one would expect the concentration of the radiative levels initially to be lower than the population density of the metastable states, but because of radiation trapping, the radiative states become repopulated.

When argon (1-3%) was introduced to a neon discharge, the number density of the metastable atoms was reduced drastically, as the metastable atoms are quenched by the argon atoms.

This can be explained by the fact that a resonance exists between the metastable state of the main gas (neon) and the ionisation potential or excited state of the added gas (argon) atoms or ions. The possible reactions are:

$$Ne_m + Ar = Ar^+ + Ne + e + K.E \qquad (8.8)$$

$$Ne_m + Ar = Ar' + Ne + K.E \qquad (8.9)$$

Where Ne_m is an excited neon metastable atom; Ar, Ar^+ and Ar' are argon gas atom, ionised and excited respectively, Ne is neon atoms and K.E is Kinetic energy. The first reaction (8.8) is more likely to occur.

When argon was used as a carrier gas, direct absorption measurements were carried out on the ArI spectral line 696.5 nm which terminates on the metastable state 4s $(3/2)_2$. Fig.45 show the variation of the number density of this metastable state of argon with the discharge current, for various pressures. The population density of the argon metastable atoms in the 4s $(3/2)_2$ state was lower than that of the neon metastable atoms in the 3s $(3/2)_2^o$ state. The saturation behaviour was also observed for concentration of the argon metastable atoms against discharge current, in agreement with the results of Delcroix et al (30).

Adding a small amount of neon (1-3%) to an argon discharge, no noticeable changes were observed on the population density of the argon metastable atoms. This is due to the fact that when excitation and ionisation potentials of the added gas (neon) are above the metastable state of the main gas (argon) no (or a very small) reaction between the two gases can occur (or very small) to affect the population density of the main gas metastable atoms, which caused no marked change in spectral or electrical characteristics of the main gas.

8.3 : THE RADIAL DISTRIBUTION OF THE METASTABLE ATOMS:

The radial distribution of the metastable atoms in a pure neon discharge was carried out by employing end viewing of the positive column, having a mesh anode through which

Fig. 45 Variation of number density of the $4s(3/2)_2$ state of argon with current for various pressures

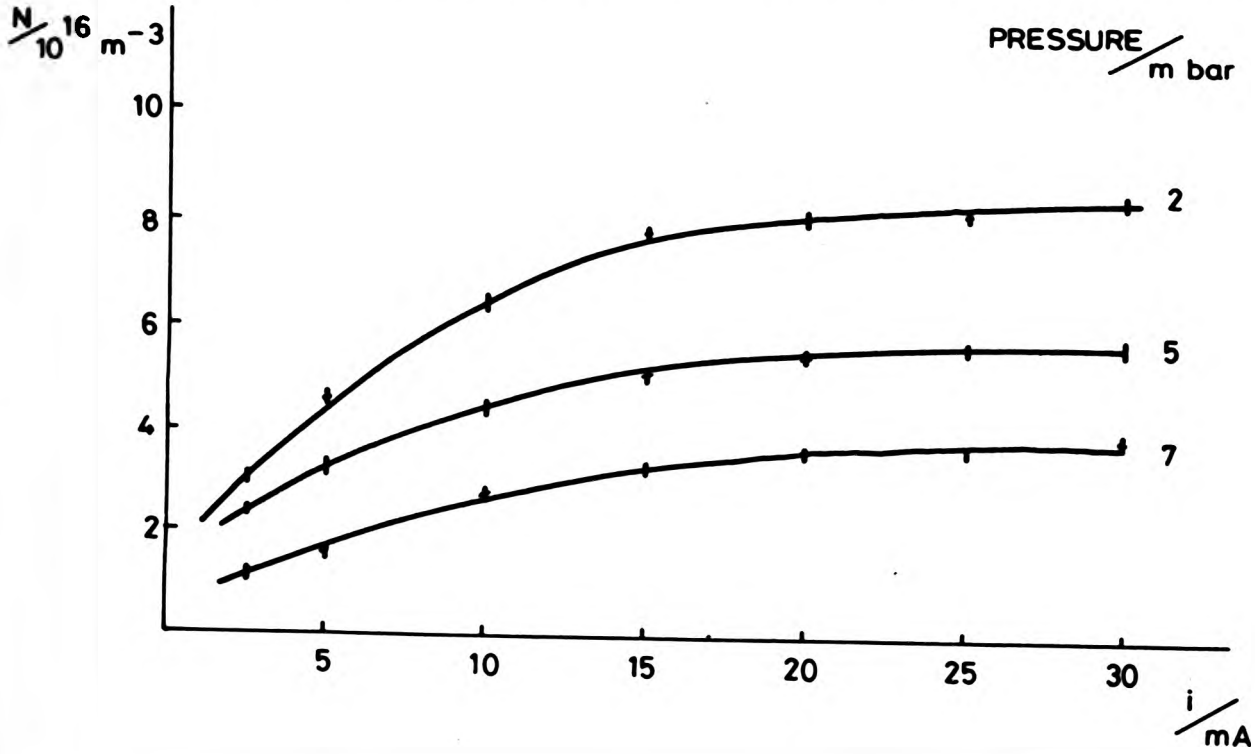

background light (microwave excited source) could pass. The experimental method of measuring radial distribution of the metastable atoms was given in section 6.4.3.

Fig. 46 shows the variation of radial distribution of the metastable atoms in 3s (3/2) state of neon with respect to the discharge current. At higher current the radial profile is wider than at higher currents. The effect of pressure on the radial distribution of the metastable is shown in Figs.47. At very low pressure the profile of these distributions is wide than at higher pressures.

These radial profiles are approximately of the form of a Bessel function of zero order. In both Figs.46 and 47 the radial distributions of the metastable atoms do not reach zero by the tube walls, because no data was obtained very close to the walls, since measurements could not be carried out very close to the tube envelope because of scattered light due to the glass joint between viewing window and the discharge tube.

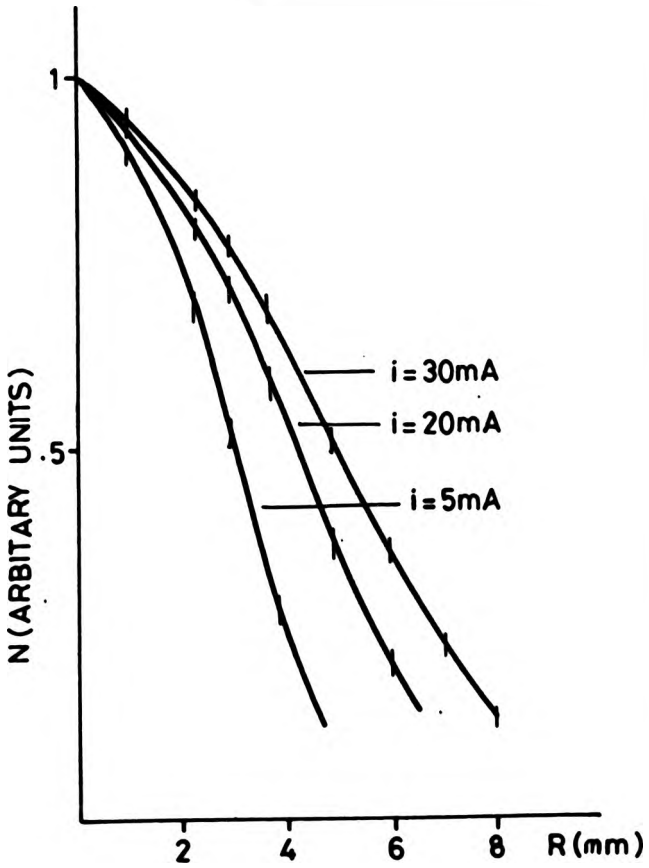

Fig. 46 Radial distribution of the $3S(3/2)^0_2$ of neon for different discharge currents

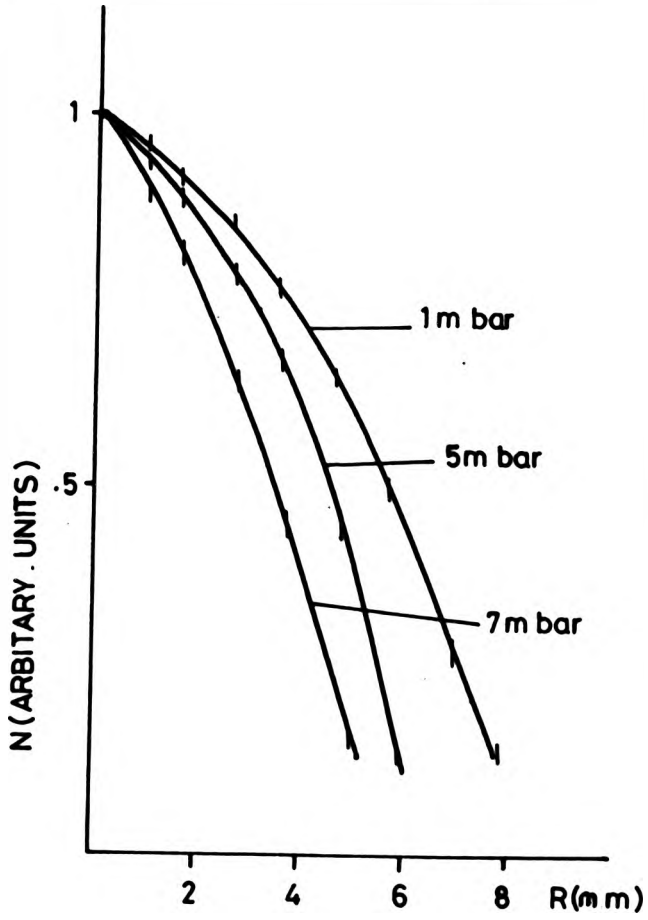

Fig. 47 Radial distribution of the $3s(3/2)^0_2$ of neon for various pressures

CHAPTER (9) INTENSITY-CURRENT (I-i) CHARACTERISTICS:

9.1 : GENERAL:

The intensity of an emission spectral line depends on the population density of the corresponding upper energy level, and the transition probability to the lower level.

$$I = \frac{N_2 \cdot A_{12} \cdot h \cdot C}{\lambda} \qquad (9.1)$$

Where I : is the intensity

N_2 : population density of upper energy level

A_{12} : transition probability

h : Planck's constant

λ : wavelength

and c : speed of light

Hence the dependence of the intensity of a spectral line on the discharge current is determined by the dependence of upper energy level population density on the current.

Many of the I-i results from the hollow cathode work by a previous worker in this laboratory, C.Howard (1) have been fitted to the I-i equation of form:

$$I = \frac{Ai(1+Ci)}{(1+Bi)} \qquad (9.2)$$

This equation is the consequence of a model that assumes that the excited state population is determined by several simple processes, the rate of which are functions of electron number density. The electron number density is assumed to increase linearly with discharge current, while

the electron energy distribution remains unchanged.

These processes and their assumed dependence on the discharge are:

Process	Dependence on Current
Single-step excitation direct from the ground state	$\propto i$
Two-step excitation via an intermediate state	$\propto i^2$ *
De-excitation by electron collision	$\propto i$
Radiative De-excitation	Independent of i

* (Assumption of the metastable population density proportional to the discharge current is not correct according to recent measurement of the metastable number density by C. Light (19) using hollow cathode discharge in neon under almost similar discharge conditions to that used by Howard).

In this work the intensity-current relationships were investigated in pure neon initially for various discharge parameters, and similar measurements were carried out using argon and argon-neon mixtures, to compare these results with those of the hollow cathode discharge.

9.2 : THE INTENSITY-CURRENT RESULTS IN PURE NEON:

It is essential to understand the nature of the dependence of the spectral lines intensity on the discharge current, the gas pressure, and the population density of the lower excited states. These relationships then assist in the interpretation of the phenomena within the light sources, since any changes in the discharge parameters inevitably alter the intensities of the spectral lines', hence the effect of discharge parameters on the line intensities are very important.

The 3p , 3p'levels of neon are populated by direct excitation from the ground state and by stepwise excitations from the 1s levels. Therefore spectral lines (3p,3p'-3s,3s'transitions) are associated not only with direct excitation of atoms, but also with secondary processes such as two-step excitation and collisions of the second kind. An excited atom may revert to its ground state without emitting light provided it can transfer its excitation energy to an electron or another particle present during the discharge. Two-stage excitation is quite important even though the probability of a collision between an excited atom and an electron is low. This is because stepwise excitation is favoured by the presence of the metastable atoms.

Emission processes, as seen from the above discussion, are closely related to the life of excited atoms; the

probability of the secondary processes increases with the lifetime of excited atoms. The intensity-current graphs for some of the NeI spectral lines for various neon pressures are given in Figs. 48 to 50, some showing a linear relationship, and some with an upward curvature (where two-step excitation can be important); some lines tended to saturate (where collisional de-excitation by electrons is dominant). Self-absorption also can cause a downward curvature on the I-i plots. Observation of the self-reversal effect for the NeI spectral lines terminating on the metastable level $3s(3/2)^{\circ}_{2}$ was evidence of high population of the metastable atoms in that state. Following the absorption measurements it was found out that the number densities of the metastable atoms are not proportional to the discharge current, so although these metastable levels could be taken as an intermediate level for two-step excitation the I-i equation (9.2) had to be modified in the light of these results.

Initially a computer program (see appendix B) was written to fit the I-i results, using equation (9.2). It was found by choosing a very small value (or zero) for B in that equation a better fit could be obtained. Since almost all the spectral lines in neon which were studied in detail in this work were those belonging to the transitions between 3s, 3s' group and 3p, 3p' group levels, and since it is apparently true that de-excitation by electron collisions is a dominant process for higher energy levels than 3p and

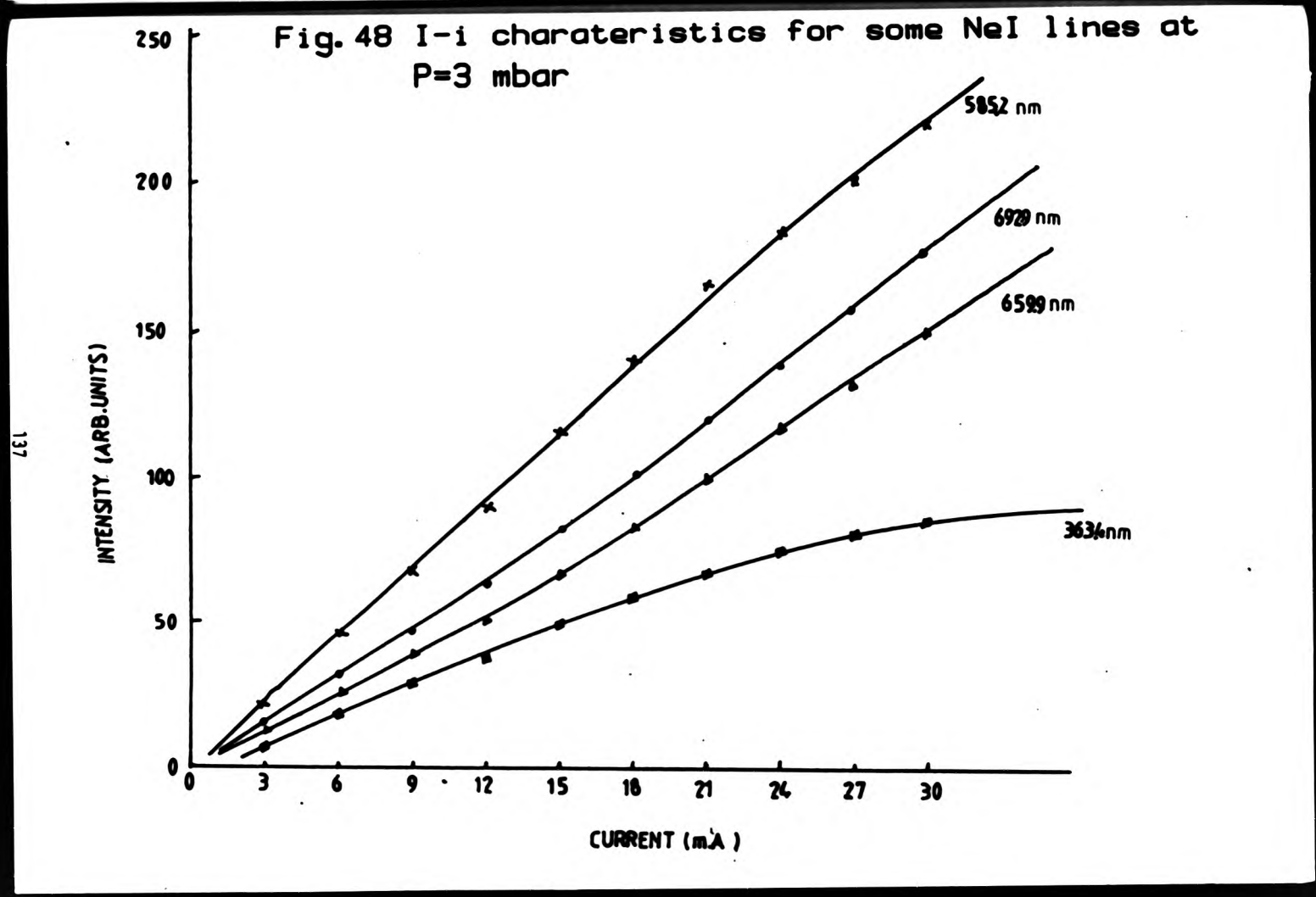
Fig. 48 I-i charateristics for some NeI lines at P=3 mbar
5852 nm
6929 nm
6599 nm
3634nm
INTENSITY (ARB.UNITS)
CURRENT (mA)
0
50
100
150
200
250
0
3
6
9
12
15
18
21
24
27
30

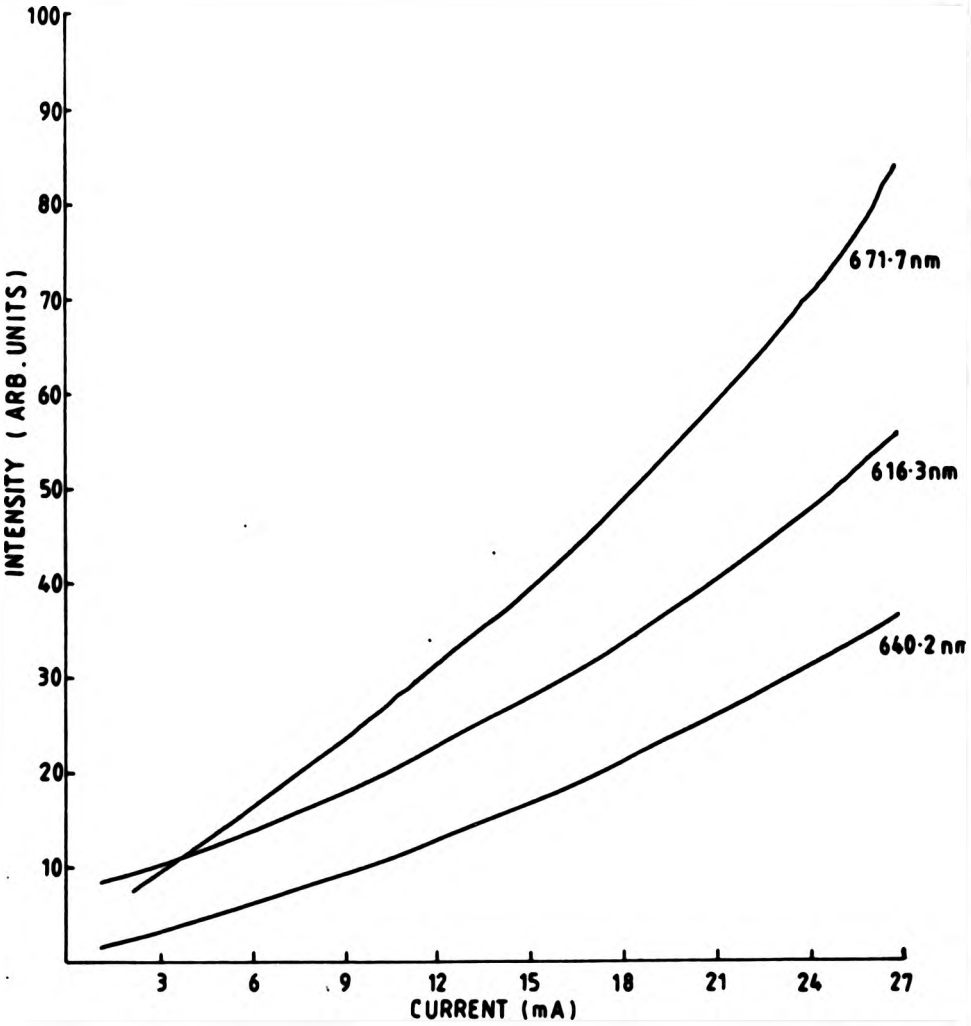

Fig. 49 I-i graphs for some NeI lines at P=5 mbar

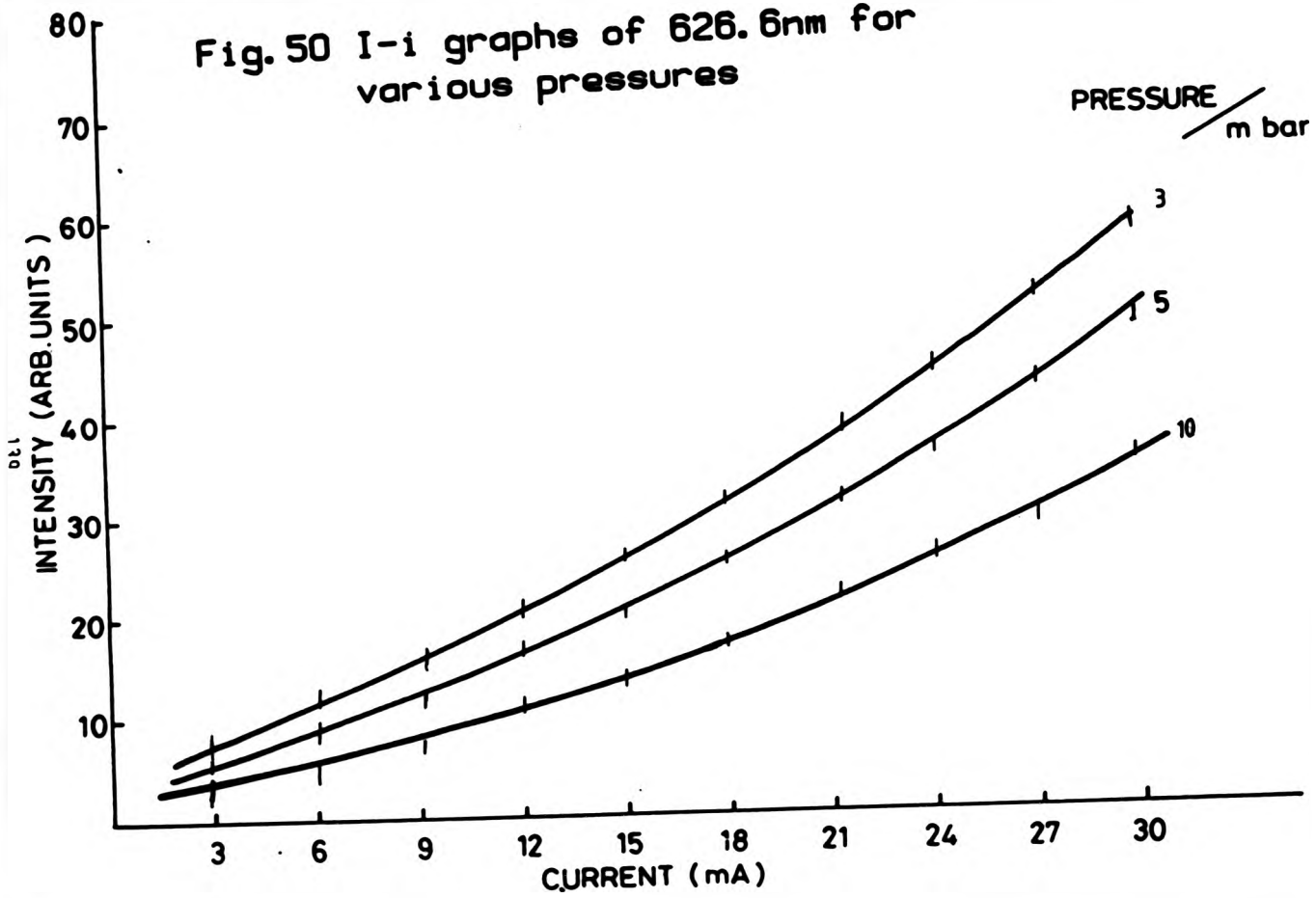
Fig. 50 I-i graphs of 626.6nm for various pressures
PRESSURE / m bar
3
5
10
INTENSITY (ARB.UNITS)
80
70
60
50
40
30
20
10
3
6
9
12
15
18
21
24
27
30
CURRENT (mA)

3p' groups, it was justified in our case to put the B value to zero. Since the number density of the metastables is not proportional to the discharge current, a modified I-i equation of the form

$$I = Ai\ (1 + B'\ N'\ (i)\ ) \qquad (9.3)$$

was used to fit the intensity-current results.

Where I : Intensity

A : Depends on the importance of single-step excitation

B' : Depends on the relative importance of two-stage excitation via an intermediate state

i : The discharge current

and N'(i) : The population density of the intermediate level.

A similar form of modified I-i equation (9.3) has been used by Light (19) to fit his results from the hollow cathode discharge. By curve fitting techniques, he has tried several forms of the I-i equation to obtain the best fits. For the spectral lines for which the I-i curves do not tend toward the origin at the lowest sustainable discharge current he has used a constant G to give the I-i equation form of

$$I = Ai\ (1 + B' \sum_{J=1}^{4} N_J(i)\ ) + G \qquad (9.4)$$

In this work another computer program (see appendix C) was

written using least square fitting for the intensity-current results. The theory of least square fitting for this computer program is given in appendix D.

To carry out the computation for I-i results, the number of current steps used was given to the computer followed by the population density of the metastable atoms (intermediate level), and the experimental intensity for each discharge current step; after execution of the program, the calculated intensity from the formula and values of A, A.B', residual, and the fractional residual were obtained and printed.

The spectral lines selected for fitting the intensity-current results were lines with negligible self-absorption.

Satisfactory fits were obtained for the intensity-current results for some NeI spectral lines when the population density of the metastable state $3s(3/2)_2^\circ$ (the highest compared with other 3s, 3s' group levels) was used, but for some other spectral lines the residual was large and less satisfactory fits were obtained, which could indicate that the probability of excitation from the metastable state is low and from the non-metastable is high.

Some authors (30,44) present effective stepwise excitation cross-section values independent of the electron energy. For that they summarized the four levels (3s, 3s' groups) to a common level with a total number density.

Much better fits were obtained when for N' (the number density of the intermediate level) the total population densities of the four lower excited state of 3s and 3s' levels were used. These four lower excited states of neon are closely spaced in energy (Fig.44), therefore electron collisions can easily change one state into another in discharge conditions and provide a strong coupling between the number densities of these four levels. Furthermore when the radiation is imprisoned (ultra-violet radiation to the ground state) in the gas, the radiative levels behave just like metastable state, so one can take these four levels (3s, 3s' groups) as one level, acting as an intermediate state for stepwise excitation.

Valignat and Leveu (44) derived an equation for the population density of the upper energy level of a given line in neon positive column discharge.

$$n_i = \frac{n_e \cdot Z_{oi} \cdot n}{\sum_j \gamma_{ij}} + \frac{n_e \cdot Z_{ji} \cdot \sum_j m_j}{\sum_j \gamma_{ij}} \qquad (9.5)$$

Where n_i : is the population density of the the ^3P level

n_e : number density of the electrons

Z_{oi} : direct excitation rate of the i level

n : population density of the ground state

γ_{ij} : relaxation frequency

Z_{ji} : stepwise excitation rate

and m_j : number density of the Jth $3s, 3s'$ level

In this equation the first term is connected with the direct

excitation from the ground state and the second term with stepwise excitation. The latter takes into account the total population densities of the metastable atoms lumped together into a single level. Table 2 shows the effective average excitation cross-section of neon 3p,3p' levels from their results (44).

LEVEL	DIRECT EXCITATION CROSS-SECTION $\overline{Q_{oi}}$ (10^{-19} cm^2)	STEPWISE CROSS-SECTION $\overline{Q_{si}}$ (10^{-16} cm^2)
$3p'(1/2)_0$	5	5
$3p'(1/2)_1$	2	4
$3p\ (1/2)_0$	0.95	1.1
$3p'(3/2)_1$	3.1	8.5
$3p'(3/2)_2$	1.6	5.7
$3p\ (3/2)_2$	2.6	15
$3p\ (3/2)_1$	1.2	6
$3p\ (5/2)_2$	1	17
$3p\ (5/2)_3$	3.8	36
$3p\ (1/2)_1$	1.3	16

TABLE 2.

Tables 10 gives values of A and B′ for the intensity-current results of NeI spectral lines 671.7, 692.9, 630.5, and 585.2 nm respectively for various neon pressures.

The Values of A and B′ for some NeI lines for various pressures.

λ (nm)	PRESSURE(mbar)	A(ARB.UNITS)*	B′(10^{-17} m^3)
671.7	1	0.91	0.37
	3	0.81	0.42
	5	0.74	0.44
	10	0.62	0.47
692.9	1	1.30	0.068
	3	1.1	0.07
	5	0.96	0.075
	10	0.73	0.08
630.5	1	1.38	0.07
	3	1.2	0.07
	5	1.1	0.074
	10	0.92	0.08
585.2	1	0.53	0.056
	3	0.51	0.058
	5	0.47	0.062
	10	0.41	0.067

TABLE 10

* Arbitary Units, constant for a given spectral line.

Comparison of the experimental and calculated intensities using the I-i equation for NeI lines at p = 2 mbar.

	λ = 638.3 nm		λ = 616.3 nm	
CURRENT (mA)	EXP. INTENSITY	CAL. INTENSITY	EXP. INTENSITY	CAL. INTENSITY
3	12	12.2	6	5.8
6	26	25.5	13	12.7
9	40	40.4	21	20.9
12	55	55.2	29	29.2
15	71	70.6	38	37.8
18	86	85.8	46	46.4
21	101	101.4	55	55.1
24	117	116.7	64	63.7
27	132	131.6	72	72.6
30	147	147.1	81	80.6
	A=2.37 (ARB.UNITS)		A=.82 (ARB.UNITS)	
	B=.061 (10^{-17} m^3)		B=.16 (10^{-17} m^3)	
	RES. = .853		RES. = .62	

TABLE 11

Fig. 51 shows the agreement of the experimental and theoretical (using equation 9.3) for intensity-current results for NeI lines 585.2 and 626.6 nm. In Fig. 52 comparisons of the experimental and theoretical I-i results are shown for NeI lines 614.3 and 640.2 nm for which the fits were less satisfactory and large residuals were obtained, which could be due to self-absorption.

Howard et al (18) suggested for the spectral lines for which their intensity versus discharge current showed a downward shape (e.g. 363.4, 470.3 nm) that the collisional de-excitation by electrons has to be taken into account, since for high lying energy levels collisional de-excitation by electron is an important process, and for these spectral lines the modified form of the I-i equation is going to be of the form.

$$I = \frac{Ai\left(1+B'\sum_{i} N'(i)\right)}{1+Ci} \qquad (9.6)$$

with the magnitude of C depending on the importance of de-excitation processes. Light (19) used this form of I-i equation to fit his I-i results for NeI lines showing downward curvature for intensity against current; also he used the equation (9.6) to fit the I-i results for NeI line 585.2 nm which showed a very linear graph for intensity versus current. The reason he has used this form of I-i equation is due to the fact that 585.2 nm has upper energy level $3p'(\frac{1}{2})$ which is the highest in the 3p group and de-

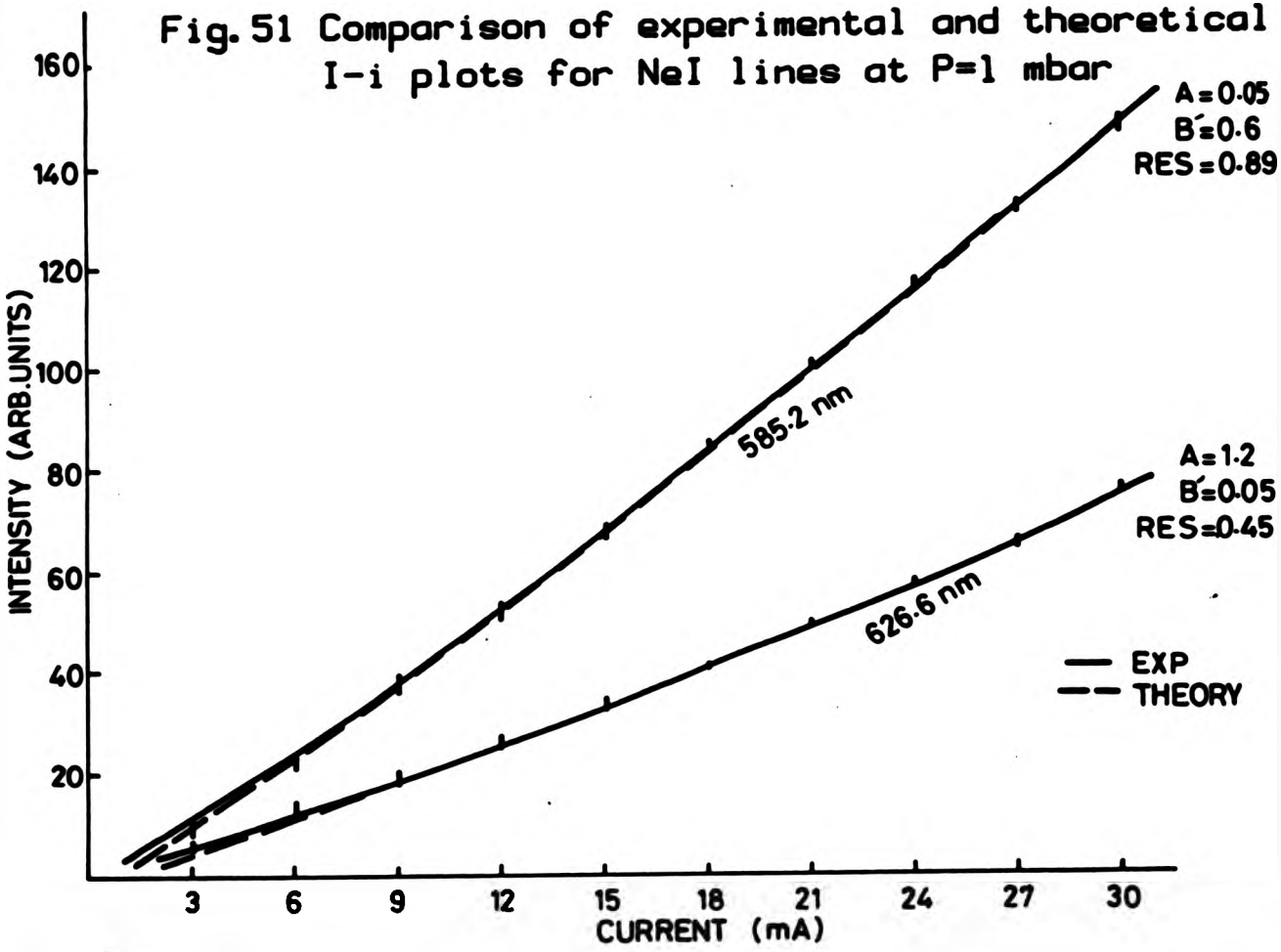

Fig. 51 Comparison of experimental and theoretical I-i plots for NeI lines at P=1 mbar

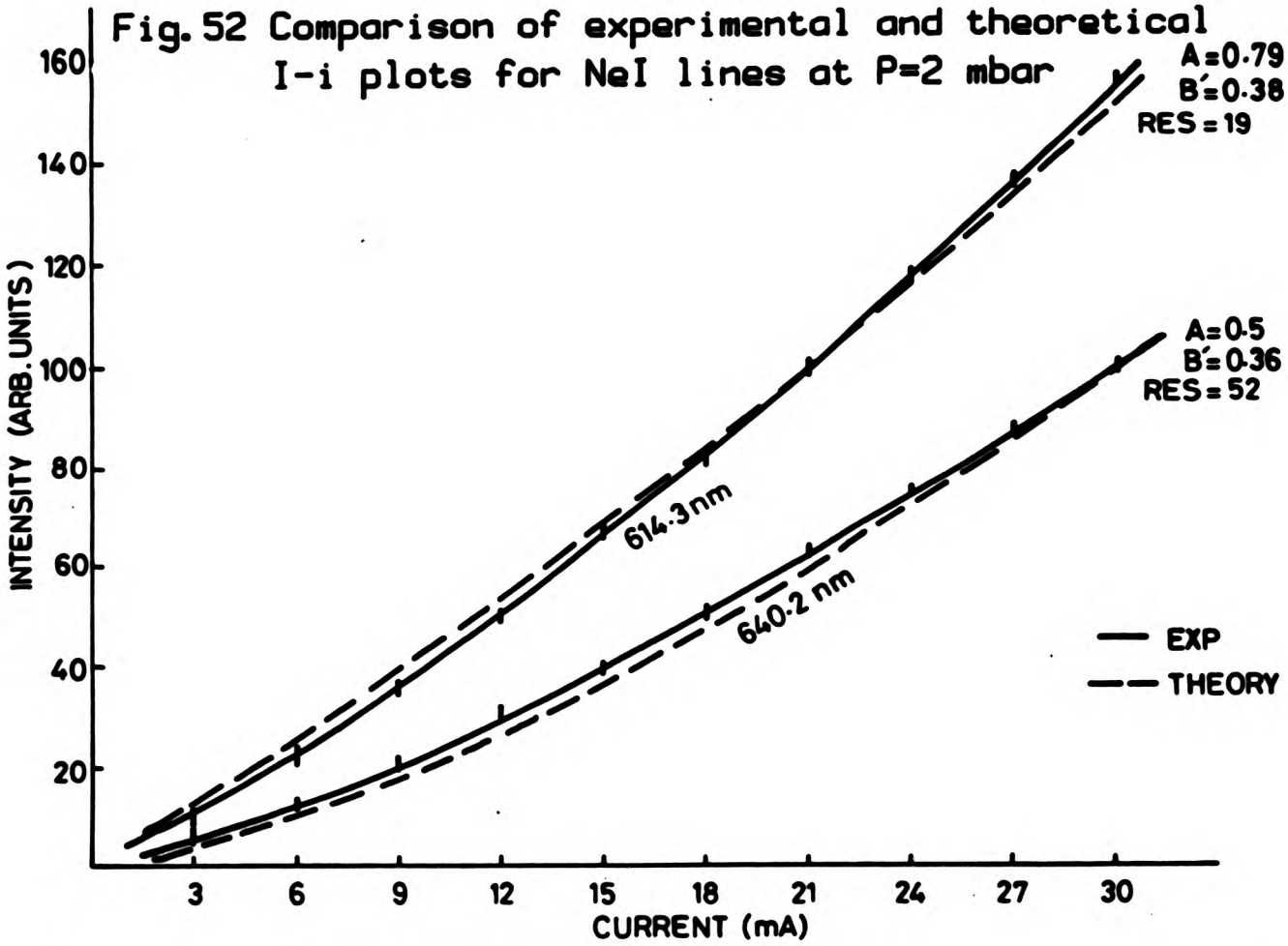
Fig. 52 Comparison of experimental and theoretical
I-i plots for NeI lines at P=2 mbar
A=0.79
B'=0.38
RES=19
A=0.5
B'=0.36
RES=52
614.3nm
640.2 nm
EXP
THEORY
INTENSITY (ARB.UNITS)
CURRENT (mA)
160
140
120
100
80
60
40
20
3
6
9
12
15
18
21
24
27
30

excitation by electrons for that level could be important. But another factor which must be considered for linearity of the I-i results for the NeI line 585.2 nm is that the ratio of the effective average cross-section for two-step and direct excitation for the $3p'(1/2)_0$ level is much lower compared with other 3p,3p' neon levels (44), therefore direct excitation may be the dominant process for this line.

The spectral lines for which the intensity-current results showed downward curvature were not studied in full detail in this work due to the low intensity of such spectral lines in the positive column discharge.

Self-absorption can change the shape of the intensity-current graphs of spectral lines. It has been suggested by Howard et al (18) that to consider this effect (self-absorption) the I-i equation (9.2) must be multiplied by a factor (1-Di) implying that the metastable population density is proportional to the discharge current. Since the rate of self-absorption of photons of a given spectral line will be proportional to the population density of the excited atoms in the lower energy level of the corresponding transition, and since the assumption of proportionality of the metastable number density to the discharge current is not true, one could bring a term of the form (1-DN'(i)) to the modified intensity-current equation, with magnitude of D depending on the importance of self-absorption.

When the intensity ratios of some neon lines against current were studied for spectral lines with common upper energy level and different lower levels (metastable, and non-metastable), the effect of self-absorption was observed for a few NeI lines corresponding to transitions terminating on the metastable state 3s $(3/2)^{o}_{1}$. The intensity ratio decreased slightly with respect to discharge current (see Fig.53). Ignoring the low current region, where error could be high, one can see 5-10% decrease of intensity ratio with current.

9.3 : THE INTENSITY-CURRENT RELATIONS IN ARGON:

In general the intensity-current curves for argon spectral lines studied in this work were very similar to those obtained for the neon lines. The argon lines for which measurements were carried out were limited, due to the fact that the strong ArI lines are above 750 nm, which is out of the range of the photomultiplier tube.

Fig. 54 shows the dependence of the intensity of some of the argon spectral lines on the discharge current. The effect of gas pressure on the I-i graphs of ArI 696.5 nm is shown in Fig.55. The modified I-i equation which was used for the neon results could also be applied for the intensity-current results for pure argon if number densities of the lower levels are known.

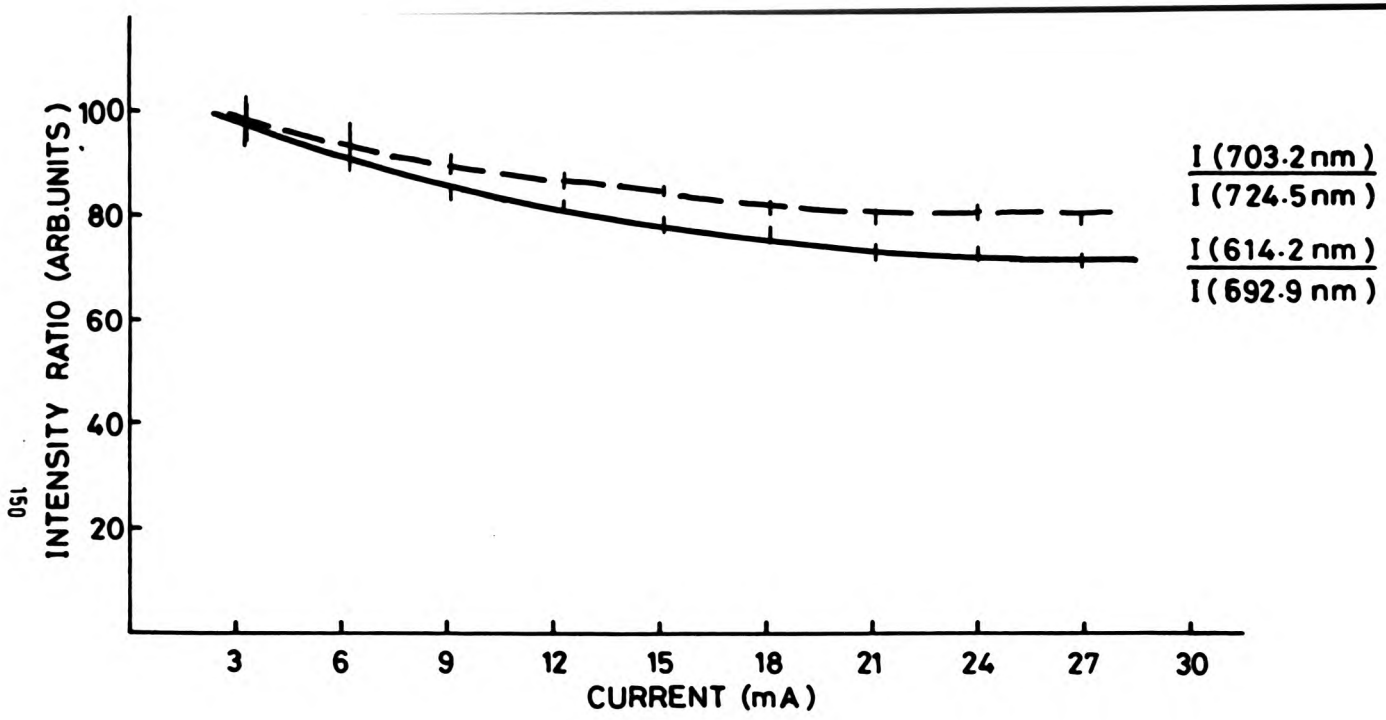

Fig. 53 Variation of intensity ratio against discharge current for NeI lines at P=5 mbar

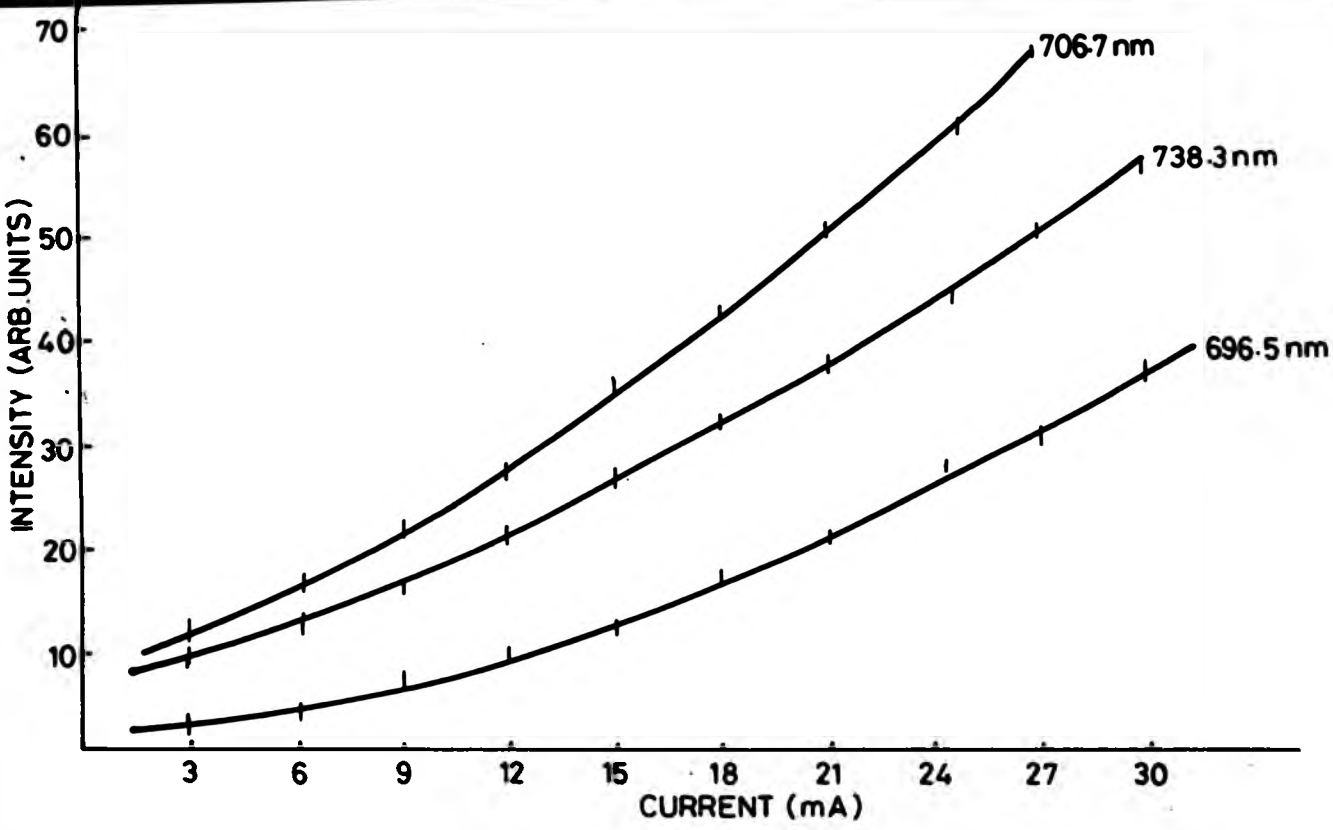

Fig. 54 Intensity-current characteristics for ArI lines at P=3 mbar

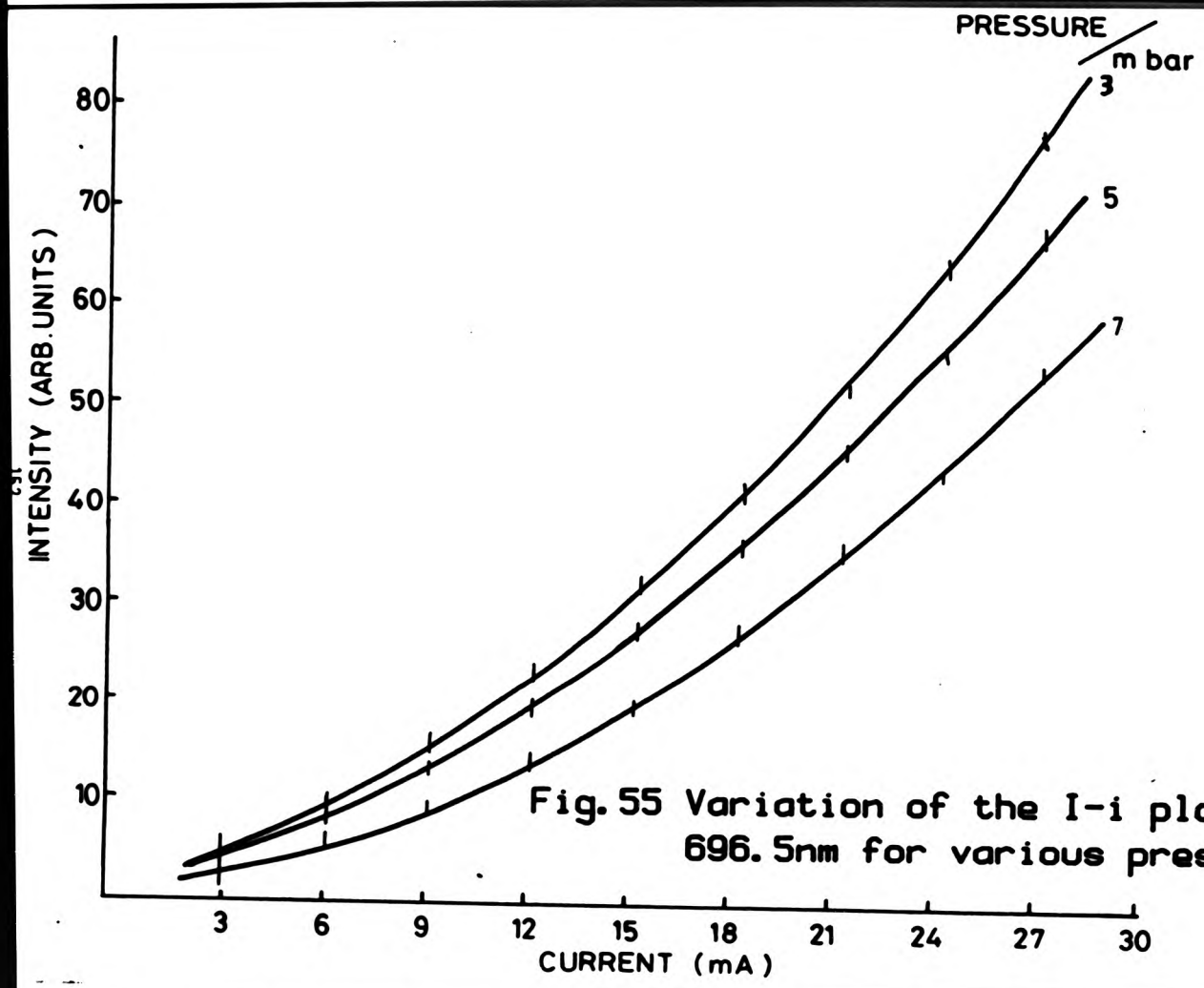

Fig. 55 Variation of the I-i plots for ArI 696.5nm for various pressures

9.4 : THE I-i RESULTS IN GAS MIXTURES (NEON-ARGON):

The effect of the various discharge parameters (current, pressure, etc) on the spectral line intensity is more difficult to establish in the case of gas mixtures than in pure gases. In this case, one must allow for changes in line intensities caused by collisions of the second kind, which may result in either intensification or weakening of the spectral lines.

When argon (1-3%) was added to a neon discharge, the upward curvature for NeI lines disappeared, indicating that two-stage excitation is no longer important, since the metastable atoms of neon are quenched by argon. This was proved when absorption measurements were carried out for neon-argon mixtures, which showed that number densities of neon decrease markedly by introducing argon to neon discharge. A linear graph was obtained for the intensity-current results of neon spectral lines having a small amount of argon added to neon discharge. Fig.56 shows the effect on the I-i graph of NeI line with 2% added argon to a neon discharge. In the equation (9.3) the term $\beta N'(i)$ will be negligible for the I-i results in neon-argon mixture since N'(i) for neon is greatly reduced in this case, and direct excitation then is the only significant process. Adding a small amount of neon to an argon discharge did not make any major change to the form of the argon I-i results.

Fig. 56 The I-i plots of NeI 626.6nm in pure neon and in argon-neon mixture

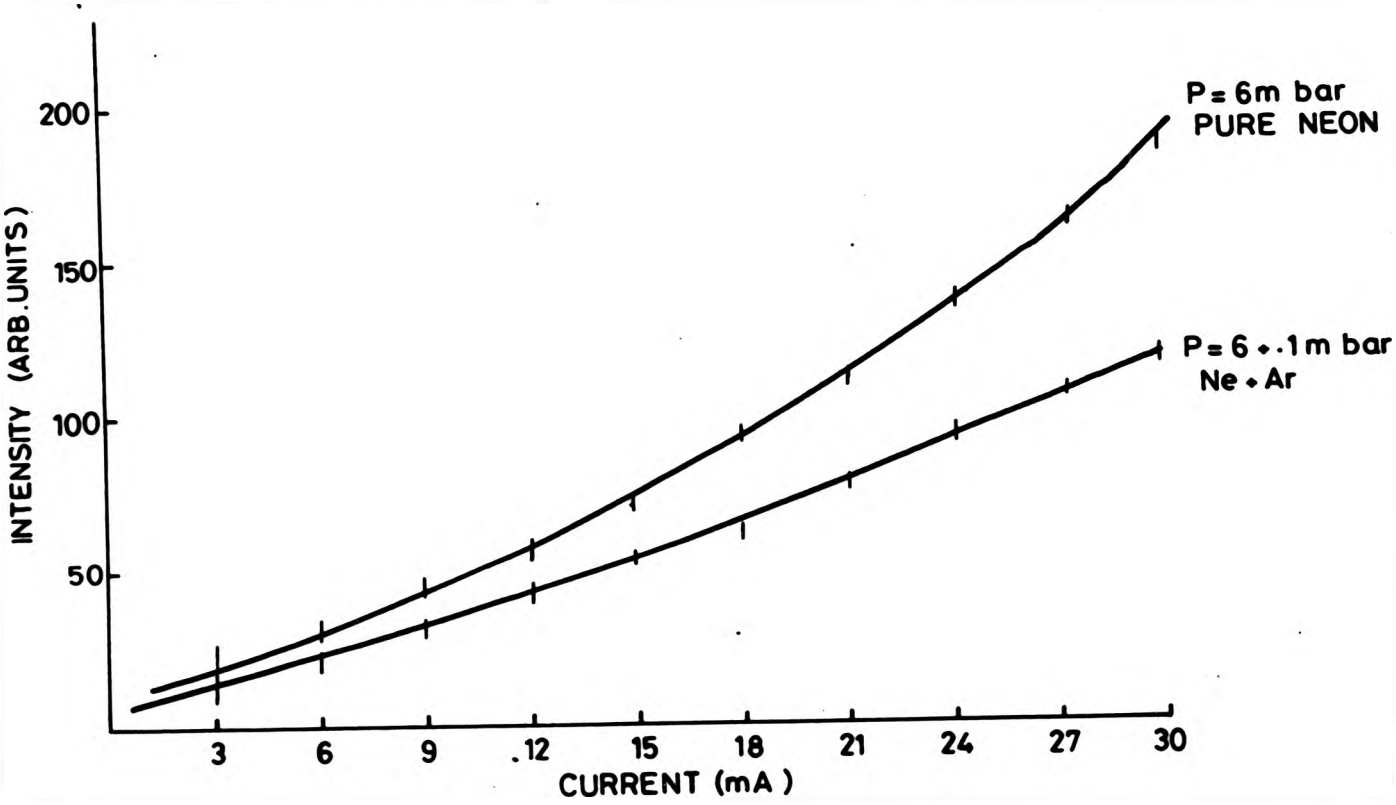

9.5 : RADIAL INTENSITY DISTRIBUTION

The higher pressure positive column discharge is characterised by a very strong constriction. This can visually be observed by looking at the light emission of such a column. It appears that this emission takes place in a narrow channel around the longitudinal axis, whereas the space between this luminous part and the tube wall remains dark.

The radial dependence of relative intensities of a number of neon spectral lines was studied, using end viewing of the positive column discharge. The radial intensity distributions for the NeI lines studied were very similar. The dependence of the radial intensity distribution on the pressure at given current for NeI spectral line (585.2 nm) is shown in Fig.57.

In case of argon as the carrier gas, the radial - distribution of intensity results were similar to those of neon, except in case of argon this contraction was more noticable.

Fig.58 shows the spatial distribution of intensity of the argon line 696.5 nm for given pressure and various discharge currents. It is clear that the intensity distribution profile contracts somewhat towards the axis with diminishing current. This contraction was more pronounced when gas pressure was higher.

Fig. 57 Radial intensity for NaI 585.2nm for different pressures

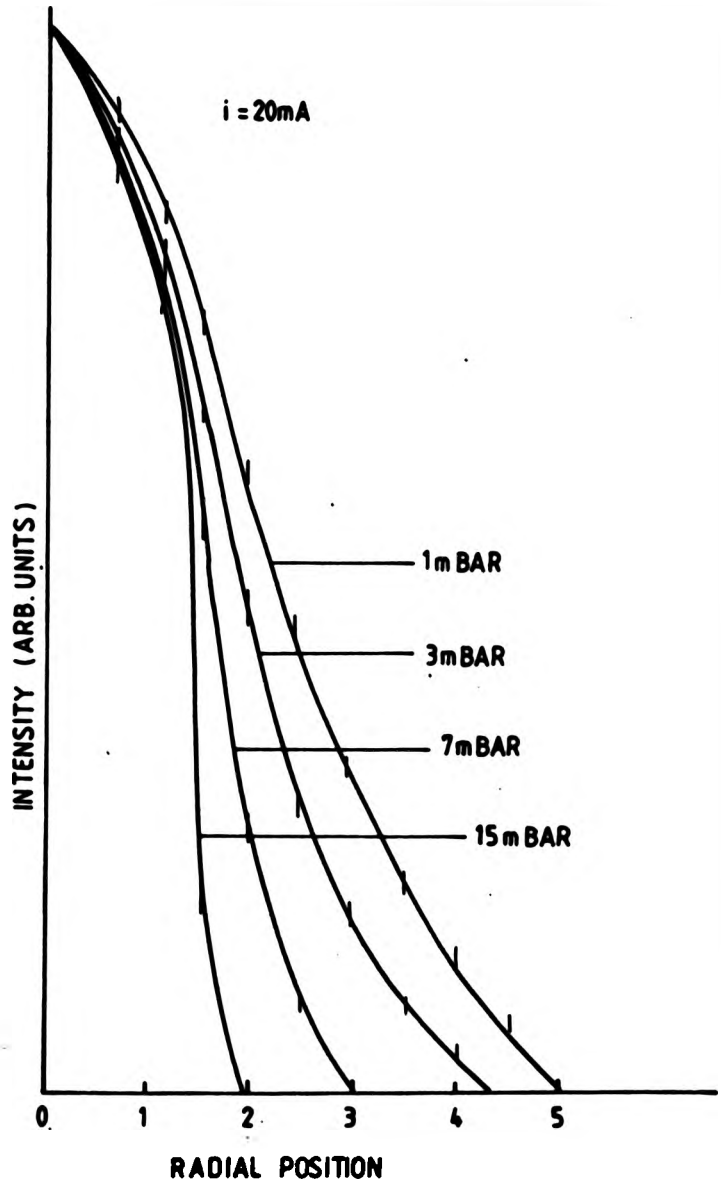

Fig. 58 Variation of radial intensity of ArI 696.5nm with discharge currents

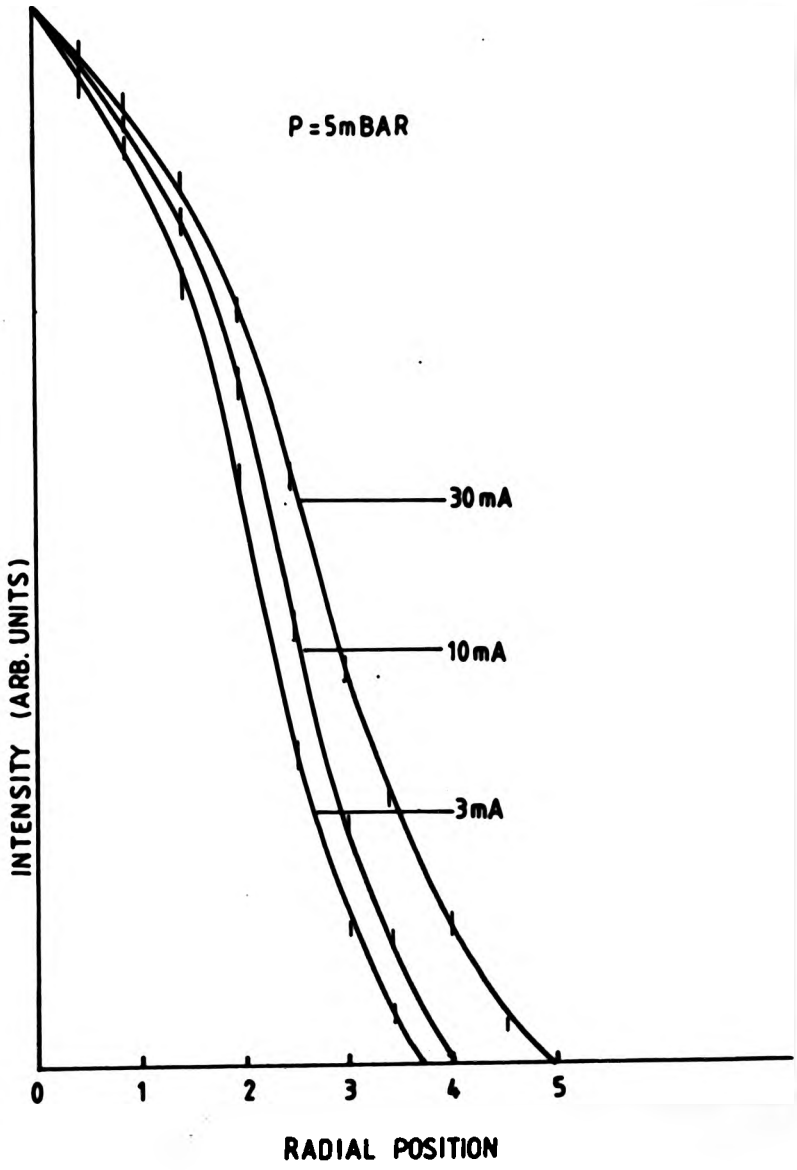

This strong constriction can be explained by the dependence of the excitation mechanisms on electron temperature. The discharge current density being much higher in the centre of the discharge tube. The radial distribution of the electrons is independent of both discharge current and pressure (45). Therefore higher gas temperature and lower gas density, (assuming pressure is constant); excitation and ionisation then takes place more in the middle part of the discharge tube.

The basic idea is that the excitation of high levels and the ionisation depends strongly on the type of tail of the electron velocity-distribution function; and the number of the fast electrons in the tail depends on the electron number density. Since the latter falls off from the centre to the edge of the discharge tube, the number of ionisations and excitations also decrease markedly, and as a result the glow intensity diminishes rapidly from the centre to the edge of discharge tube.

CHAPTER (10) SUMMARY AND CONCLUSION:

In this work the electrical and spectral characteristics of the low pressure positive column discharge were investigated under various discharge conditions.

To avoid the effects due to sputtering from a plane cathode, and extend the pressure and discharge current range, hollow or heated filament cathodes were employed in the positive column discharge tubes. This also allowed a better estimation of the electric field strength along the positive column to be made due to the lower tube voltage required compared with a plane cathode.

Tube voltage was monitored for each set of measurements, and voltage versus current curves were checked with time to asertain their reproducibility and to show any changes in gas purity. The electrical characteristics of the positive column discharge were found to be reproducible under similar conditions, unless gas was left inside the vacuum system for long period of time, when the results were less reproducible due to contaminations.

All the measurements were carried out under maximum purity; since the cathode surface (when a plane cathode was used) was fully covered by negative glow an abnormal discharge was obtained and voltage-current graphs had an increasing positive slope. When a hollow cathode was used in the positive column tube the v-i curves showed a flat

characteristic known as hollow cathode effect.

The Fabry-Perot interferometer emission scans of NeI spectral lines terminating on the metastable state of neon $3s(3/2)^{\circ}_{1}$ showed a self-reversal effect when end viewing of the positive column was employed for investigation, indicating a high concentration of the metastable atoms in that level; the F.P.I. emission scans of NeI lines terminating on the other 3s and 3s' group levels did not exhibit any sign of self-reversal.

Consequently the number densities of the 3s, 3s' levels of neon were determined by direct absorption measurements. The absorption results showed that population density of the metastable atoms depends on the discharge current at low current, and as the discharge currents increased the population density of the metastable atoms reaches a saturation level at a certain discharge current. this saturation behaviour was less pronounced at lower pressures (less than 1.0 mbar) where diffusion of the metastable atoms to the discharge tube walls is high. The number densities of the radiative states against current did not show a saturation effect; a gradual increase with discharge current was observed (in general agreement with (19,44)). The population densities obtained for the excited states 3s and 3s' levels of neon are the same order of magnitude as in other published work (33,44).

The variation of the population density of the argon metastable level 4s $(3/2)_2$ with respect to the discharge current was similar to that obtained for the neon metastable, but the number density of this metastable state of argon was an order of magnitude less than the neon metastable atoms in the $3s(3/2)_2^o$ state. In the cases of neon and argon the lowest radiative state is located less than one-tenth of an electron volt above the lowest metastable state, so that process of excitation to a nearby higher radiating state is energetically possible in thermal collisions. The upper metastable state in neon and argon could be destroyed by de-excitation to lower radiating state, as well as excitation to the upper radiative level.

The intensity-current results for neon spectral lines showed three forms of graphs, neutral gas atom lines with transitions between 3p,3p'-3s,3s' some showed linear graphs (indicating that direct excitation is important), and some showed upward curvature (indicating that two-step excitation via an intermediate state is important as well as direct excitation from the ground state), and those with transitions amongst the high lying levels (e.g. 363.3 nm) tended to saturate (where de-excitation by electrons play an important role). Self-absorption can also effect the I-i curves and cause the graphs to exhibit slight downward curvature.

The I-i results from the hollow cathode discharge (1,19) showed a very similar pattern to those obtained from the positive column discharge in this work. The I-i equation suggested by Howard et al (18) was modified and used for fitting the present intensity-current results.

$$I = Ai \left(1 + B' \sum_{j=1}^{4} N_j' (i) \right) \qquad (10.1)$$

Good fits for the I-i results were found when the total population densities of the four lower excited states (3s, 3s' groups) of neon were used in the modified I-i equation for the intensity versus current results. Even better fits and lower residuals were obtained for the I-i results when the values of number densities and the experimental intensities corresponding to low discharge current (1,2,3 mA) were neglected for computation due to their larger errors. The value of A in the I-i equation decreases as pressure increases and that of B' increases slightly with pressure. This may be explained by variation in the energy distribution of electrons with pressure, so that the proportion of low energy electrons compared with high ones increases with gas pressure. The B' values for lines with common upper level are roughly equal (Table 10 gives data for NeI lines 692.9 and 630.5 nm). Less satisfactory fits were obtained for the intensity-current results for spectral lines which could be self-absorbed (terminating to the metastable state). It has been suggested by Howard et al (18) for these sort of spectral lines a factor of (1-Di)

be used in the I-i equation, but in the modified form of the I-i relationship, it will be in the form

$$I = Ai\ (1 + B' \sum_{J=1}^{4} N'_J\ (i))\ \ (1-D\sum_{i} N'(i)) \qquad (10.2)$$

The upward curvature for the NeI spectral lines disappeared when a small amount of argon (a few percent) was introduced to a neon discharge, indicating that two-stage excitation is not important any more, since by adding argon to a neon discharge the intermediate level (metastable state of neon) for stepwise excitation is quenched and destroyed by argon. Removal of the self-reversal effects on the NeI lines and marked reduction of the population densities of metastable atoms of neon when a small amount of argon was introduced to a neon discharge were good evidence for this (disappearing of upward curvature for the intensity-current curves of neon spectral lines). Quenching of the population density of the metastables, will reduce the probability of two-step excitation and change the form or shape of the intensity versus discharge current graphs. An attempt was made all the time to carry out the measurements under maximum purity, so that contaminations would not alter the results.

The intensity-current graphs for the ArI spectral lines showed a very similar pattern to those obtained for neon lines. In this case adding a small amount of neon to argon discharge did not make significant change to the form of the I-i curves of argon lines. This is in agreement with

measurements of population density of the argon metastable state $4s(3/2)_2$ in an argon-neon mixture where no significant changes was observed on the number density of $4s(3/2)_2$ state when neon (by a small amount) was introduced to an argon discharge.

Separation of gases (cataphoresis) in neon-argon mixtures was observed, specially in longer positive column tubes, but to avoid the effects due to this, the area of discharge tube near anode was used for all the measurements.

Pressure and current both have a marked influence on the radial intensity distribution; by increasing pressure, constricted discharge was observed, and the intensity distribution profiles became narrower. Reduction of the discharge current resulted in the profiles contracting somewhat toward the axis.

REFERENCES

1 Howard., C., MPhil Thesis, C.N.A.A., (1983)

2 Pillow, M.E., Spectrochim. Acta, 36B, No.8, 821-843, (1981)

3 Klarfeld, B., J.Techn. Phys. USSR, 4, 44, (1937) 5, 725, (1938)

4 Gross, O., Z. Physik, 88, 741, (1934), A

5 Francis, G., The Glow Discharge at Low Pressure, Handbuch Der Physik, XXII, 154-161

6 Guntherschulze, A., Z. Physik, 41, 718, (1927)

7 Schellenmeier, H., Z. Physik, 122, 269, (1944)

8 Golobovskii, YU.B., Kagan, YU.M., and Lyagushchenko, R.L., Opt. Spect., 20, 317, (1966)

9 Headrick, L.B., and Duffenduck, O.S., Physical Rev., 37, 737-755, (1931)

10 Hackam, R., spectroscopy Let., 6 (11), 653-658, (1973)

11 Loeb, L.B., J. Appl. Phys., 29, 1369, (1958)

12 Santorum, C., Physica, 83c, 367-372, (1976)

13 Gaur, J.P. and chanin, L.M., J. Appl. Phys., 40, 256, (1969)

14 Kagan, YU.M., Lyagushenko, R.L., and Khakhaev, A.D., Opt. Spect., vol., 14, 317-322, (1963)

15 Golobovskii, Y U.B., Ivanov, V.A., and Kagan, YU.M., Opt. Spect., vol., 32, 464-467, (1972)

16 Frisch, S.E., and Kagan, YU.M., zh.Exp.Teor. Fiz., 11, 286, (1941)

17 Musha, T., J.Phys. Soc. Japan, 17, 1440, (1962)

18 Howard, C., Pillow, M.E., Steers, E.B.M., and Ward, D.W., Analyst, vol., 108, 145-152, (1983)

19 Light, C.E. Private Communication (1987)

20 Mouwen, C.A.M., PhD Thesis, Eindhoven University of Technology, (1971)

21 Golobovskii, YU.B., Kagan, YU.M., and Lyagushchenko, R.L, Opt.Spect., vol. xxI, No. 5, 295-297, (1965)

22 Milenin, V.M., Opt.Spect., 46, 1209-1210, (1979)

23 Gofmeister, V.P. and Kagan, YU.M., Opt.Spect., 25, 185, (1968)

24 Strauss, J.A., Ferreira, N.P., and Human, H.G.C., Spectrochimica Acta, vol. 37B, No., 11, 947-957, (1982)

25 Soldatov, A.N., Evtusheko, G.S., and Muraveu, I.I., Opt.Spect., vol.34, No., 2, 6-8, (1973)

26 Smits, R.M.M., and Prins, M., Physica, 80c, 571-584, (1975)

27 Van Schaik, N., Steenhuijsen, L.W.G., Van Bommel, P.J.M., Van Nieuwenhuyzen, J.C.A.M., J.De. Physique Colleque C7, 27-28 (1979)

28 Akhmedzhovov, R.A, Polushkin, I.N., Khanin, YA.I., and Yazenkov, V.V., Fiz. Plazmy, 8, 333-338, (1982)

29 Golobovskii, YU.B., Kagan, YU.M., and Komarova, L.L., Opt.Spect., vol., 33, 440-441, (1972)

30 Delcroix, J.L., Ferreira, c.M., and Ricard, A., Principles of Laser Plasma Chapter (5), 159-233

31 Lisitsyn, V.N., Provorov, A.S., and Chebotaev, C.P., Opt.Spect., vol., 29, 119-122, (1971)

32 Mityureva, A.A. and Penkin, N.P., Opt.Spect., vol., 38, No.2 229-230, (1975)

33 Behnke, J.F, Deutsch, H., and Scheibner, H., Beitr. Plasma Phys., 25, 41-56, (1985)

34 Van Deldhuizen, E.M., PhD Thesis, University of Technology of Eindhoven, (1983)

35 Smits, R.M.M., Lammers, P.H.M., Baghuts, L.C.J, Hagedooren, H.L., and Heide, J.A.V.D., Beitr. Plasma Phys., 5, 157-168, (1974)

36 Reed, A.M., PhD Thesis, C.N.A.A., (1980)

37 Stocker, B.J., BR.J. Applied Phys., 12, 465, (1961)

38 Atomic Transition Probability, N.B.S. 4, 126-129

39 Mitchell and Zemansky, Resonance Radiation and Excited Atoms, Cambridge Univ. Press., (1934, 1971)

40 Jarrett, S.M., Franken, P.A, J. Opt.Soc. Amer., 35, 1603, (1965)

41 Stacy, D.N., Vaughan, J.M., Phys. Let., 11, 105, (1964)

42 Vaughan, J.M., Proc. Roy.Soc., A295, 164, (1966)

43 Fried, B.D., and Conte, S.D., The Plasma Dispersion Function, New York, Academic Press., (1961)

44 Valignat, s., Leveau, J., Physica, 104C, 441-450, (1981)

45 Yarnold, G.D., and Holmes, S., Phil.Mag., 22, 988, (1936)

ADDITIONAL LITERATURE:

Thorne, A.P., Spectrophysics, (1974)

Kuhn, H.G., Atomic Spectra 2nd Ed. (1969)

Von Engel, A., Ionized Gases, 2nd Ed., (1964)

American Inst. of Phys. Handbook, 2nd Ed., p.7-122

Weston, G.F., Cold Cathode Glow Discharge Tubes, (1968)

Acton, J.R., and Swift, J.D., Cold Cathode Discharge Tubes, (1963)

APPENDIX : A

"MENU"

```
10 CLEAR
20 DISP "Digitize data                    1"
30 DISP "Check data                       2"
40 DISP "Correct data                     3"
50 DISP "Display log ratio                4"
55 DISP "Plot original curves             5"
60 DISP "Quit programme                   6"
70 INPUT V
80 IF V=1 THEN CHAIN "TRY1"
90 IF V=2 THEN CHAIN "TRY2"
100 IF V=3 THEN CHAIN "TRY4"
110 IF V=4 THEN CHAIN "TRY5"
115 IF V=5 THEN CHAIN "TRY6"
120 END
```

```
1 REM TRY1
10 PLOTTER IS 705
20 DIM T$[32]
30 DISP "ENTER FILENAME TO BE USED - UP TO 6 CHARACTERS"
40 DISP "THE FILES USED SO FAR ARE" @ CAT ":D701"
45 D$=":D701"
50 INPUT A$
55 A$=A$&D$
60 CREATE A$,100
70 DISP "ENTER DATA TITLE - NO MORE THAN 32 CHARACTERS"
80 INPUT T$
90 ASSIGN# 1 TO  A$
100 PRINT# 1 ; T$
110 DIM X(10,50),Y(10,50)
120 DISP "MOVE SIGHT TO START OF BASELINE  - PRESS ENTER ON GRAPH PLOTTER"
130 DIGITIZE X1,Y1,P1
135 PRINT# 1 ; X1,Y1
140 DISP "MOVE SIGHT TO END OF BASELINE - PRESS ENTER ON GRAPH PLOTTER"
150 DIGITIZE X2,Y2,P2
155 PRINT# 1 , X2,Y2
156 DISP "ENTER THE WAVENUMBER DIFFERENCE BETWEEN START AND END POINTS"
157 INPUT W
158 PRINT# 1 ; W
160 DISP "ENTER NUMBER OF POINTS TO BE DIGITIZED" @ INPUT N1
170 DISP "ENTER NUMBER OF CURVES TO BE DIGITIZED" @ INPUT N2
180 PRINT# 1 ; N1,N2
190 DX=(X2-X1)/(N1-1)
200 N=1
210 PLOT X1,Y1
220 FOR K=1 TO N2
230 DISP "MOVE SIGHT TO CURVE ";K
240 DISP "PRESS ENTER ON PLOTTER"
250 DIGITIZE X(K,N),Y(K,N),P
251 IF ABS ((X(K,N)-X1)/X1)<.01 THEN GOTO 270
252 PLOT X1,Y1
253 GOTO 230
270 PRINT# 1 ; X(K,N),Y(K,N)
280 NEXT K
290 X1=X1+DX
300 N=N+1
310 IF N>N1 THEN GOTO 330
320 GOTO 210
330 FOR N=1 TO N1
340 FOR K=1 TO N2
350 DISP Y(K,N);
360 NEXT K
370 DISP
380 NEXT N
390 ASSIGN# 1 TO  *
395 PAUSE
396 CHAIN "MENU"
400 END
```

```
1 REM TRY2
10 PLOTTER IS 1
20 DIM X(10,50),Y(10,50)
30 DIM T$[32]
40 DISP "ENTER FILENAME - THE FILES AVAILABLE ARE:-" @ CAT ":D701"
45 D$=":D701"
50 INPUT A$
55 A$=A$&D$
60 ASSIGN@ 1 TO  A$
70 READ@ 1 ; T$
80 DISP T$
85 READ@ 1 ; X1,Y1,X2,Y2
86 READ@ 1 ; W
90 READ@ 1 ; N1,N2
100 DISP N1,N2
110 FOR N=1 TO N1
120 FOR K=1 TO N2
130 READ@ 1 ; X(K,N),Y(K,N)
140 NEXT K
150 NEXT N
160 ASSIGN@ 1 TO  *
170 GCLEAR
180 FOR K=1 TO N2
190 MOVE X(K,1),Y(K,1)
200 FOR N=2 TO N1
210 DRAW X(K,N),Y(K,N)
220 NEXT N
230 NEXT K
231 PAUSE
232 CHAIN "MENU"
240 END
```

```
1 REM TRY3
10 PLOTTER IS 1
20 DIM X(10,50),Y(10,50)
30 DIM T$[32]
40 DISP "ENTER FILENAME - THE FILES AVAILABLE ARE:-" @ CAT
50 INPUT A$
60 ASSIGN@ 1 TO  A$
70 READ@ 1 ; T$
80 DISP T$
85 READ@ 1 ; X1,Y1,X2,Y2
86 READ@ 1 ; W
90 READ@ 1 ; N1,N2
100 DISP N1,N2
110 FOR N=1 TO N1
120 FOR K=1 TO N2
130 READ@ 1 ; X(K,N),Y(K,N)
140 NEXT K
150 NEXT N
160 ASSIGN@ 1 TO  *
170 GCLEAR
180 FOR K=2 TO N2
190 FOR N=1 TO N1
200 DISP N,LOG ((Y(1,N)-Y1)/(Y(K,N)-Y1))
210 NEXT N
220 NEXT K
230 GCLEAR
240 SCALE 0,N1,0,1.5
250 FOR K=2 TO N2
260 FOR N=1 TO N1
270 IF N=1 THEN MOVE N,LOG (Y(1,N)/Y(K,N))
280 DRAW N,LOG (Y(1,N)/Y(K,N))
290 NEXT N
300 NEXT K
301 PAUSE
302 CHAIN "MENU"
310 END
```

```
1 REM TRY4
10 PLOTTER IS 705
20 DIM X(10,50),Y(10,50)
30 DIM T$[32]
40 DISP "ENTER FILENAME - THE FILES AVAILABLE ARE :-" @ CAT ": D701"
45 D$=":D701"
50 INPUT A$
55 A$=A$&D$
60 ASSIGN@ 1 TO  A$
70 READ@ 1 ; T$
80 DISP T$
85 READ@ 1 ; X1,Y1,X2,Y2
90 READ@ 1 ; N1,N2
100 DISP N1,N2
110 FOR N=1 TO N1
120 FOR K=1 TO N2
130 READ@ 1 ; X(K,N),Y(K,N)
140 NEXT K
150 NEXT N
160 ASSIGN@ 1 TO  *
170 DISP "ENTER NUMBER OF CURVE WHICH HAS ERROR" @ INPUT K
180 FOR N=1 TO N1
190 PLOT X(K,N),Y(K,N)
200 DISP "IS THIS CORRECT Y OR N " @ INPUT Q$
210 IF Q$ <> "N" THEN GOTO 240
220 DISP "MOVE SIGHT TO CORRECT POSITION - PRESS ENTER" @ DIGITIZE X(K,N),Y(K,N)
.P
240 NEXT N
250 ASSIGN@ 1 TO  A$
260 PRINT@ 1 ; T$,X1,Y1,X2,Y2
270 PRINT@ 1 ; N1,N2
290 FOR N=1 TO N1
290 FOR K=1 TO N2
300 PRINT@ 1 ; X(K,N),Y(K,N)
310 NEXT K
320 NEXT N
330 ASSIGN@ 1 TO  *
331 PAUSE
332 CHAIN "MENU"
340 END
```

```
1 REM TRY5
10 PLOTTER IS 705
20 DIM X(10,50),Y(10,50)
25 DIM S(10)
30 DIM T$[32]
40 DISP "ENTER FILENAME - THE FILES AVAILABLE ARE:-" @ CAT ":D701"
45 D$=":D701"
50 INPUT A$
55 A$=A$&D$
60 ASSIGN# 1 TO  A$
70 READ# 1 ; T$
80 DISP T$
85 READ# 1 ; X1,Y1,X2,Y2
86 READ# 1 ; W
90 READ# 1 ; N1,N2
100 DISP N1,N2
110 FOR N=1 TO N1
120 FOR K=1 TO N2
130 READ# 1 ; X(K,N),Y(K,N)
140 NEXT K
150 NEXT N
160 ASSIGN# 1 TO  *
170 GCLEAR
180 FOR K=2 TO N2
190 FOR N=1 TO N1
191 IF Y(K,N)<Y1 THEN GOTO 205
195 Y(K,N)=LOG ((Y(1,N)-Y1)/(Y(K,N)-Y1))
200 GOTO 210
205 Y(K,N)=Y(K,N-1)
210 NEXT N
220 NEXT K
230 YM=0
240 FOR K=2 TO N2
250 N6=INT (N1/2)-5 @ N7=N6+10
251 FOR N=N6 TO N7
260 IF Y(K,N)>YM THEN YM=Y(K,N)
270 NEXT N
280 NEXT K
292 DISP "PRESS P1 ON PLOTTER - THEN PRESS ENTER"
300 DIGITIZE X3,Y3,P3
310 DISP "PRESS P2 ON PLOTTER - THEN PRESS ENTER"
320 DIGITIZE X4,Y4,P4
330 SCALE X3,X4,0,1.2*YM
340 DISP "PUT PAPER IN PLOTTER THEN PRESS CONT"
350 PAUSE
360 PEN 2
361 MOVE .1*(X4-X3),.9*YM @ LABEL T$
370 FOR K=2 TO N2
380 FOR N=1 TO N1
390 IF N=1 THEN MOVE X(K,N),Y(K,N)+.1*YM
400 DRAW X(K,N),Y(K,N)+.1*YM
410 NEXT N
420 NEXT K
430 K=1
440 FOR N=1 TO N1
450 MOVE X(K,N),.1*YM @ DRAW X(K,N),.12*YM
460 NEXT N
461 MOVE X(K,1),.1*YM @ DRAW X(K,N1),.1*YM
470 DISP "ENTER START POINT FOR INTEGRATION" @ INPUT I1
480 DISP "ENTER END POINT FOR INTEGRATION" @ INPUT I2
490 LINE TYPE 4
500 MOVE X(1,I1),.1*YM @ DRAW X(1,I1),YM
510 MOVE X(1,I2),.1*YM @ DRAW X(1,I2),YM
520 LINE TYPE 1
530 FOR K=2 TO N2
```

```
540 S1=0
550 S1=S1+Y(K,I1)/2
560 FOR N=I1+1 TO I2-1
570 S1=S1+Y(K,I1)
580 NEXT N
590 S1=S1+Y(K,I2)/2
591 S(K)=S1*W/(N1-1)
592 NEXT K
595 FOR K=2 TO N2
600 DISP K,S(K)
601 MOVE .8*(X4-X3),K*.05*YM+.5*YM @ LABEL USING "DD.DDD" ; S(K)
610 NEXT K
611 PAUSE
612 CHAIN "MENU"
620 END
```

```
1 REM TRY6
10 PLOTTER IS 705
20 DIM X(10,50),Y(10,50)
25 DIM S(10)
30 DIM T$[32]
40 DISP "ENTER FILENAME - THE FILES AVAILABLE ARE:-" @ CAT ":D701"
45 D$=":D701"
50 INPUT A$
55 A$=A$&D$
60 ASSIGN# 1 TO  A$
70 READ# 1 ; T$
80 DISP T$
85 READ# 1 ; X1,Y1,X2,Y2
86 READ# 1 ; W
90 READ# 1 ; N1,N2
100 DISP N1,N2
110 FOR N=1 TO N1
120 FOR K=1 TO N2
130 READ# 1 ; X(K,N),Y(K,N)
140 NEXT K
150 NEXT N
160 ASSIGN# 1 TO  *
170 GCLEAR
175 PEN 2
180 FOR K=1 TO N2
190 FOR N=1 TO N1
195 IF N=1 THEN MOVE X(K,N),Y(K,N)
200 DRAW X(K,N),Y(K,N)
210 NEXT N
220 NEXT K
611 PAUSE
612 CHAIN "MENU"
620 END
```

APPENDIX: B

```
10 CLEAR
20 DISP " DRAW AND LABEL AXES          1"
30 DISP " DRAW THEORETICAL CURVE       2"
40 DISP " ENTER DATA POINTS            3"
50 DISP " EXIT FROM PROGRAMME          4"
60 DISP
70 DISP " ENTER NUMBER OF ROUTINE REQUIRED" @ INPUT R
80 IF R=1 THEN GOTO 120
90 IF R=2 THEN GOTO 140
100 IF R=3 THEN GOTO 160
110 IF R=4 THEN GOTO 180
120 GOSUB DRAUGHT
130 GOTO 10
140 GOSUB THEORY
150 GOTO 10
160 GOSUB DINPUT
170 GOTO 10
180 END
190 DRAUGHT:
200 PLOTTER IS 705
210 NTH=0
220 DX=1 @ DY=1
230 CLEAR
240 DEG
250 DISP "MAX CURRENT";@ INPUT IMX
260 DISP "MAX INTENSITY";@ INPUT INX
270 IMAX=5*(INT (IMX/5)+1)
280 INMAX=5*(INT (INX/5)+1)
290 IF IMAX>30 THEN DX=2
300 IF INMAX>30 THEN DY=2
310 IF INMAX>100 THEN DY=4
320 IF IMAX>100 THEN DX=4
330 GCLEAR @ SETGU
340 LDIR 0
350 MOVE 60,10 @ LABEL "Current-mA"
360 LDIR 90
370 MOVE 5,40 @ LABEL "Intensity-Arbitrary Units"
380 LOCATE 15,120,20,90
390 SCALE 0,IMAX,0,INMAX
400 LAXES -5,5,0,0,DX,DY
410 MOVE 0,INMAX @ DRAW IMAX,INMAX @ DRAW IMAX,0
420 MOVE 0,0
430 RETURN
440 THEORY:
450 NTH=NTH+1
460 SCALE 0,IMAX,0,INMAX
470 DISP "ENTER VALUES OF CONSTANTS"
480 DISP " A=";@ INPUT A
490 DISP " B=";@ INPUT B
500 DISP " C=";@ INPUT C
510 DISP " D=";@ INPUT D
520 IF NTH>1 THEN GOTO 540
530 MOVE IMAX*.05,INMAX*.95 @ LDIR 0 @ LABEL "   A     B      C      D"
540 MOVE IMAX*.05,INMAX*.95-NTH*INMAX*.05 @ LABEL USING "D.DDD,X,D.DDD,X,D.DDD,X
,D.DDD" ; A,B,C,D
550 MOVE 0,0
560 FOR K=0 TO IMAX STEP IMAX/1000
570 Y=A*K*(1+C*K)*(1-D*K)/(1+B*K)
```

```
580 IF Y>INMAX OR Y<0 THEN GOTO 610
590 DRAW K,Y
600 NEXT K
610 MOVE 0,0
620 RETURN
630 DINPUT:
640 ALPHA @ CLEAR
650 DISP "CURRENT";@ INPUT I@ DISP "INTENSITY";@ INPUT B
660 IF I<0 THEN GOTO 710
670 MOVE I-.01*IMAX,B @ DRAW I+.01*IMAX,B
680 MOVE I,B+.01*INMAX @ DRAW I,B-.01*INMAX
690 MOVE 0,0
700 GOTO 640
710 RETURN
```

APPENDIX : C

```
5 PRINTER IS 701
10 REM ***LEAST SQ FIT TO INT=AI*(1+BN(I))***
20 REM ***INPUT OF STORED DENSITY FROM FILE***
25  DISP "PLACE DATA DISC INTO DRIVE 1"
27 CAT ":D701"
35 DISP "ENTER DATA FILE NAME" @ INPUT F$
40 CREATE F$&":D701",1
50 ASSIGN# 1 TO  F$&":D701"
60 INPUT ID
70 FOR I=1 TO ID
80 INPUT C(I),N(I)
90 NEXT I
100 ASSIGN# 1 TO  * !
110 REM ***INPUT EXP INTENSITIES***
120 FOR I=1 TO ID
130 DISP "CURRENT",C(I),
135 DISP "INTENSITY"
140 INPUT Z(I)
150 NEXT I
160 REM
170 PRINT ""
180 PRINT ""
190 REM **CALCULATE COEFFS FOR LEAST SQ FIT**
200 P=0 @ Q=0 @ R=0 @ S=0 @ T=0 @ RES=0 @ FR=0
210 FOR I=1 TO ID
220 P=P+C(I)*C(I)
230 Q=Q+C(I)*C(I)*N(I)
240 R=R+C(I)*Z(I)
250 S=S+C(I)*C(I)*N(I)*N(I)
260 T=T+C(I)*N(I)*Z(I)
270 NEXT I
280 PRINT "CALC. A=",AN
300 BN=(T*P-Q*R)/(P*S-Q*Q)
310 REM **TABULATION OF EXP AND THEO CURVE**
320 PRINT "CALC A*B=",BN
330 PRINT "CURRENT EXP INTENSITY   CALC INTENSITY"
340 FOR I=1 TO ID
350 ZN(I)=AN*C(I)+BN*C(I)*N(I)
360 DISP C(I),Z(I),ZN(I)
370 PRINT C(I),Z(I),ZN(I)
380 RES=(Z(I)-ZN(I))*(Z(I)-ZN(I))+RES
390 FR=RES/(Z(I)*Z(I))+FR
395 NEXT I
400 DISP "RESIDUAL=",RES,"FRACTIONAL RESIDUAL=",FR
410 PRINT "RESIDUAL=",RES,"FRACTIONAL RESIDUAL=",FR
420 DISP "NEW INTENSITY      1"
430 DISP "NEW DENSITY        2"
435 DISP "NEW AN             3"
440 DISP "EXIT               4"
450 DISP
460 DISP "ENTER NUMBER OF ROUTINE REQUIRED" @ INPUT K
470 IF K=1 THEN GOTO 110
480 IF K=2 THEN GOTO 25
485 IF K=3 THEN GOTO 95
490 IF K=4 THEN GOTO 510
500 STOP
510 END
```

APPENDIX: D

Theory for least square fitting:

$$Z = A\,x.\,(1+By)$$

Where Z: Intensity

x: Discharge Current

y: Number density of intermediate level

$$Z = Ax + Cx\,y$$

Where $C = A.B$

Deviation from fit $= Z - (Ax + Cx\,y)$

For least square fit, A and C chosen such that

$$D = \sum_i (Z_i - Ax_i - Cx_i y_i)^2 \text{ is a minimum}$$

i.e.

$$\frac{\partial D}{\partial A} , \frac{\partial D}{\partial C} = 0$$

$$\frac{\partial D}{\partial A} = \sum_i 2\,(Z_i - Ax_i - Cx_i y_i)\,(-x) = 0$$

i.e. $\sum x^2 A + C\sum x^2 y - \sum x\,Z = 0 \qquad (1)$

$$\frac{\partial D}{\partial C} = \sum_i 2\,(Z_i - Ax_i - C\,x_i y_i)\,(-xy) = 0$$

i.e. $A\sum x^2 y + C\sum x^2 y^2 - \sum xy\,Z = 0 \qquad (2)$

Let $\sum x^2 = P$, $\sum x^2 y = q$, $\sum xZ = r$

$\sum x^2 y^2 = s$, $\sum xy\,Z = t$

Then from (1) = $PA + qC - r = 0$

from (2) = $qA + sc - t = 0$

$$A = \frac{vs - qt}{ps - q^2} \quad , \quad C = \frac{tp - qr}{ps - q^2}$$

In the basic program:

Z(I): Experimental intensity

C(I): Discharge current

N(I): Number density of intermediate level

ZN(I): Intensity calculated from formula

A = AN

A.B = BN

ID: Number of current steps

$$\text{Residual} = \frac{1}{ID} \sum (ZN(I) - Z(I))^2$$

$$\text{Fractional residual} = \frac{1}{ID} \sum \left(\frac{ZN(I) - Z(I)}{Z(I)}\right)^2$$

APPENDIX E:

SAC 86/3RD/BNASS
BRISTOL (1986)

ELECTRICAL AND SPECTRAL CHARACTERISTICS OF THE POSITIVE COLUMN OE A LOW PRESSURE DISCHARGE IN INERT GASES

E.B.M. Steers and A. Zendehnam
Department of Electronic & Communications Engineering & Applied Physics,
Polytechnic of North London

Intensity-current relationships for selected Ne I and Ne II lines emitted from a hollow cathode discharge in pure neon are in general agreement with a model involving the balance between one-step and two-step excitation processes, and de-excitation by radiation and electron collisions[1]; subsequently number density of neon metastable atoms has been measured[2].

Comparative measurements from the positive column of a d.c. discharge in neon have been made, using various tubes with bores 3-20 mm, pressure range 0.1-15 mbar and current 0-30 mA. The merits of the various cathode systems used (plane, hollow cathode and heated coated) will be discussed.

The dependence of the intensity of selected neon lines on the discharge current has been recorded over a wide range of parameters (pressure, length, diameter and different orientation of the positive column) with the voltage-current characteristics also recorded in each case.

A Fabry-Perot interferometer was employed to record emission and absorption line profiles. The variation of self-reversal and of the population of metastable atoms with pressure, current and the discharge condition will be reported. Similar experiments have been carried out using argon and argon-neon mixtures.

The extent to which these experimental measurements can be fitted to the model proposed and the limitations of the model for conditions in the positive column region will be discussed.

[1] Howard, C, Pillow, M E, Steers, E B M and Ward, D W, Analyst 1983, 108, 145
[2] Light, C E, Steers, E B M, Proc. of the 8th Inter.Conf. on Gas Discharges and Their Applications, 1985, p.559

21ST CSI
GARMISH (1985)

POPULATION OF METASTABLE NEON ATOMS IN HOLLOW CATHODE AND OTHER LOW PRESSURE DISCHARGES

C.E. Light, E.B.M. Steers and A. Zemdehnam,

School of Applied Physics, The Polytechnic of North London,
Holloway, London, N7 8DB, U.K.

1. INTRODUCTION

The variation with current, i, of the intensity, I, of neon spectral lines emitted by a demountable neon/iron hollow cathode lamp has been studied as part of an investigation of the excitation processes in hollow cathode discharges. The results indicate that two-step excitation is important for many neon lines, [1], with the metastable state $3s[3/2]_2^o$ as the probable intermediate level [2]. I-i relationships from the positive column of a discharge in low pressure neon have also been investigated for comparison. To assist in interpreting the I-i results, data on the metastable populations in both types of source are required, and high resolution absorption measurements have been made on selected Ne I lines.

Methods usually used to determine number densities of metastable atoms are based on those described by Mitchell and Zemansky [3]; all contain assumptions on the form and constancy of the line profiles. These uncertainties can be avoided by deriving the absorption line profile, k(σ), from Fabry-Perot measurements of the primary source and transmitted line profiles [4]. The number density, N, of absorbing atoms is given by

$$N = \frac{8\pi\, g_2\, c}{\lambda_o^2\, g_1\, A_{12}} \int k(\sigma)\, d\sigma$$

where g_1 and g_2 are the statistical weights of the upper and lower levels, respectively, A_{12} the Einstein transition probability and λ_o the central wavelength.

2. EXPERIMENTAL DETAILS

Demountable discharge tubes were used on u.h.v. systems to give high purity conditions; the vacuum system for the positive column tubes was similar to that for the hollow cathode [2]. In both cases, the discharge tubes were filled with research grade neon to the required pressure, and a getter used to maintain purity.

The hollow cathode assembly was mounted in a 64 mm I.D. 4-way cross (Fig.1); the open-ended cylindrical, mild steel cathode, 50 mm long and 15 mm bore, was held horizontally by three support rods. The cathode and chamber were earthed and glass and mica sheaths used to prevent strav discharges. Pressures to 1 to 5 torr were used, and currents in the range 1-50 mA.

A glass or fused silica discharge tube was used for measurements on the positive column; after preliminary experiments with cold cathodes, hollow cathodes and a heated coated cathode, the last was chosen for most of the measurements. The form of the tube (Fig.2), with alternative anodes (1 and 2) giving different length positive columns, allowed an estimate to be made of the field strength. Neon pressures between 0.1 and 15 torr were used, with currents up to 30 mA.

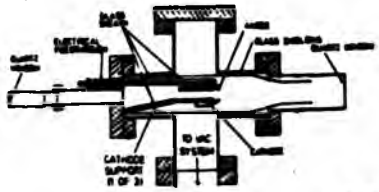

Fig. 1: Section through the hollow cathode chamber

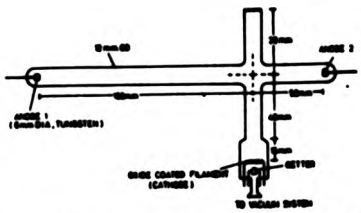

Fig. 2: Positive column discharge tube (mounted with long arm vertical)

A neon, microwave excited, electrodeless discharge lamp (EDL) was used as the primary source for the absorption measurements. Ne I spectral lines emitted by the EDL were isolated by the monochrometer and profiles recorded by means of the pressure scanning Fabry-Perot interferometer [2] with the discharge off (i = 0) and with it switched on (Fig.3). This was carried out for spectral lines with transitions terminating on $3s[3/2]^o_2$ (e.g. Ne I 640.2 and 614.3 nm) and on the other three levels of the 3s,3s' group. Measurements were made at various pressures and discharge currents. The instrument function of the interferometer was determined by recording the profile of the Ne I 632.8 nm line emitted by a mode-stabilized laser.

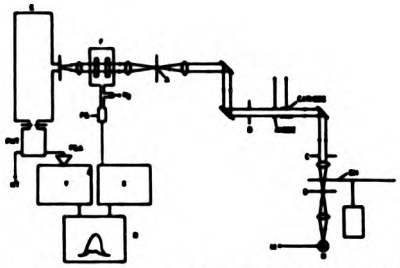

Fig. 3: Arrangement for interferometer measurements for hollow cathode discharge. A,B,C,D: Apertures; E: Eagle monochromator; F: Fabry-Perot Interferometer and housing; M: Microwave power supply; N: Neon EDL primary source; X,Y: X & Y axis control circuits; R: X-Y recorder; CH: Chopper; H_2: To gas pressure supply and needle valve; PS: Pressure sensor.

For positive column the probe beam was focussed at the centre of the tube.

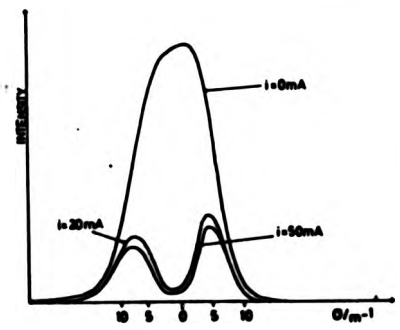

Fig. 4: Fabry-Perot profiles of Ne I 640.2 nm transmitted through the hollow cathode discharge (neon pressure: 2 torr).

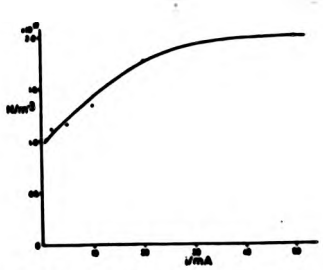

Fig. 5: Plot of number density of metastable state $3s[3/2]^o_2$ against current, i, for a hollow cathode discharge in neon, pressure 1 torr

3. RESULTS

Fig.4 shows an example of the Fabry-Perot scans for Ne I 640.2 nm. From such data, the variation of k(σ) with wavenumber σ can be derived; a correction for instrument profile must be made, but this is small and has been neglected for preliminary calculation of results. Fig.5 is a plot of number density of the $3s[3/2]^o_2$ state against current for a hollow cathode discharge at 1 torr. Both sources show the same type of dependence of metastable population on current, with a tendency to saturate with increasing current, in agreement with the results of van Veldhuizen and de Hoog [5]; number densities from both sources are of the same order of magnitude, but those for the hollow cathode discharge showed very little variation with pressure, whilst the positive column results have a marked dependence on pressure. Further experimental work is in progress and more detailed analysis of the results is being carried out, and will be presented.

We wish to thank Cathodeon, Ltd., Cambridge, for the provision of a range of specially designed discharge tubes for the positive column experiments.

REFERENCES

1. Howard, C., Pillow, M.E., Steers, E.B.M. and Ward, D.W., Analyst, 108.145-152(1983)
2. Light, C.E. and Steers, E.B.M., Analyst, 110. 439-441 (1985)
3. Mitchell, A.C.G. and Zemansky,M.W..Resonance Radiation and Excited Atoms, C.U.P. (1961)
4. Light, C.E. and Steers, E.B.M., Proc. of 8th Int.Conf. on gas Discharges and their Applications, Oxford (1985), *in press*
5. van Veldhuizen, E.M. and de Hoog, F.J., J.Phys.D., 17, 953-968 (1984)

XVIII ICPIG
SWANSEA (1987)

EXCITATION MECHANISMS IN THE POSITIVE COLUMN OF LOW CURRENT DISCHARGES IN NEON AND ARGON

B.B.N. Steers and A. Zendehnam

Department of Electronic and Communications Engineering and Applied Physics,
The Polytechnic of North London, Holloway, London, N7 8DB, U.K.

Introduction

The variation with the current, i, of the intensity, I, of neon spectral lines emitted from a low pressure positive column discharges has been studied as part of an investigation of excitation processes in these discharges. The results indicate that two-stage excitation is important for many neon lines [1], with the metastable level 3s [3/2]$_2$ as the probable intermediate level [2]. Measurements of emission lines profiles have been made using a pressure scanned Fabry-Perot interferometer.

High resolution absorption measurements have been carried out to give data on the populations of the metastable states, and their variation with pressure and current, to assist in interpreting the intensity *versus* current (I-i) results. Figure 1 shows the optical arrangements.

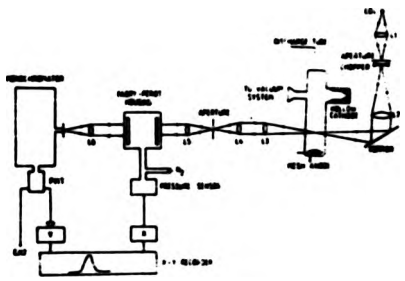

Figure 1. The optical arrangement used for measurement of emission and absorption profiles. The interferometer was removed for I-i results.

The measurements were made using a variety of discharge tubes with diameters from 3 to 20 mm, with currents up to 30 mA and neon pressures between 0.1 and 15 mbar. For comparison, measurements were also made with argon and neon-argon mixtures. A high vacuum system was used to give high purity conditions with glass or fused silica demountable positive column tubes and various cathode systems, (cold plane, hollow and heated coated). The relative merits of the various cathode systems used will be discussed.

The I-i and emission and absorption profile measurements were carried out for two orientations of the discharge tubes (end-on and side-on views). The profile of the Ne I 6328 Å line emitted from a helium-neon laser was recorded to determine the instrument function of the interferometer.

Results and Discussion.

Axial intensity *versus* current measurements at various gas pressures were made for selected Ne I lines. A linear I-i graph was obtained for a few spectral lines: some lines gave upward curvature, indicating that two stage excitation plays an important role in their excitation, but lines from higher energy levels (e.g. 3633 Å), where collisional de-excitaion processes are likely to be more significant, showed downward curvature (Figure 2).

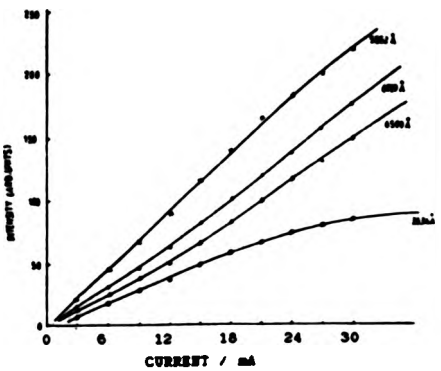

Figure 2. Graphs of intensity *versus* current for some Ne I lines.
Neon pressure: 5 mbar

The upward curvature for the Ne I lines disappeared when argon was added to the neon discharge; neon metastable atoms were quenched by argon, so that two-step excitation was then not significant.

Most of the Ne I lines corresponding to transitions to the metastable state 3s [3/2]$_2$ exhibited varying degrees of self-reversal (Figure 3); this was not observed for transitions terminating on the other three levels of the 3s,3s' group.

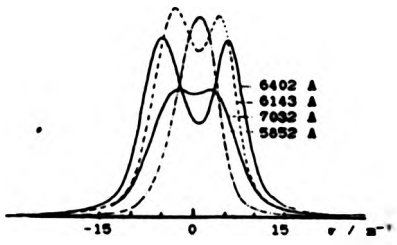

Figure 3. Fabry-Perot scans of some Ne I lines. Neon pressure: 2 mbar. Current 20 mA.

When argon was used, I-i curves for Ar I lines showed a very similar behaviour to that for Ne I spectral lines. Self-reversal was not observed for argon lines terminating on the metastable states, but the strongest lines at about 8000 Å were outside the range of the equipment.

Preliminary analysis of the data has been carried out without a correction for the instrumental profile, thus giving an "apparent" absorption coefficient. The number densities of the metastable and radiative states have been calculated by graphical integration over the line profile of the apparent absorption coefficient for Ne I lines [3]. Plots of the number density of the 3s [3/2]$_2$ level against current for various pressures are given in Figure 4.

The number density of this state tends to a constant value for higher currents as both the excitation process and the loss of metastable atoms by further excitation and ionisation by electrons are approximately proportional to the current. This saturation behaviour is much less for radiative levels, where the dominant loss process is not dependent on the current.

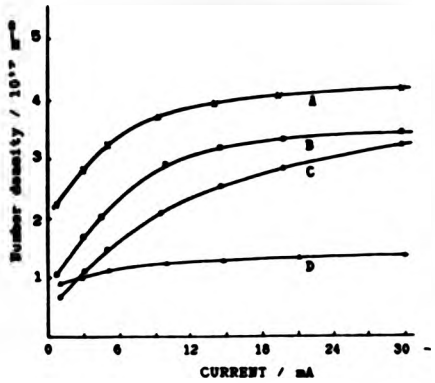

Figure 4. Plot of number density of the 3s [3/2]$_2$ level against current for various pressures:- A,2 mbar; B,1 mbar; C,0.6 mbar and D,10 mbar

The results of this work are in good agreement with the trends shown in the results of van Veldhuizen and de Hoog [4] and Smits and Prins [5].

We wish to thank Mr D.V. Ward of Cathodeon Ltd, Cambridge, for his interest in this project and for supplying the special discharge tubes used.

References

[1] Howard, C., Pillow, M.E., Steers, E.B.M. and Ward, D.V., 1983, Analyst 108, 145-152

[2] Light, C.E. and Steers, E.B.M., 1985, Analyst 110, 439-441.

[3] Light, C.E., 1985, Proc. 8th Int. Conf. on Gas Discharges and their Applications (GD85), *Leeds Univ. Press*, 559-561

[4] van Veldhuizen, E.M. and de Hoog, F.J., 1984, J. Phys D, 17, 963-966

[5] Smits, R.M.M. and Prins, M., 1975, Physica 80C, 571-584

TITLE Excitation Processes In The Positive Column of Electrical Discharges In Inert Gases

AUTHOR A. ZENDEHNAM